EUTROPHICATION PROCESSES AND MICROBIAL ECOLOGY OF LAKE MENDOTA, WISCONSIN

by

Emily Louise Kara

A dissertation submitted in partial fulfillment of

the requirements for the degree of

Doctor of Philosophy

(Civil and Environmental Engineering)

at the

UNIVERSITY OF WISCONSIN-MADISON

2012

Date of final oral presentation: 6/7/2012

The dissertation is approved by the following members of the Final Oral Committee:

Katherine D. McMahon, Associate Professor, Civil and Environmental Engineering
Chin H. Wu, Professor, Civil and Environmental Engineering
Joel A. Pedersen, Professor, Soil Science
Eric E. Roden, Professor, Geology
Paul C. Hanson, Research Professor, Natural Science

Abstract

Eutrophication of Lake Mendota, Wisconsin co-occurred with deforestation of the watershed by settlers in the mid 1850's. The characteristics of this aquatic ecosystem are representative of eutrophication occurring throughout the world in lakes, rivers and marine systems (abundant harmful algal blooms [HABs]), anoxic hypolimnia, and altered food webs). Although the flow of nutrients through lakes and the microbial communities responsible for cycling have been a topic of scientific study for more than a century, our understanding of the efficacy of nutrient management, HAB and heterotrophic bacterial community prediction, and phosphorus speciation at the in-lake level remains limited.

Enhanced nutrient management in the watersheds of impaired or threatened surface waters is the most common tool for mitigation of eutrophication, and is understood to be an effective tool to improve or prevent degradation of surface water due to excess nutrients. We used a mass balance approach to determine the net effects of nutrient management changes in the Lake Mendota, Wisconsin watershed occurring between 1995 and 2007, including farmers' adoption of enhanced nutrient management plans, reduced use of chemical feed supplements for dairy cattle, and an urban phosphorus ban. These three factors were attributed to be the cause of reduced, but positive accumulation in 2007, indicating that efforts to improve nutrient management have had limited effect on the overall P budget.

We setup, calibrated, and validated an aquatic ecosystem model to test its ability for the short- and long-term prediction of the dynamics of HABs in Lake Mendota. We found biological variables to have the poorest fit with observations, particularly at time scales > 1 month, with the use of high-frequency water quality observations and predictions, and assessed using wavelet

analysis. We used numerical simulations to assess the effects of climate change scenarios on water quality, and to identify the most potentially important external factors for HAB dynamics in the lake.

Beyond HABs, heterotrophic bacterial communities are responsible for important ecosystem functions in lakes, and the interactions of heterotrophic bacteria with each other, with HABs, and with environmental variables over long time series is unknown. We determined the drivers of bacterial community characteristics (including diversity and co-occurrence network structure) using a decade-long record of bacterial community composition together with a long-term ecological research dataset and local similarity analysis. We found season to drive the complexity of interaction networks and patterns in diversity; variation of environmental variables did not explain the patterns observed.

Finally, the chemical structure and dynamics of phosphorus compounds in Lake Mendota across space and time was assessed by ^{31}P nuclear magnetic spectroscopy (NMR) to determine the prevalence and nature of non-reactive phosphorus in particulate and dissolved fractions. We found particulate and dissolved fractions from all locations observed had significant temporal variability, while epilimnetic particulate P was more stable over 5 months, and was associated with dissolved reactive P dynamics.

This work addresses phosphorus cycling and microbial ecology of a eutrophic lake, leveraging and building upon the body of literature on anthropogenic eutrophication processes and microbial ecology in lakes.

Acknowledgements

My advisor, Dr. Katherine McMahon, gives her students every opportunity to succeed. With her guidance, I have grown into a scientist with many dimensions and a self-knowledge of my own capacities, cultivated through the organic process of research in her lab. I look to Trina as a role model for her leadership, unending enthusiasm, positivity, creativity, and persistence. I am grateful to Trina for seeing in me the potential for research in environmental engineering, and especially for showing me how important personal connections are for professional growth and success.

Dr. Paul Hanson, my co-advisor, sees the world from a larger perspective than most people do. As such, he demands frequent identification and re-identification of goals, which helps me to stay more relevant and focused than I would be otherwise. Paul's creativity and innovation has been refreshing and inspirational during our work together. I thank Paul for being present for me as an advisor in all aspects of my doctoral research, including by mentoring me as a student leader in the Global Lake Ecological Observatory Network.

I am ever grateful to my parents who have wholeheartedly supported me in countless material, emotional, and spiritual ways throughout my life, and continue to today. Their guidance and love have made me the person I am. My dad frequently reminds me that I am capable of reaching any goal I set out to attain, and my mom teaches me the value of meeting the present moment with kindness, compassion, curiosity, and humility. My fiancé, Jordan, is a role model to me by embodying his core values in everyday life: integrity, loyalty, honesty, and diligence. Learning by example makes me a better scientist and human being. I have thoroughly enjoyed

the completion of the PhD journey with him at my side, both literally and figuratively, and I look forward to the rest of our lives together.

I am grateful for support and humor from siblings Adeline, Charlie, and Phil, and from friends Rebecca Kosick, Jaime Cesarz, Haemi Kim, Carol Warden, Tracy Stacy, Allie Sanders, Jessica Lucido, and Tracy Cadkin. Colleagues and friends Ashley Shade, Luke Winslow, Kevin Rose, Lucas Beversdorf, Steve Powers, Ryan Batt, and Amanda Stone: I am so happy to have had the chance to work with you and learn from you in various ways. Many thanks to McMahon lab members Ashley Shade, Ryan Newton, Shaomei He, Stuart Jones, and Jason Flowers for showing me the ropes while we were at UW together, and to Jay Hawley, and Ben Crary our work together more recently. I am indebted to James Mutschler, Katie VanGheem, and Aaron Besaw for assistance in the lab. I am grateful to colleagues at the Center for Limnology and in the Global Lake Ecological Observatory network for enriching my doctoral experience by sharing your research and letting me share mine, and for the productive collaborations that have grown out these interactions. I am grateful to Dave Harring, Ted Bier, and Aaron Stephenson for technical assistance at the Center for Limnology, and to Dean Maly, Gary Pine, and Janet Newlands for support at the Microbial Sciences Building.

Finally, I am grateful for my funding sources: the National Science Foundation, Gordon and Betty Moore foundation, the Becker Family, and the Anna Grant Birge Family.

Table of Contents

Table of Contents

List of Figures

List of Tables

Chapter 1 - Introduction

Emily L. Kara

The second decade of the 21st century marks the approximate 150 year anniversary of the deforestation of the Lake Mendota, Wisconsin watershed and subsequent eutrophication of the Yahara chain of lakes: Mendota, Monona, Waubesa, and Kegonsa. The sediment record of Lake Mendota indicates that the watershed was cleared of native forests to make way for agriculture in the mid 1850's, soon after Wisconsin attained statehood in 1848. Likely since the mid-1800s, and certainly since 1889 (Trelease, 1889), Lake Mendota has exhibited the telltale signs of excess nutrient loading: 'blue-green algal' (now known as *Cyanobacterial*) blooms. Although nutrient management efforts, beginning in the 1950s, have had a pronounced effect on the in-lake phosphorus concentrations (Lathrop, 2007), phosphorus loading to the lake remains high, and the dissolved oxygen record of Birge and Juday from the 1906 indicates that the lake's tropic status is not significantly different than that observed in the late 1970s by Brock and others (Birge & Juday, 1911; Brock, 1985), nor that monitored currently by the North Temperate Lakes Long Term Ecological Research Program (NTL LTER). This evidence indicates that despite the best efforts of the community and regulatory bodies to improve water quality, it remains impaired.

In the past two decades, a renewed effort to maintain and recover water quality in the Yahara lakes has been led by the Wisconsin Departments of Natural Resources (WDNR) and Agriculture, Trade, and Consumer Protection (WDATCP), and the City of Madison, together with stakeholders and interested parties including University of Wisconsin scientists, lake associations, and regional private consulting firms, in what is known as the Yahara Capital Lakes Environmental Assessment and Needs partnership. The partnership aims to 'establish clear and achievable goals and an implementation plan for cleaning the lakes' (Jones et al., 2010), and

overrides WDNR requirements for water quality of hydrologic inflows and in-lake water quality criteria, based on the recognition that the Yahara lakes are a special case that requires a more delicate and diplomatic regulation than other state waters, due to the diversity of stakeholders: farmers, area businesses, the University of Wisconsin, area residents, land managers, and legislators. A concerted effort started in the 1990's to reduce nutrient loading to Lake Mendota by half, the Lake Mendota Priority Watershed Project, were not met by 2009 (Jones et al., 2010).

Scientific research of eutrophic Lake Mendota has occurred for nearly as long as the lake has been eutrophied, beginning with the work of Birge and Juday (e.g. Birge, 1915; Birge & Juday, 1911; Juday, 1914). Research has continued into the 21st century on topics including phosphorus loading and cycling (Bennett et al., 1999; Carpenter et al., 2007; Kamarainen et al., 2009; Lathrop et al., 1998b; Soranno et al., 1997), phosphorus speciation (Brock & Clyne, 1984; Eisenreich & Armstrong, 2000; Sommers et al., 2008), microbial ecology (Ingvorsen & Brock, 1982; Jones et al., 2009; Newton & McMahon, 2011; Pedrós-Alió & Brock, 1982; Shade et al., 2007), and *Cyanobacterial* dynamics (Brock, 1985; Brock & Clyne, 1984; Fallon & Brock, 1980; Konopka & Brock, 1978; Miller & McMahon, 2011). Yet questions remain: Have recent efforts to manage nutrients affected the standing stock of P in the watershed? At what spatial and temporal scales can harmful *Cyanobacterial* blooms be forecasted? How do exogenous drivers such as magnitude and quality of nutrients loaded affect water quality variables, including harmful blooms? How do microbial communities in Lake Mendota vary through time; are the underlying communities' dynamics related to water quality?

The research presented in this dissertation focuses on processes and factors of eutrophication related to the efficacy of nutrient management at the watershed-scale, in-lake phosphorus speciation and cycling, mechanistic prediction of water quality, and the long-term

underlying microbial communities of Lake Mendota, Wisconsin. Here, I address research questions related to nutrient, management, nutrient cycling and bioavailability, water quality forecasting, and the patterns of microbial populations that underlie aquatic ecosystem functioning. The research is focused on a single system, but has applicability to other eutrophic systems, for nutrient managers, microbial ecologists, and water quality modelers.

In Chapter 2, a quantitative analysis of the impact of a decade of phosphorus (P) management in the Lake Mendota watershed is presented. The effects of changes in regulation and best management practices on the P budget for the watershed are assessed, and potential mitigation scenarios and the impact on P loading to the watershed are investigated (Kara et al., 2012). Chapter 3 takes a mechanistic approach to the issue of *Cyanobacterial* blooms in Lake Mendota, and aims to determine the success of a predictive hydrodynamic-biogeochemical water quality model at across a time scales using traditional goodness-of-fit techniques and wavelet analysis (Kara et al., 2012). Chapter 4 assesses the sensitivity of that mechanistic model's response variables to potential future climate change, including temperature and nutrient scenarios. Chapter 5 analyzes an unprecedented decade-long observational record of bacterial communities from Lake Mendota using a novel analytical approach, network analysis. Microbial communities underlie nutrient cycling and perform critical roles in maintenances of water quality and nutrient availability, and the drivers of long-term dynamics remain largely unknown. Finally, Chapter 6 is a closer look at the composition of P at the molecular level using ^{31}P nuclear magnetic resonance spectroscopy (^{31}P NMR), discriminating the types of P entering and existing in the system over 1 year, from within the lake and from its major hydrologic inflows. The finding of Chapter 6 are relevant to aspects of each of the other chapters, and I anticipate the

research will future research in the fields of nutrient management, water quality modeling, and aquatic microbial ecology of eutrophic lakes.

References

Bennett, E. M., Reed-Andersen, T., Houser, J., Gabriel, J. R., & Carpenter, S. R. (1999). A Phosphorus Budget for the Lake Mendota Watershed. *Ecosystems*, *2*(1), 69-75. doi:10.1007/s100219900059

Birge, E. (1915). The heat budges of American and European lakes. *Transactions of the Wisconsin Academy of Sciences, Arts, and Letters*, *18*(166-213).

Birge, E., & Juday, C. (1911). The inland lakes of Wisconsin. *Wisconsin Geological and Natural History Survey Bulletin*, *22*(7), 259.

Brock, T D, & Clyne, J. (1984). Significance of algal excretory products for growth of epilimnetic bacteria. *Applied and environmental microbiology*, *47*(4), 731-4.

Brock, Thomas D. (1985). *A Eutrophic Lake: Lake Mendota, Wisconsin* (p. 308). Springer Verlag.

Carpenter, S. R., Benson, B., Biggs, R., Chipman, J. W., Foley, J. A., Golding, S. A., Hammer, R. B., et al. (2007). Understanding Regional Change : A Comparison of Two Lake Districts. *BioScience*, *57*(4), 323-335.

Eisenreich, S. J., & Armstrong, D. E. (1977). Chromatographic Investigation of Inositol Phosphate Esters in Lake Waters. *Environmental Science & Technology*, *11*(5), 497-501.

Fallon, R. D., & Brock, T. D. (1980). Planktonic blue-green algae: Production, sedimentation, and decomposition in Lake Mendota, Wisconsin. *Limnology and Oceanography*, *25*(l), 72-88.

Ingvorsen, A. K., & Brock, T. D. (1982). Electron Flow Via Sulfate Reduction and Methanogenesis in the Anaerobic Hypolimnion of Lake Mendota. *Limnology*, *27*(3), 559-564.

Jones, S. E., Newton, R. J., & McMahon, K. D. (2009). Evidence for structuring of bacterial community composition by organic carbon source in temperate lakes. *Environmental microbiology*, *11*(9), 2463-72. doi:10.1111/j.1462-2920.2009.01977.x

Jones, S., Josheff, S., Presser, D., & Steinhorst, G. (2010). *The Yahara Capital Area Environmental Assessment and Needs 2010 Report* (p. 138). Madison, WI. Retrieved from www.yaharawatershed.org

Juday, C. (1914). The Inland lakes of Wisconsin: the Hydrography and Morphoemetry of the Lakes. *Wisconsin Geological and Natural History Survey Bulletin*, *27*(9).

Kamarainen, A. M., Yuan, H., Wu, C. H., & Carpenter, S. R. (2009). OCEANOGRAPHY : METHODS Estimates of phosphorus entrainment in Lake Mendota : a comparison of one-dimensional and three-dimensional, 553-567.

Kara, E. L., Hanson, P. C., Hamilton, D. P., Hipsey, M. R., Mcmahon, K. D., Read, J. S., Winslow, L., et al. (2012). Environmental Modelling & Software Time-scale dependence in numerical simulations : Assessment of physical , chemical , and biological predictions in a stratified lake at temporal scales of hours to months. *Environmental Modelling and Software*, *35*, 104-121. Elsevier Ltd. doi:10.1016/j.envsoft.2012.02.014

Kara, E. L., Heimerl, C., Killpack, T., Bogert, M. C., Yoshida, H., & Carpenter, S. R. (2012). Assessing a decade of phosphorus management in the Lake Mendota, Wisconsin watershed and scenarios for enhanced phosphorus management. *Aquatic Sciences*, *74*(2), 241-253. doi:10.1007/s00027-011-0215-6

Konopka, A., & Brock, T. D. (1978). Effect of temperature on blue-green algae (cyanobacteria) in lake mendota. *Applied and environmental microbiology*, *36*(4), 572-6.

Lathrop, R. (2007). Perspectives on the eutrophication of the Yahara lakes. *Lake and Reservoir Management*, *23*(4), 345-365. doi:10.1080/07438140709354023

Lathrop, R., Carpenter, S. R., Stow, C., Soranno, P., & Panuska, J. (1998). Phosphorus loading reductions needed to control blue-green algal blooms in Lake Mendota. *Spring*.

Miller, T. R., & McMahon, K. D. (2011). Genetic diversity of cyanobacteria in four eutrophic lakes. *FEMS microbiology ecology*, *78*(2), 336-48. doi:10.1111/j.1574-6941.2011.01162.x

Newton, R. J., & McMahon, K. D. (2011). Seasonal differences in bacterial community composition following nutrient additions in a eutrophic lake. *Environmental microbiology*, *13*(4), 887-99. doi:10.1111/j.1462-2920.2010.02387.x

Pedrós-Alió, C., & Brock, T. D. (1982). Assessing biomass and production of bacteria in eutrophic Lake Mendota, Wisconsin. *Applied and environmental microbiology*, *44*(1), 203-18.

Shade, A., Kent, A. D., Jones, S. E., Newton, R. J., Triplett, E. W., & McMahon, K. D. (2007). Interannual dynamics and phenology of bacterial communities in a eutrophic lake. *Limnology and Oceanography*, *52*(2), 487-494. doi:10.4319/lo.2007.52.2.0487

Sommers, L. E., Harris, R. F., Williams, J. D. H., Armstrong, D. E., Syers, J. K., & Mar, N. (2008). Determination of Total Organic Phosphorus in Lake Sediments. *Limnology*, *15*(2), 301-304.

Soranno, P., Carpenter, S. R., & Lathrop, R. (1997). Internal phosphorus loading in Lake Mendota : response to external loads and weather. *Methods*, *1893*, 1883-1893.

Trelease, W. (1889). The “working” of the Madison lakes. *Transactions of the Wisconsin Academy of Sciences*, *7*, 121-129.

Chapter 2 - Assessing a decade of phosphorus management in the Lake Mendota, Wisconsin watershed and scenarios for enhanced phosphorus management

Emily L. Kara, Chad Heimerl, Tess Killpack,
Matthew C. Van de Bogert, Hiroko Yoshida, Stephen R. Carpenter

(Published in Aquatic Sciences (2012) 74:241-253)

2.1 Abstract

A phosphorus (P) budget was estimated for the watershed of Lake Mendota, Wisconsin, to assess the effects of nutrient management on P accumulation in the watershed soils. We estimated how nutrient management programs and legislation have affected the budget by comparing the budget for 2007 to a budget calculated for 1995, prior to implementation of the programs. Since 1995, inputs decreased from 1,310,000 kg P/yr to 853,000 kg P/yr (35% reduction) and accumulation decreased from 575,000 kg P/yr to 279,000 kg P/yr (51% reduction). Changes in P input and accumulation were attributed primarily to enhanced agricultural nutrient management, reduction in dairy cattle feed supplements and an urban P fertilizer ban. Four scenarios were investigated to determine potential impacts of additional nutrient management tactics on the watershed P budget and P loading to Lake Mendota. Elimination of chemical P fertilizer input has the greatest potential to reduce watershed P accumulation and establishment of riparian buffers has the greatest potential to prevent P loading to Lake Mendota.

2.2 Introduction

Excess nutrient loading impairs water quality in surface waters worldwide. Although excess phosphorus (P) runoff to freshwater exceeds planetary boundaries for global water quality

targets (Carpenter and Bennett 2011), P fertilizer availability limits agricultural production in some parts of the world, and some have argued that non-renewable global P reserves are declining (Cordell et al. 2009). Management of phosphorus loading to surface waters from agricultural runoff, urban fertilizers, storm water drainage, and wastewater effluent is crucial to prevention and control of cultural eutrophication (Schindler et al. 2008; Carpenter 2008), and for conservation of a limited resource upon which global food production depends (Carpenter and Bennett 2011; Cordell et al. 2009).

For decades, eutrophication of Lake Mendota, Wisconsin (WI) has generated attention in the public realm and scientific community (Lathrop 2007; Carpenter and Lathrop 2008; Brock 1985). For lakes in general, and for Lake Mendota specifically, the relationship between external P loading and water quality is well established (Schindler 1977; Schindler et al. 2008; Lathrop et al. 1999; Vollenweider 1976; Smith et al. 2006). Efforts to manage phosphorus loading in the Lake Mendota watershed began in the 1950's, nearly 70 years after nuisance algal blooms were first observed (Brock 1985), and have continued into the 21st century. Eutrophication persists in Lake Mendota due to nonpoint agricultural sources of phosphorus in the watershed (Betz et al. 2002), as well as recycling from hypolimnetic and sediment P (Soranno et al. 1997; Kamarainen et al. 2009). Eutrophication in Lake Mendota appears to be reversible (Carpenter and Lathrop 2008; Lathrop et al. 1998).

Nonpoint pollution of Lake Mendota prompted researchers to compute a P budget (inputs, outputs, and accumulation) for the Lake Mendota watershed in order to understand the sources of high P inputs (Bennett et al. 1999). In the years since the publication of the 1995 budget, significant changes in agricultural practices, manure management, and fertilizer use may have occurred due to new regulations and changes in agricultural practices. To investigate this

possibility, we updated the P budget for the Lake Mendota watershed for 2007. To examine comparative effects of additional P management tactics, we analyzed scenarios of altered watershed P budgets and nutrient loading to Lake Mendota. The results suggest a comparison of the efficiency (cost per unit of reduced loading) of different nutrient management tactics within the context of a managed watershed that may be relevant to water quality managers and policy-makers worldwide.

2.3 Materials and Methods

Lake Mendota is located in south central Wisconsin, USA (43°06′24″N; 89°25′29″W). The lake and watershed have been described in detail elsewhere (Kitchell 1992; Brock 1985; Bennett et al. 1999). Approximately 88% of the watershed is contained within Dane County, WI; the remaining 12% is within Columbia County, WI.

Using a mass-balance approach, we calculated the inputs, outputs, and accumulation of P in the Lake Mendota watershed for 2007 using the methods of Bennett et al (1999). We assumed a 'best case' scenario for 2007: full compliance by residents and farmers with local ordinances, nutrient management plans, and best management practices. To test the effect of additional P management techniques not currently employed in the watershed, we simulated four scenarios in order to represent the largest possible reduction in P loading to the watershed and to Lake Mendota at several control points (Figure 2.1). The scenarios included (1) elimination of imported chemical fertilizer P, (2) elimination of imported animal feed supplements, (3) implementation of anaerobic manure digesters, and (4) implementation of riparian buffers to reduce P loss to Lake Mendota. The scenarios are intended to represent alternative control points in the watershed as a guide for future management within the watershed, as compared to the

'best case' scenarios for our calculated 2007 budget and the 1995 budget as estimated by Bennett et al. (1999).

Methods for calculating the 2007 phosphorus budget were based on the work of Bennett et al. (1999) and supplemented with information from publications, municipal reports, and local agricultural experts regarding relevant changes in local nutrient management practices since 1995. Detailed methods and examples are given in the Appendix. Inputs and outputs of P were calculated using 2007 data from various sources (Table 2.1). Where necessary, data were scaled to the watershed from studies aggregated at coarser scales, as described below and in the Appendix

We obtained values for cropland area, crop export, animal inventory and export, and animal products export from the United States Department of Agriculture National Agricultural Statistics Services (USDA-NASS) 2007 Census of Agriculture aggregated to Dane County (USDA-NASS 2009a, b). The county values were scaled to the watershed based on the proportion of the county's agricultural land within the watershed boundary. This proportion was estimated using 2005 land use coverage layers for Dane County (http://www.countyofdane.com/lio) and Columbia County (ftp://www.co.columbia.wi.us/lid), and watershed boundaries delineated by the Wisconsin Department of Natural Resources (ftp://dnrftp01.wi.gov/geodata). We assumed that the proportion of cropland area, export, animal inventory and export, and animal product export for the small fraction of watershed area within Colombia County (12%) was the same as for Dane County, WI.

Phosphorus inputs to the watershed included fertilizer for crops and urban lawns, feed supplements for cattle, commercial biosolid applications, and atmospheric deposition. Fertilizer for urban lawns was calculated based on the percent of turf-covered urban area in the watershed

(Bennett et al. 1999; Bannerman et al. 1993) and the recommended fertilization rates (Soldat and Petrovic 2008). Mass of phosphorus imported in animal feed supplements was estimated using data particular to south-central Wisconsin dairy herds (Powell et al. 2002). Values for atmospheric P deposition were assumed to be the same as those calculated in a previous study (Lathrop 1979) and used in the 1995 P budget (Bennett et al. 1999).

Assumptions about fertilizer and dairy cattle feed supplements were different for the 2007 and 1995 budgets. For both budgets, estimates of agricultural fertilizer use were based upon recommendations for each crop by made by the University of Wisconsin Cooperative Extension (UWEX). In contrast to the 1995 budget (Bennett et al. 1999), the 2007 budget assumed that many goals for agricultural P management had been met. We assumed (1) farmers measured soil P concentration and chemical P was applied at a rate recommended by the UWEX for soil based on the outcome of that measurement, which would typically prescribe no P application for most crops grown in Mendota watershed soils (L. Lambert, Dane County Land Conservation Division, pers. comm.; Bennett et al. 1999); (2) P addition to crops as land-applied manure was credited by farmers as P fertilizer (Laboski et al. 2006), (J.M. Powell, US Dairy Forage Research Center, University of Wisconsin, pers. comm.); (3) a P ban on chemical fertilizer for urban lawns and turf was in effect (Dane County Code of Ordinances Chapter 80); and (4) dairy cattle P feed supplements did not exceed the animals' physiological requirements (Satter et al. 2005).

Phosphorus output included crops for human consumption (excluding forage crops), animal products (dairy and eggs), animals (cattle, hogs and pigs) and export to Lake Mendota. Export data for 2007 crops, dairy products, and animals were obtained from the USDA Census of Agriculture and scaled to the watershed as described above. Exports in eggs were determined using the number of laying hens in the watershed, the average annual egg

production per layer, and P concentration of eggs (USDA-NASS 2009a; USDA-AMS 2000; Lorimor et al. 2000). Forage crops grown in the watershed were assumed to remain in the watershed for animal feed and were not counted as exports (J.M. Powell, US Dairy Forage Research Center, University of Wisconsin pers. comm.). Phosphorus exported via crops, animals, and animal products was calculated using conversion rates particular to the product (Lorimor et al. 2000; Laboski et al. 2006). Export to Lake Mendota was estimated using the mean annual P load to the lake for the years 1976 to 2005 as reported by Carpenter and Lathrop (2008).

Budget values that included uncertainties other than simple scaling from the county to the watershed scale were bracketed with minimum and maximum estimates based on extremes of plausible assumptions. All calculations of minimum and maximum values can be found in the Appendix. More uncertainty exists in estimates for inputs than outputs because agricultural exports are more consistently and clearly reported than are imported feed supplement and fertilizer use.

Within the budget, control points for P management were identified (Figure 2.1). These control points were selected for their expected contribution to watershed P accumulation and loading to Lake Mendota. The effects of the elimination of chemical P fertilizer (Scenario 1) and feed supplement (Scenario 2) imports to the watershed were evaluated by simulating removal of all chemical P inputs for fertilizer and feed from the mass balance. In the manure digester scenario (Scenario 3), we assumed that 85% of the phosphorus in manure processed by digesters would be exported from the watershed as a solid by-product. The remaining 15% of the phosphorus remains in liquid form and would be used as fertilizer within the watershed (Strand Associates 2009). Not all manure is collectable; for this scenario, we assumed that 64% of total

manure produced was collected and processed by digesters (Powell et al. 2005). In this case, manure exported that would otherwise have been credited as crop fertilizer was balanced with corresponding increases in the import of agricultural P fertilizer. The fourth scenario simulated reduced P output from the watershed to Lake Mendota by implementing riparian buffers along all waterways within the watershed, as outlined by Diebel and others (Diebel et al. 2009). The following assumptions for the scenario were made (M. Diebel, Center for Limnology, University of Wisconsin-Madison, pers. comm.): buffers in this scenario only affected agricultural runoff (70% of P load); 45% of the agricultural P load was delivered in winter (Dec through April) and 55% in the remaining months; of the winter P load, 75% was dissolved and of this, 90% passed through buffers; approximately half of the particulate P was retained by buffers during winter; of the summer P load, 25% is dissolved and half of the dissolved fraction passed through buffers; and the remaining 75% of summer P load was particulate and of this, 90% was retained by buffers.

2.4 Results

Assuming compliance with local ordinances, nutrient management plans, and best management practices, we estimated the 2007 inputs of P to the Lake Mendota watershed within a range of 275,000 kg P/yr to 1,130,000 kg P/yr, with a most likely estimate of 854,000 kg P/yr (Table 2.2). Fertilizer for corn accounted for the largest input of P (41%), with feed supplements for cattle (16%) and fertilizer for soybeans (12%) as the second and third largest inputs. Dry and wet deposition contributed to approximately 7% of the P inputs, while human-imported P (chemical fertilizer and animal feed supplements) made up 93% of total P inputs to the watershed.

The most likely estimate of P output for 2007 was 574,000 kg P/yr, with minimum and maximum estimates of 555,000 and 613,000, respectively (Table 2.3). Exports of P in corn accounted for 56% of all exports from the watershed, followed by soybeans (15%) and dairy products (12%). Loss of P to Lake Mendota represented 6% of the total output (34,000 kg P/yr). The most likely estimate of imports and exports yielded a calculated accumulation of 279,000 kg P/yr in the Lake Mendota watershed in 2007. The maximum and minimum estimates of net P accumulation are 522,000 and -280,000 kg P/yr, respectively (Table 2.2 and 2.3), where negative values indicates net loss of P from the watershed. The most notable differences between the 1995 and 2007 budgets are the reduction in accumulation of P stored in the soil and overall P inputs to the watershed. Phosphorus accumulation in soils was reduced by 52% from 1995 to 2007, while inputs to soil were reduced by 35%. Over 12 years, outputs from the watershed decreased by 27%, primarily due to reduced corn export.

Net results of implementing P control at various points in the watershed are summarized in figure 2. Under Scenario 1, assuming application of agricultural and urban chemical P fertilizer was eliminated, total P inputs would be reduced to 255,000 kg P/yr, a 75% decrease from estimated 2007 inputs. Assuming export was maintained at current levels, this scenario decreased stored P by 214%, from 279,000 kg P/yr accumulation in the watershed to 319,000 kg P/yr depletion. Eliminating inputs to the watershed as agricultural P feed supplements in Scenario 2 reduced inputs by 21%, from 854,000 kg P/yr to 671,000 kg P/yr. Assuming outputs remain unchanged, this scenario reduced accumulation from 279,000 kg P/yr to 96,500 kg P/yr. Implementation of manure digesters, Scenario 3, increased both input and output of P from the watershed. Digesters increased input to 919,000 kg P/yr and output to 763,000 kg P/yr. The net result was reduced P accumulation in the watershed to 155,000 kg P/yr, a 44% decrease in

accumulation from the 2007 budget. Scenario 4, implementation of riparian buffers, reduced the P load to Lake Mendota by 76%, to 8070 kg P/yr. This scenario did not affect any other inputs or outputs and had the net effect of reducing the P exported from the watershed by about 5% to 548,000 kg P/yr. Annual accumulation of P within watershed soil was increased in this scenario by 29%, to 360,000 kg P/yr.

2.5 Discussion

2.5.1 Nutrient Management in the Lake Mendota Watershed

Implementation of the Lake Mendota Priority Watershed Project (PWP), an effort to control and reduce non-point sources of pollution to the lake by 50% (Betz et al. 2002), played a large role in the reduced estimates of urban and agricultural fertilizer use for 2007. Comparison of the 1995 and 2007 'best case' budgets revealed a 37% reduction in agricultural fertilizer application attributed to more stringent nutrient management by farmers, according to reports by area experts. The PWP's ten-year implementation period began in 1998 and included changes to agricultural as well as urban nutrient management practices that affect water quality. Cropland was the target of changes in nutrient and water management and erosion control. The mid-term results of the project indicate that between 1998 and 2000 the majority of rural landowners had committed to implementing best management practices (Betz et al. 2002). Implementation of the PWP and the use of nutrient management plans on farms have reduced P fertilizer application and established rules regarding manure crediting. These changes are thought to have caused a decrease in P fertilizer use on agricultural land. This inference is supported by statistics on P fertilizer purchases adjusted for price and farm area, which indicated an 11% reduction in

purchase of agricultural fertilizer in the watershed area between 1992 and 2007 (DATCP 2009). Nonetheless, the lack of direct data on P fertilizer application in the watershed or county scale leaves this component of the budget uncertain. If the actual reductions in P applications were smaller than believed by our sources of information, then the 2007 budget would be more similar to the 1995 budget.

A further debit in P inputs derives from the 41% reduction in imported feed supplements since 1995, even though animal numbers in the watershed have remained the same (USDA-NASS 2009a). Since 1995, farmers have been advised that supplements purchased for their protein or energy value contain varying amounts of phosphorus, sometimes in excess of an animal's physiological needs (Satter et al. 2005). This information may have caused farmers to purchase supplements that balance animal protein and energy needs with phosphorus levels in the diet (J.M. Powell, US Dairy Forage Research Center, University of Wisconsin, personal communication).

Finally, the Urban Phosphorus Ban enacted in Dane County in 2005 (Dane County Code of Ordinances Chapter 80) prompted our estimate of an 82% reduction of urban P fertilizer use from 1995 rates. The ordinance prohibits the use of P fertilizer on established lawns, golf courses, and other turf in the county; exceptions are granted when soil tests indicate limiting levels of soil P, though application for such exceptions in the county are rare (D. Soldat, Soil Science Extension, University of Wisconsin, personal communication).

2.5.2 Nutrient Management Scenarios

The nutrient management scenarios we presented act by two mechanisms: prevention of P from entering the watershed using legislation and collection/retention of P within the

watershed (Figure 2.2). Nutrient management scenarios 1 and 2 require management of P imports for agriculture. More stringent regulation of agricultural chemical P application would reduce the overall 2007 P inputs by as much as 61%, as estimated in Scenario 1. Soil P data (Peters 2010; Lathrop 2009) and UW Extension fertilizer recommendations (Laboski et al. 2006) indicate presence of ample P concentration in the majority of urban and agricultural soils in the watershed for growing turf and regional crops. A reduction in P application would likely not harm farmers' economic success, but rather enhance the profitability (Valentin et al. 2004) and promote conservation of this non-renewable resource (Cordell et al. 2009). Similarly, in Scenario 2, elimination of P mineral feed supplements would likely have little effect on the productivity of dairy cattle in southeast Wisconsin (Satter and Wu 1999), but the downstream effects on water quality in Lake Mendota could be potentially improved by measures banning chemical P supplements to mature dairy cows. Reduction in mineral P supplements would decrease manure P, thereby reducing the quantity of potentially unnecessary land-applied P-rich manures under this scenario.

Scenarios 3 and 4 use infrastructure to collect and/or retain P within the watershed. Diversion of manure to anaerobic digesters as described in Scenario 3 could eventually contribute to improved water quality by decreasing P soil accumulation and export to surface water during precipitation events, thereby mitigating eutrophication due to external P loading (Figure 2.2). Currently, uncollected manure accounts for significant P inputs to surface water during rain events (J.M. Powell, US Dairy Forage Research Center, University of Wisconsin, pers. comm.), though the magnitude of the loading is not well quantified and we do not account for the direct effect of reduced export to surface water in this scenario. Scenario 3 would provide incentives to farmers to collect manure, rather than applying it to land, reducing additional

accumulation of soil P (Figure 2.2). This scenario could also provide methane gas production for electrical generation or other use and would generate products including liquid fertilizer and bedding derived from manure solids. Implementation of riparian buffers, as described in Scenario 4, would directly reduce the P load to Lake Mendota and could thereby reduce the occurrence of nuisance algal blooms. This reduction would have immediate implications for the recreational services provided by the lake as well as enhancing flood control and soil retention. The scenario has little effect on the P budget of the watershed, however, since its sole purpose is to increase P retention within the terrestrial landscape. Whereas buffers may have the greatest immediate benefit to the lake, management actions such as those explored in the other scenarios will be of long-term benefit as P is reduced in soils that may eventually be eroded due to conversion of agricultural land to other uses.

2.5.3 Uncertainty

The 2007 budget was informed by changes in regional nutrient management policies, information from local agricultural experts, current animal census, and crop export data. Particularly for P inputs from fertilizer and feed supplements, a large plausible range exists, representing uncertainty in the importation and use of P in agriculture. Bennett et al (1999) also found a similarly large range of potential rates, but their estimates were, on average, much higher than those made here. The 'best case' scenario for the 2007 budget indicates that P is still accumulating, but more slowly than in 1995.

County-level soil P data were used by Bennett et al. (1999) to corroborate their results; we also used soil P data to estimate net change of P in soil for comparison against findings from the budget presented here (Figure 2.3, data derived from the University of Wisconsin-Madison

Soil and Plant Analysis Lab 2011). Assuming total soil mass in the watershed of 4.67×10^{11} kg (after Bennett et al. 1999), annual rates of change in P storage can be estimated from soil P concentration. Net changes in soil P estimated in this manner suggest net loss of ~ 467,000 kgP/yr from the watershed between 2004-2009, whereas the 'best case' mass balance presented here indicates a 280,000 kgP/yr accumulation. This discrepancy is within the range of uncertainties in both the budget and county soil P datasets. Our estimated range of plausible inputs was large compared to magnitude of output and net change, approximately 1,000,000 kgP/yr (Table 2.2 and 2.3). Likewise, soil P data should be interpreted with caution, as soil P is heterogeneous. A spatially explicit assessment of soil P variability in Dane County revealed a 99% confidence interval for soil P concentration ranging more than a thousand-fold (~1-1000 mgP/kg soil, Bennett et al. 2005). Thus, the difference in estimates from the mass-balance budget and county soil P data is not unexpected, given the variance in soil P and the potential range of P inputs to the soil.

The modest changes and high variability in soil P are consistent with the high inter-annual variation and lack of trend in annual P inputs to Lake Mendota (Carpenter and Lathrop 2008). The lack of trend in input to the lake may be related to the long residence time of P in watershed soil. Because of this long residence time, P inputs to soil must be decreased for a long time in order to shift inputs to the lake (Carpenter 2005). Therefore, interventions that decrease erosion and retard P flow to the lake, such as vegetated buffers, have an important role in water quality management, especially while soil P levels remain elevated (Carpenter et al. 1998).

2.6 Conclusions

Lake Mendota exemplifies the many agricultural watersheds that have unbalanced nutrient budgets (MacDonald et al. 2011; Vitousek et al. 2009). In developed countries, the imbalance is generally in the direction of over-application of fertilizers, as has occurred in the Lake Mendota watershed. Meanwhile, in under-developed countries, P fertilizer is more expensive and less available to farmers, leading to P-deficient agricultural soils in regions with fewer resources and high population growth (Cordell et al. 2009). Watershed nutrient budgets are needed to mitigate excessive P inputs to P-rich watersheds, and allocate fertilizers to regions where agricultural production is most impaired by low nutrient availability (MacDonald et al. 2011). Yet very few countries collect nutrient balance data, and globally, water quality management is hampered by lack of information on terrestrial nutrient balances (Vitousek et al. 2009). Our study has shown how this data gap can be filled. Clearly, a great deal more work is needed to establish regional, continental and global views of agricultural nutrient imbalance and its consequences for water quality.

2.7 Acknowledgments

We thank Monica Turner, Jake Vander Zanden, Jim Lorman, Chris Kucharik, Dave Lewis, Bill Provencher, the participants in the UW-Madison Ecosystems Services course for thoughtful feedback on the paper. We thank them and Pete Nowak, J. Mark Powell, Dick Lathrop, Lauri Lambert, and Doug Soldat for their helpful discussion and direction.

2.8 References

Bannerman RT, Owens DW, Dodds RB, Hornewer NJ (1993) Sources of Pollutants in Wisconsin Stormwater. Water Science and Technology 28 (3-5):241-259

Bennett EM, Carpenter SR, Clayton MK (2005) Soil phosphorus variability: scale-dependence in an urbanizing agricultural landscape. Landscape Ecology 20 (4):389-400. doi:10.1007/s10980-004-3158-7

Bennett EM, Reed-Andersen T, Houser JN, Gabriel JR, Carpenter SR (1999) A phosphorus budget for the Lake Mendota watershed. Ecosystems 2 (1):69-75

Betz C, Jopke P, Connors K, Lathrop R (2002) Mid-term results of the Lake Mendota priority watershed project. http://wwwsoilswiscedu/extension/FAPM/2002proceedings/Betz-Conf-2002pdf

Brock TD (1985) A Eutrophic Lake, Lake Mendota, WI. Ecological Studies: Analysis and Synthesis, vol 55, 1st edn. Springer-Verlag, New York

Carpenter SR (2005) Eutrophication of aquatic ecosystems: Bistability and soil phosphorus. Proceedings of the National Academy of Sciences of the United States of America 102 (29):10002-10005. doi:10.1073/pnas.0503959102

Carpenter SR (2008) Phosphorus control is critical to mitigating eutrophication. Proceedings of the National Academy of Sciences of the United States of America 105 (32):11039-11040. doi:Doi 10.1073/Pnas.0806112105

Carpenter SR, Bennett EM (2011) Reconsideration of the planetary boundary for phosphorus. Environmental Research Letters 6 (1):014009

Carpenter SR, Caraco NF, Correll DL, Howarth RW, Sharpley AN, Smith VH (1998) Nonpoint pollution of surface waters with phosphorus and nitrogen. Ecological Applications 8 (3):559-568

Carpenter SR, Lathrop RC (2008) Probabilistic estimate of a threshold for eutrophication. Ecosystems 11 (4):601-613. doi:Doi 10.1007/S10021-008-9145-0

Cordell D, Drangert J-O, White S (2009) The story of phosphorus: Global food security and food for thought. Global Environmental Change 19 (2):292-305

DATCP (2009) Wisconsin Agricultural Statistics-2008. Wisconsin Department of Agriculture, Trade, and Consumer Protection, Madison, WI

Diebel M, Maxted J, Robertson D, Han S, Vander Zanden M (2009) Landscape Planning for Agricultural Nonpoint Source Pollution Reduction III: Assessing Phosphorus and

Sediment Reduction Potential. Environmental Management 43 (1):69-83. doi:Doi 10.1007/S00267-008-9139-X

Kamarainen AM, Yuan HL, Wu CH, Carpenter SR (2009) Estimates of phosphorus entrainment in Lake Mendota: a comparison of one-dimensional and three-dimensional approaches. Limnology and Oceanography-Methods 7:553-567

Kitchell JF (1992) Food web management : a case study of Lake Mendota. Springer series on environmental management. Springer-Verlag.

Laboski A, Peters J, Bundy L (2006) Nutrient application guildelines for field vegetable and fruit crops in Madison, WI. University of Wisconsin-Madison Extension

Lathrop RC (1979) Dane County water quality plan. Madison, WI

Lathrop RC (2007) Perspectives on the eutrophication of the Yahara Lakes. Lake and Reservior Management (23):345-365

Lathrop RC (2009) Controlling eutrophication in the Yahara Lakes: Challenges and opportunities. Presented at Community Environmental Forum, UW Madison Nelson Institute of Environemental Studies

Lathrop RC, Carpenter SR, Robertson DM (1999) Summer water clarity responses to phosphorus, *Daphnia* grazing, and internal mixing in Lake Mendota. Limnology and Oceanography 44 (1):137-146

Lathrop RC, Carpenter SR, Stow CA, Soranno PA, Panuska JC (1998) Phosphorus loading reductions needed to control blue-green algal blooms in Lake Mendota. Canadian Journal of Fisheries and Aquatic Sciences 55 (5):1169-1178

Lorimor J, Powers W, Sutton A (2000) Manure Characteristics. Iowa State University MidWest Plan Service

MacDonald GK, Bennett EM, Potter PA, Ramankutty N Agronomic phosphorus imbalances across the world's croplands. Proceedings of the National Academy of Sciences. doi:10.1073/pnas.1010808108

MacDonald GK, Bennett EM, Potter PA, Ramankutty N (2011) Agronomic phosphorus imbalances across the world's croplands. Proceedings of the National Academy of Sciences 108 (7):3086-3091. doi:10.1073/pnas.1010808108

Peters J (2010) Wisconsin Soil Test Summary: 2005-2009. New Horizons in Soil Science 3

Powell JM, Jackson-Smith DB, Satter LD (2002) Phosphorus feeding and manure nutrient recycling on Wisconsin dairy farms. Nutrient Cycling in Agroecosystems 62 (3):277-286

Powell JM, McCrory DF, Jackson-Smith DB, Saam H (2005) Manure collection and distribution on Wisconsin dairy farms. Journal of Environmental Quality 34 (6):2036-2044. doi:Doi 10.2134/Jeq2004.0478

Satter L, Wu Z (1999) Phosphorus requirements in dairy cattle. In Maryland Nutrition Conference, Baltimore, MD

Satter LD, Klopfenstein T, Erickson G, Powell JM (2005) Phosphorus and dairy-beef nutrition. Phosphorus, Agriculture, and the Environment. ASA-CSSA-SSSA Monograph N. 46. American Society for Agronomists, Madison, WI

Schindler DW (1977) Evolution of Phosphorus Limitation in Lakes. Science 195 (4275):260-262

Schindler DW, Hecky RE, Findlay DL, Stainton MP, Parker BR, Paterson MJ, Beaty KG, Lyng M, Kasian SEM (2008) Eutrophication of lakes cannot be controlled by reducing nitrogen input: Results of a 37-year whole-ecosystem experiment. Proceedings of the National Academy of Sciences of the United States of America 105 (32):11254-11258. doi:Doi 10.1073/Pnas.0805108105

Smith VH, Joye SB, Howarth RW (2006) Eutrophication of freshwater and marine ecosystems. Limnology and Oceanography 51 (1):351-355

Soldat DJ, Petrovic AM (2008) The Fate and Transport of Phosphorus in Turfgrass Ecosystems. Crop Science 48 (6):2051-2065. doi:Doi 10.2135/Cropsci2008.03.0134

Soranno PA, Carpenter SR, Lathrop RC (1997) Internal phosphorus loading in Lake Mendota: response to external loads and weather. Canadian Journal of Fisheries and Aquatic Sciences 54 (8):1883-1893

Strand Associates (2009) Community manure management facilities planCommunity manure management facilities plan. Dane County Office of Lakes and Watersheds and Lakes and Watershed Commission.

State of Wisconsin Annual Soil Test Summary Report (2011) http://uwlab.soils.wisc.edu/madison. Accessed 25 May 2011

USDA-AMS (2000) United States standards, grades, and weight classes for shell eggs. United States Department of Agriculture Agricultural Marketing Service, Washington, DC

USDA-NASS (2009a) Census of Agriculture 2007. vol 1. United States Department of Agriculture National Agricultural Statistics Service, Washington, DC

USDA-NASS (2009b) Quick Stats Wisconsin County Data. United States Department of Agriculture National Agricultural Statistics Service, Washington, DC

Valentin L, Bernardo DJ, Kastens TL (2004) Testing the empirical relationship between best management practice adoption and farm profitability. Review of Agricultural Economics 26 (4):489-504. doi:Doi 10.1111/J.1467-9353.2004.00195.X

Vitousek PM, Naylor R, Crews T, David MB, Drinkwater LE, Holland E, Johnes PJ, Katzenberger J, Martinelli LA, Matson PA, Nziguheba G, Ojima D, Palm CA, Robertson GP, Sanchez PA, Townsend AR, Zhang FS (2009) Nutrient Imbalances in Agricultural Development. Science 324 (5934):1519-1520. doi:10.1126/science.1170261

Vollenweider A (1976) Advances in defining critical loading levels for phosphorus in lake eutrophication. Memorie dell'Istiuto italiano di Idrobiologia 33:53

2.9 Tables

Table 2.1 Sources of data used to calculate the 2007 phosphorus budget for the Lake Mendota watershed.

Component	*Subcomponent*	*Source*
INPUTS		
Fertilizer for agricultural crops	Amount of land planted in each crop	USDA-NASS 2009a
	Recommendations for fertilizer application rates by crop and soil P concentration.	Laboski et al. 2006
	Dane County Soil P Concentrations	Bennett et al. 1999
Feed supplements for dairy cattle	Average feed consumed per cow per day in South Central WI	Powell et al. 2002
	Percent of P in feed that is homegrown versus imported	Powell et al. 2002
	Number of cattle in Dane County	USDA-NASS 2009a
	Herd structure of cattle South Central WI	Powell et al. 2002
Fertilizer for urban lawn	Urban land area in the watershed	Bennett et al. 1999
	Percent of urban area that is lawn	Bannerman et al. 1993
	Recommended fertilization rates	Soldat and Petrovic 2008
Atmospheric Deposition	Dry deposition	Lathrop 1979
	Wet deposition	Lathrop 1979
OUTPUTS		
Crops harvested	Amount of each crop harvested in Dane County	USDA-NASS 2009a
	% P in each crop	Laboski et al. 2006
Animal products	Number of hogs, cattle and calves sold in Dane County	USDA-NASS 2009a
	% P in cattle and hogs	Lorimor et al. 2000
	Milk produced in Dane County, 2007	USDA-NASS 2009b
	Number of Layers in Dane County, 2007	USDA-NASS 2009a
	Eggs per layer per year, Wisconsin, 2007	USDA-NASS 2009b
	Mass of eggs	USDA-AMS 2000
	% P in milk and eggs	Lorimor et al. 2000
Hydrologic export to Lake Mendota	Hydrologic export to Lake Mendota	Lathrop et al. 1998

Table 2.2 Estimates of phosphorus inputs to the Lake Mendota Watershed. Minimum and maximum values represent the range of plausible values.

INPUTS (kg P/yr)	Minimum	Most Likely	Maximum
Dry deposition	43,000	43,000	43,000
Wet deposition	18,000	18,000	18,000
Biosolids	53,400	53,400	53,400
Feed supplements	79,000	141,000	203,000
Fertilizer for urban lawn	0	15,500	33,000
Fertilizer for corn	81,600	346,000	409,000
Fertilizer for soybeans	0	121,000	147,000
Fertilizer for oats	0	1,420	2,300
Fertilizer for wheat	0	12,700	17,100
Fertilizer for barley	0	151	224
Fertilizer for forage crops	0	101,000	206,000
Fertilizer for peas and beans	0	291	516
Fertilizer for tobacco	0	290	535
Sum	275,000	854,000	1,130,00

Table 2.3 Estimates of phosphorus outputs from the Lake Mendota watershed.

OUTPUTS (kg P/yr)	**Minimum**	**Most Likely**	**Maximum**
Dairy products	70,900	70,900	70,900
Eggs	397	397	397
Cattle	45,400	45,400	45,400
Hogs and pigs	0	0	5,640
Corn	320,000	320,000	320,000
Soybeans	86,700	86,700	86,700
Oats	1,750	1,750	1,750
Wheat	14,000	14,000	14,000
Barley	81	81	81
Forage	0	0	0
Peas and Beans	530	530	530
Tobacco	600	600	600
Export to ME	15,000	34,000	67,000
Sum	562,000	576,000	598,000

2.10 Figures

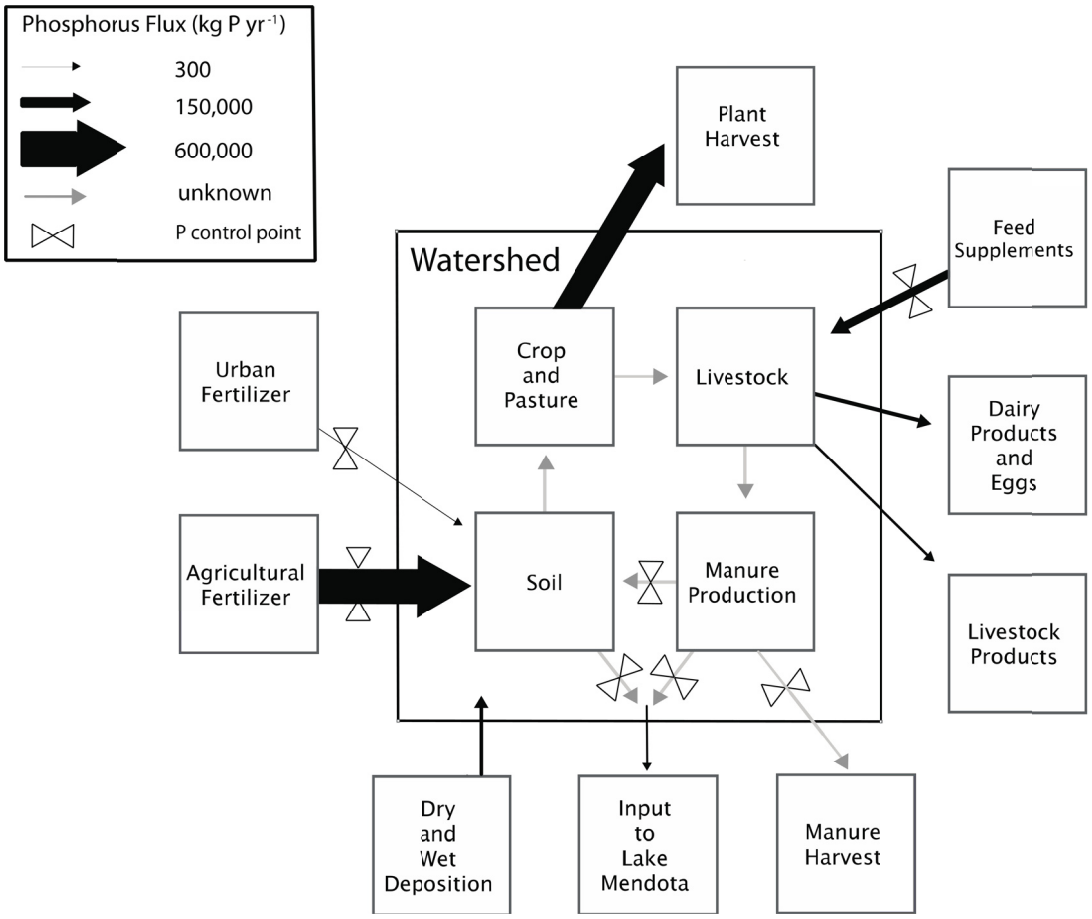

Figure 2.1 Conceptual diagram for the 2007 Mendota watershed P budget. Inputs and outputs are represented by arrows whose width corresponds to the magnitude of the flux; boxes represent sources, sinks, or pools of P. Bowties represent control points identified in management scenarios. Agricultural fertilizer and plant harvest represent the largest input and output, respectively.

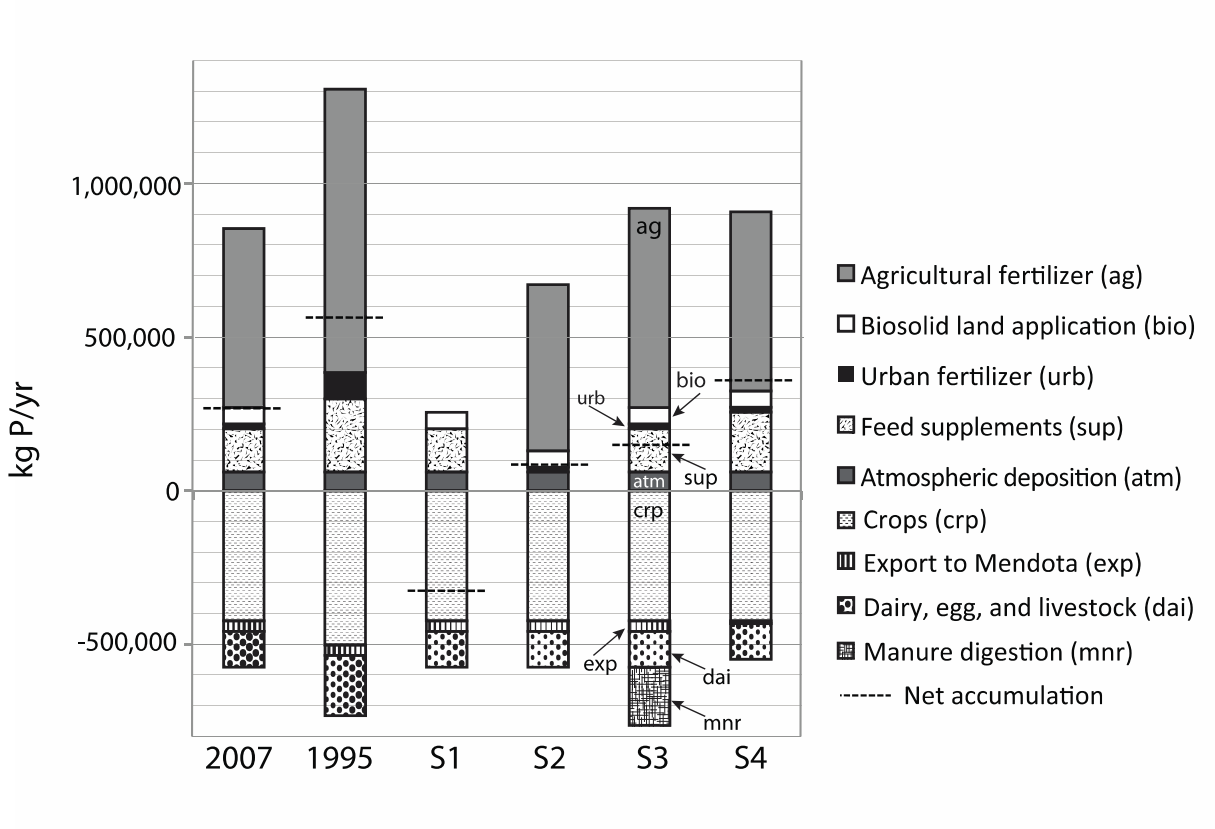

Figure 2.2 Summary of budgets. 2007 and 1995 represent the budget presented here and by Bennett et al (1999), respectively. Scenarios are represented by S1-S4. Dashed line indicates net watershed phosphorus accumulation. S1 results in largest net negative accumulation of P from watershed soil.

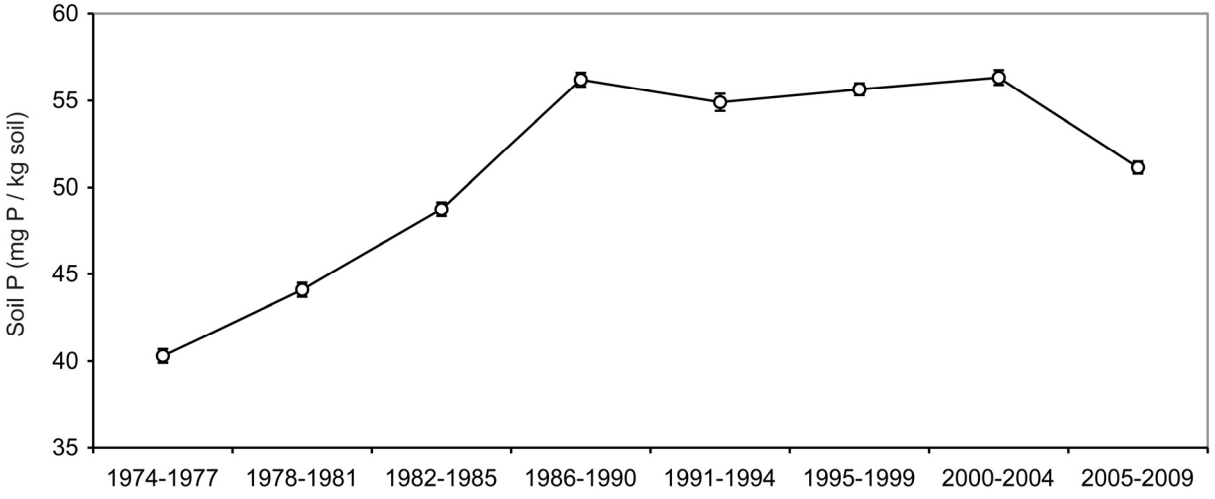

Figure 2.3 Dane County soil P test (mg P/kg soil) levels for 35 years from the State of Wisconsin Annual Soil Test Summary Report (University of Wisconsin-Madison Soil and Plant Analysis Database 2011). Error bars represent 95% confidence intervals.

2.11 Appendix

This appendix was created as a detailed record of how the phosphorus budget for the Lake Mendota, WI watershed was derived. It is also a record of the numerous assumptions that we made in converting numbers available to us from various sources to watershed scale P imports and exports.

2.11.1 Converting county values to watershed values

In order to convert values for agricultural components of the budget which were only available to us at the county scale to the watershed scale, we divided the values by the area of agricultural land in the county to normalize to agricultural area. We then multiplied this by the agricultural area within the watershed which includes a small proportion of land in neighboring Columbia County. We assumed that agricultural practices in the Columbia County portion of the watershed were adequately represented by Dane County data.

e.g. $$\frac{DaneCty\ Cattle}{DaneCty\ AgArea} * Watershed\ AgArea = WatershedCattle$$

where "DaneCty AgArea" was 395,369 acres and "Watershed AgArea" was 80,475 acres based on the 2007 USDA NASS Cropland Data Layer (as cited within the main body of the paper). This resulted in a factor of 0.204 to multiply by Dane County values to obtain watershed scale estimates.

These assumptions differed slightly from the Bennett et al. (1999) approach, which assumed that the distribution of livestock and crops in the watershed was proportional to the distribution in the county. Our approach allowed for the distribution of agricultural land to be

different within the watershed than for the county as a whole. The net effect of this difference is small. If we followed the Bennett et al. convention our factor above would be 0.220 (686 km^2 / 3113 km^2, or watershed area divided by county area).

2.11.2 Calculating exports

2.11.2.1 Dairy Products

Milk production for Dane County was obtained from the USDA-NASS Quick Stats website for 2007. This value was scaled to the watershed as described above and converted to P using the weight-weight conversion of 0.0009 units P per unit milk.

2.11.2.2 Eggs

Our calculated mass of P exported in eggs differed by two orders of magnitude from the Bennett et al. value for 1995 (1999). The number of layers (hens of laying age) in the watershed was available from the USDA Census of Agriculture for 1992, 1997, 2002, and 2007. Of these four years, the 2007 value was the highest. By this metric alone, we would have expected to have higher P exported in eggs in 2007 than 1995, though Dane County Data specifically for 1995 are not available through the USDA NASS online database. The number of layers in Dane County was 63,914 in 1992 and 75,052 in 2007.

We calculated egg P export as follows. The number of layers in Dane County was scaled to the watershed as described above.

The number of eggs per layer per year was estimated for statewide data because county-specific data is not reported for years after 1992. For years 1981 through 1992 where data are available for both the state and county, there was no statistically significant difference between

the mean for state and county numbers, though the year-to-year variance was greater for the county than the state. We used the mean value for the state as the most-likely estimate for eggs per layer per year (278). We bounded this mean value with a minimum, which was the historical low value for Dane County (215) and a maximum, which was the most likely value, plus approximately half of the historic range of the Dane County values in order to account for the increasing trend in egg yield (308).

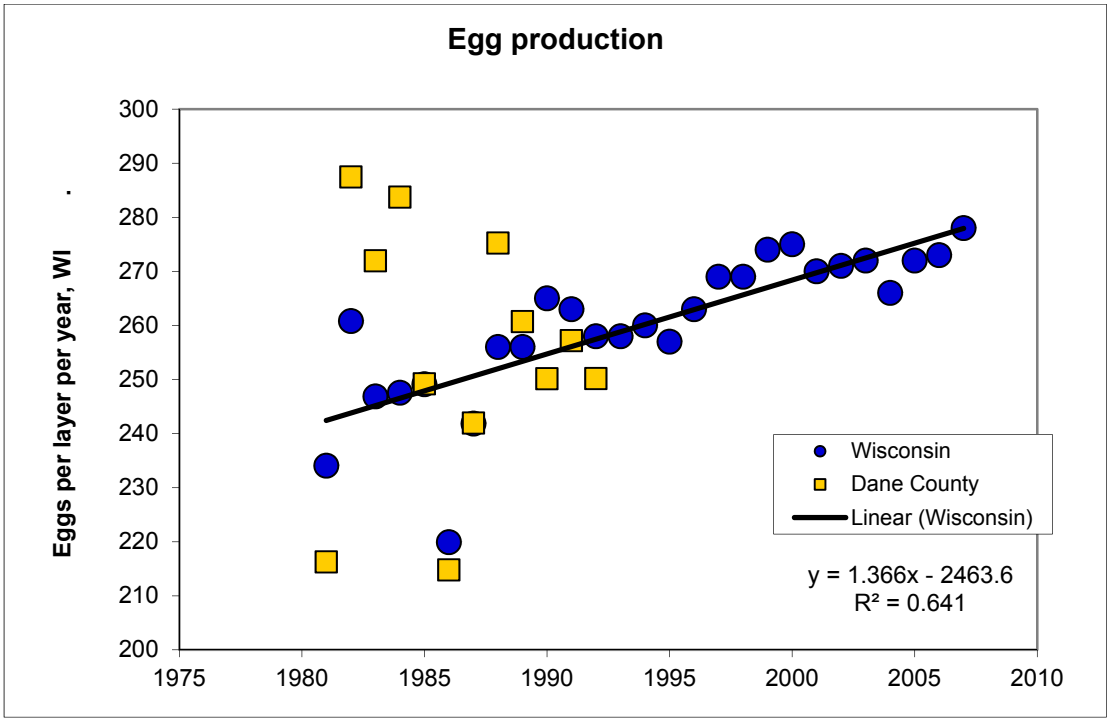

Figure A.1. Egg yield for hens in Dane County and Wisconsin.

To estimate mass of each egg, we bounded the calculation assuming that all eggs were "medium" in the minimum case, large/extra large in the most likely case, and "jumbo" in the maximum case according to the USDA grading standards for table eggs (USDA-AMS 2000). These corresponded to masses of 50, 60, and 71 grams per egg, respectively.

All eggs were assumed to have 0.0021 grams P per gram of egg (Lorimor et al. 2000).

Thus the minimum P exported in eggs was:

Number of layers * minimum yield * minimum egg size * proportion P, or

(75,052 * 0.204) layers * 215 eggs per layer per year * 0.05 kg per egg * 0.0021 kg P per kg egg = 346 kg P per year.

The maximum value was (75,052 * 0.204) layers * 308 eggs per layer per year * 0.071 kg per egg * 0.0021 kg P per kg egg = 703 kg P per year.

2.11.2.3 Animal export

2.11.2.3.1 Cattle

The number of cattle sold in Dane County was reported in the Census of Agriculture for 2007. This is broken down into categories of calves (<500 lbs) and cattle (>500 lbs).

Calves sold for veal can be sold immediately after birth to be raised in a dedicated veal farm or can be raised on location to full slaughter weight. We bracketed the mass of calves sold using these two extremes, with the mean as the most likely case. In the minimum, we assumed all calves were sold (and exported from the watershed) soon after birth at a weight of 100 lbs. In the maximum, we assumed all calves were raised within the watershed to a veal slaughter weight of 300 lbs.

Cattle (>500 lbs) sold are likely a combination of mature Holstein cows, which are being culled from the herd along with beef cows, and dairy steers. Cattle raised for beef have an average slaughter weight of 1140 lbs (Greiner 2002), while mature Holstein cows in Wisconsin have an average weight of 1500 lbs (Hoffman et al. 1992). We used these two values as minimum and maximum values for cattle export with the mean as the most likely.

For the proportion of P in cattle, we used 0.007 (Lorimor et al. 2000).

2.11.2.3.2 Hogs and pigs

According to communication with area experts, there are no longer any commercial swine operations within the Lake Mendota watershed (P. Nowak, University of Wisconsin-Madison, personal communication). Therefore, our minimum and most likely estimates for Hogs and Pigs export is set at zero. Our maximum estimate is calculated as if the watershed has a proportional share of Dane County's swine population.

The 2007 Census of Agriculture reported the total number of hogs and pigs sold from the county. In 1997 and years prior, this was split between feeder pigs (40-80 lbs) and non-feeder pigs. According to the data available, approximately 30% of the pigs sold in years with these data were feeder pigs. Therefore we estimated that 30% of the pigs sold were on average 60 lbs, while the remaining 70% were an average of 250 lbs.

2.11.2.3 Crop Export

2.11.2.3.1 Corn, wheat, barley, oats, and rye for grain; soybeans (for beans); and tobacco

Total harvest for the crops above was obtained for Dane County from the 2007 Census of Agriculture. These were converted to watershed values as described above. Harvest was

converted from yield units to P mass using conversion factors from Laboski et al. (2006, Table 4.3) for each crop.

2.11.2.3.2 Green peas and snap beans

Peas and beans were a minor component of the budget but were included to be consistent with the 1995 budget of Bennett et al. (1999).

County level harvest data for peas has not been reported since 2003. However acres planted in peas has continued to be reported. We used annual yields and acres planted from 1968 to 2003 to develop a linear model for yield (tons/acre) over that time period. Yield increased linearly from 1968 to 2003 (R^2=0.56). Predicted yield for 2003 was 2.45 tons per acre and as this was the last year data were available for Dane County yields. We did not extrapolate beyond 2003 and instead used the 2003 prediction as a conservative yield prediction for 2007. We did not use the actual 2003 yield as it appeared to be an outlier (see chart below).

Interestingly, there has been a very steady decline in acres planted in peas in Dane County over the 35 year record, from 11,000 acres to approximately 500 acres.

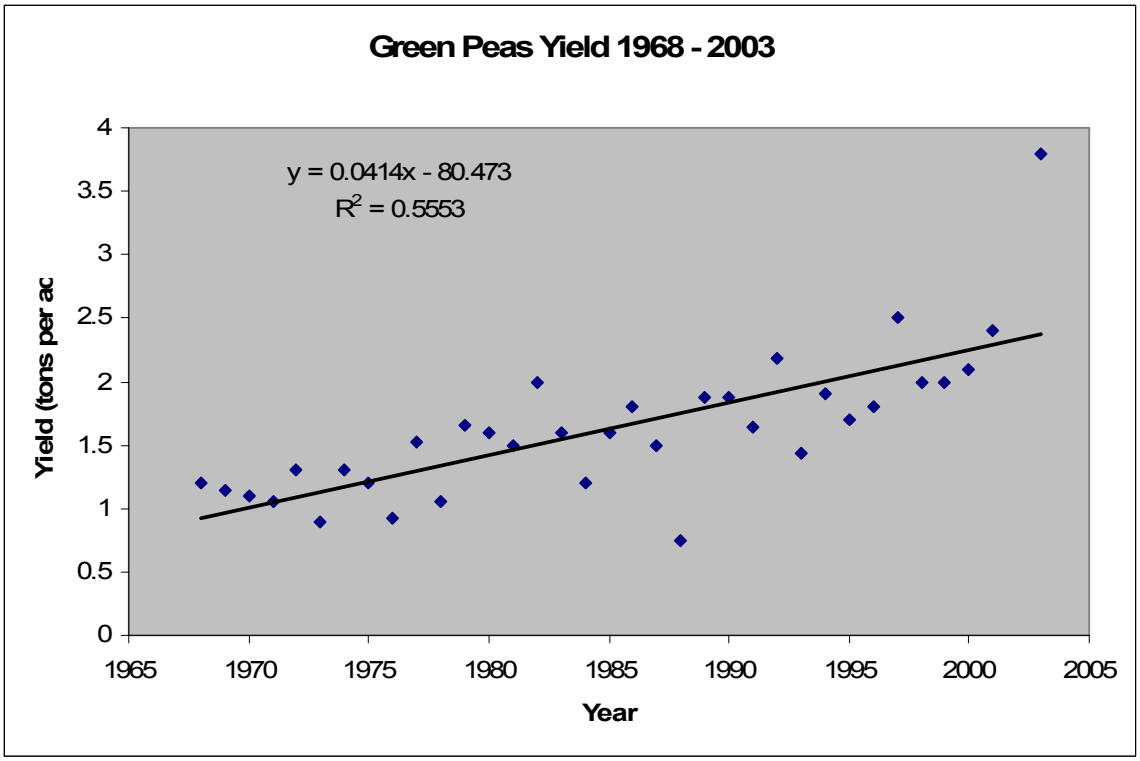

Figure A.2.2 Yield of Green Peas (tons per acre) for Dane County, WI. Data were not reported after 2003.

Similar to green peas, harvest data for snap beans has not been reported for the county level since 2001. Acres planted in beans was reported in the 2007 data, however. We used the linear prediction for 2001 yield as a conservative estimate for 2007 yield as in the case for green peas. For both peas and beans we converted from mass harvested to mass P using conversions found in Laboski et al. (2006).

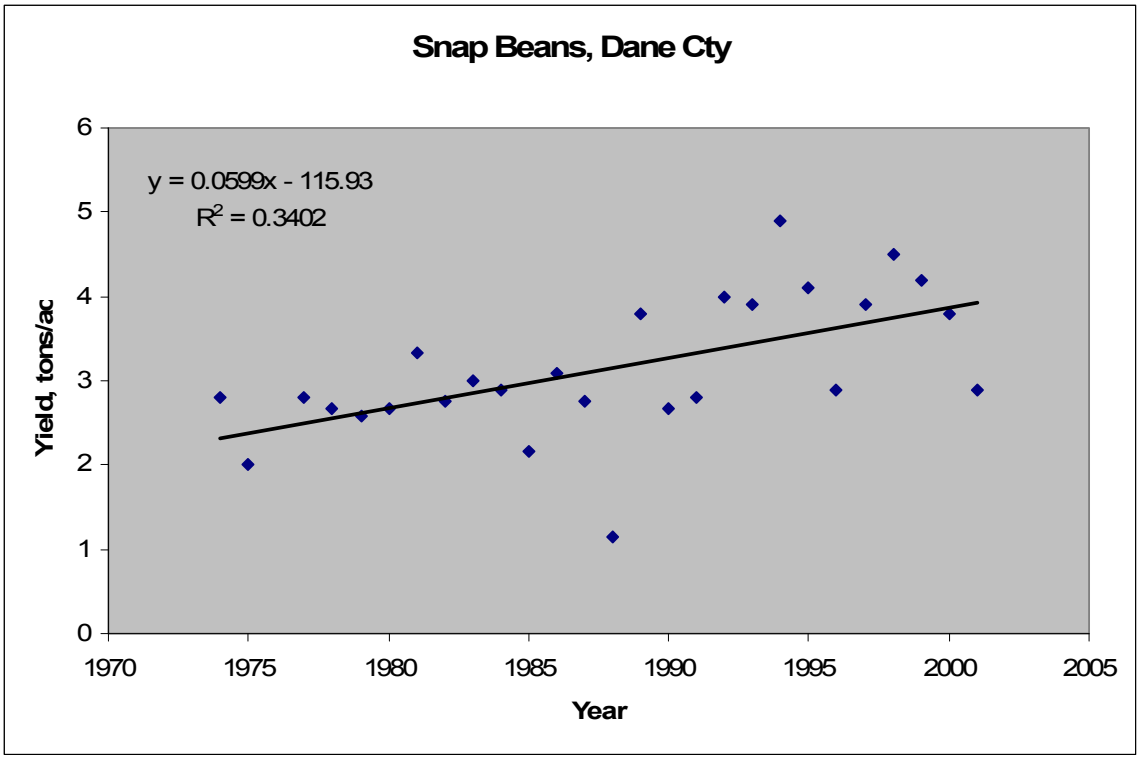

Figure A.2.3 Yield of snap beans (tons per acre) for Dane County, WI. Data were not reported after 2001.

2.11.2.4 Forage Crops

Forage crops were assumed to stay within the watershed as these tend not to be cash crops but rather are grown to support livestock on the farm (J.M. Powell, US Dairy Forage Research Center, University of Wisconsin, pers. comm.). Therefore these were not counted as exports from the watershed.

2.11.2.5 Export to Lake Mendota

Export to Lake Mendota was estimated to be the mean value of the Lake Mendota P load reported in Carpenter and Lathrop (2008). Minimum and maximum values were the 10th and 90th percentiles of the data, respectively.

2.11.3 Calculating Imports

2.11.3.1 Feed Supplements

Feed supplements were calculated based on a study of supplements to South Central Wisconsin dairy farms by J.M. Powell et al. (2002). Powell et al. reported the average mass of food consumed per cow per day, the percentage of that feed that is P, and the proportion of that feed that is from forage vs. mineral supplements. In personal communication with J.M. Powell, he suggested that amount of P supplements fed to cattle has decreased steadily over the last decade for reasons outlined in the main text of our paper (J.M. Powell, US Dairy Forage Research Center, University of Wisconsin, pers. comm.). We bounded our estimates of total feed supplements using a maximum value where all cows in the watershed receive supplements, a minimum where only lactating cows receive supplements, and a most likely value that is an average of the two.

2.11.3.2 Urban fertilizer

Our minimum estimate of urban fertilizer assumed that only lawns low in P were fertilized. To be in compliance with the Dane County P ordinance for lawns (Ord 80), a soil test demonstrating P-deficient soils needs to be conducted in order to legally apply chemical P to lawns. Since the ordinance went into effect, only 200 lawns have been tested in the watershed, and of those only 20% show low P. Thus of the approximately 200,000 lawns in the watershed, only 40 of them (0.02 percent) can legally apply P (D. Soldat, University of Wisconsin Soil Science Extension, personal communication). We therefore used zero as our minimum estimate for urban P fertilizer use. Maximum estimates assumed that 20% of the 200,000 lawns in the watershed were fertilized twice a year which is a baseline recommended rate of application

(Soldat and Petrovic 2008). The most likely estimate was an average of the maximum and minimum estimates.

2.11.3.3 Agricultural fertilizer

The import of chemical P fertilizer is one of the biggest uncertainties of this budget due to the lack of data available publicly at the county or watershed scale.We know that recommended rates of P application have declined and that Nutrient Management Plans in the watershed have made farmers more aware of their P needs and management.

Our estimates of fertilizer imports are based on recommendations for each crop at each of three different soil P test levels from the University of Wisconsin Extension – Nutrient application guidelines for field, vegetable, and fruit crops in Wisconsin (Laboski et al. 2006). On average, Dane county soils fall into the "Excessively High" phosphorus category for which the recommended P application to soils is zero. An exception is reluctantly made in the guidelines for applying starter fertilizer for corn crops even in excessively high phosphorus soils. Our minimum values for P imports thus include zero imports for all crops with the exception of a low rate of starter fertilizer application for corn in the watershed.

Despite the recommendation of zero P fertilizer, we suspected that farmers apply some P fertilizer in hopes that it will provide a "bumper" crop (P. Nowak, University of Wisconsin-Madison, personal communication). Therefore our "most-likely" values for fertilizer application used the recommendations for "high" soil P instead of "excessively high" soil P. In the maximum case, we used recommendations for the "optimal" soil test P category which allows for P to be applied at approximately the same rate as it is removed in crops.

In all cases, the amount of chemical P imported was reduced by the amount of manure P in the watershed available to be spread and credited. For the crediting, we assumed 64% of the manure was able to be collected and that, 60% of the manure P was plant-available and therefore credited.

2.11.4 Manure production in the watershed

The 2007 Census of Agriculture categorized cattle and cows into 3 categories: beef cows, milk cows, and other cattle. The "other cattle" category included heifers (cows which have not yet calved), and all male cattle (beef steers, dairy steers, bulls, and calves). In order to use these data with the Midwest Plan Service manure P production rates, we needed to further divide these categories to match the MPS categories as follows.

Previous years of the agricultural census further divided the "other cattle" category between heifers and male cattle and we used these data to determine the proportion of this category which were heifers (54%) versus male cattle (46%).

Cattle categorized as "milk cows" were further divided between lactating (84%) and dry (16%) cows based upon the ratio found for south central Wisconsin dairy farms by Powell and others (2002). All cows in these two categories were assumed to be full grown, mature Holstein cows (1500 lbs).

Cattle in the "beef cows" category were all assumed to be full grown and were assumed to be the average size for mature beef cows (1139 lbs, Greiner 2002).

Cattle in the heifers category were divided between "young" and "mature" groups using mean data from south central Wisconsin herds (Powell et al, 2002). "Young" heifers are between 0 and 7 months old and account for 42% of heifers. "Mature" heifers are older than 7

months but not yet 24 months and account for 58% of heifers. We used a linear age-weight relationship (Hoffman 2006) and assumed a uniform distribution of ages within each of these two categories to determine the mean size of heifers in each.

Male cattle (beef and dairy) are primarily used for veal and beef production with a very small number kept as bulls. We assumed all cattle in this category were steers and raised until age 13 months at which point they are exported from the watershed. Within this category, we assumed a uniform age distribution such that the mean age was 6.5 months. This was potentially a high estimate as it assumes all males are raised to full size. More likely, because this is a predominately dairy watershed, a significant portion of these would be veal calves and the mean age would be much lower.

Manure production rates (lbs maure/lbs animal), as well as P concentrations in manure, were obtained from Lorimor et al (2000) for heifers, lactacting cows, dry cows, beef cows, and beef steers. We multiplied these rates by the numbers and mean size of cattle in each of these categories to estimate the total amount of manure produced in the watershed.We bounded our estimates for cattle by +/- 30% (Lorimor et al. 2000).

Chicken manure was estimated for layers and broilers using manure P production data from Lorimor et al. (2000).

Hog manure was set to zero for our minimum and most likely values for the same reasons as hog and pig export above. The maximum value assumed hogs in the watershed are proportional to the county as a whole. However we did not have age/size structure data for hogs and pigs. Here we assume the average hog is 150 lbs, half-way to market weight, and used the Lorimor (2000) values for manure P production.

Table A2.1 Estimates of manure production within the watershed. Scenario 3 manure digesters increase in output includes several loss terms related to collection and separation, which are described in the Methods of the main text.

	Minimum	Most likely	Maximum
Cattle manure P	308,120	440,170	572,220
Chicken manure P	3,180	3,180	3,180
Hog manure P	0	0	35,620
Total manure P	311,300	443,350	611,020

2.11.5 Uncertainty in estimates

More uncertainty was associated with P inputs compared to outputs in the watershed. Uncertainties arose when estimating P fertilizer applied to agricultural soil because comprehensive and accurate fertilizer application and manure spreading rates in the watershed are not compiled or available publicly. Uncertainties in estimates of P fertilizer application to urban lawns also existed due to lack of reported fertilizer application rates on residential, commercial and industrial lawns. Estimates of animal feed supplements also introduced uncertainties in terms the quantity of supplements and to which types of cows the farmers are giving supplements to. Because of this lack of concrete data, we were forced to estimate based on recommended rates of fertilizer and feed supplement use combined with personal accounts and publications of scientists who investigate those areas.

Uncertainty in estimates also arises in converting county data to watershed data. This analysis assumes that agricultural practices are distributed uniformly across the agricultural land of the county. However, we have heard anecdotal evidence that the north-east part of the county may have more dairy operations, while the south west half of the county is more dominated by cash-grain operations (R. Lathrop, Wisconsin Department of Natural Resources, personal

communication). If this is indeed the case, we may be overestimating agricultural fertilizer use while underestimating feed supplements, manure production, export of milk and cattle, etc.

Fewer uncertainties in outputs existed because production data and P content for crops are readily available in public databases. Uncertainties in outputs arose in estimates of P in livestock export because this is dependent on the size and type of animal exported. We attempted to capture the range of variability by examining exports at plausible extremes of animal sizes.

Nutrient management at the watershed scale would be greatly aided by aggregation of data at that scale rather than at political, county or state boundaries.

2.11.6 References not included in main text

Greiner, S.P. 2002. Beef cattle breeds and biological types. Virginia Cooperative Extension Publication 400-803.

Hoffman, P.C. 2006. Strategies to reduce growth variance and improve feed efficiency in dairy heifer management. Milk Production Reference Library. www.MilkProduction.com

Hoffman, P. C., D.A. Funk, and T.D. Syverud. 1992. Growth rates of Holstein replacement heifers in selected Wisconsin dairy herds. College of Agriculture and Life Sciences Research Report. R551. University of Wisconsin-Madison.

Chapter 3 - Time-scale dependence in numerical simulations: Assessment of physical, chemical, and biological predictions in a stratified lake at temporal scales of hours to months

Emily L. Kara, Paul Hanson, David Hamilton, Matthew R. Hipsey,
Katherine D. McMahon, Jordan Read, Luke Winslow, John Dedrick,
Kevin Rose, Cayelan C. Carey, Stefan Bertilsson, David da Motta Marques,
Lucas Beversdorf, Todd Miller, Chin Wu, Yi-Fang Hsieh, Evelyn Gaiser, and Tim Kratz

(Published in Environmental Modelling and Software (2012) 35:104-121)

3.1 Abstract

We evaluated the predictive ability of a one-dimensional coupled hydrodynamic-biogeochemical model across multiple temporal scales using wavelet analysis and traditional goodness-of-fit metrics. High-frequency in situ automated sensor data and long-term manual observational data from Lake Mendota, Wisconsin, USA, were used to parameterize, calibrate, and evaluate model predictions. We focused specifically on short-term predictions of temperature, dissolved oxygen, and phytoplankton biomass over one season. Traditional goodness-of-fit metrics indicated more accurate prediction of physics than chemical or biological variables in the time domain. This was confirmed by wavelet analysis in both the time and frequency domains. For temperature, predicted and observed global wavelet spectra were closely related, while observed dissolved oxygen and chlorophyll fluorescence spectral characteristics were not reproduced by the model for key time scales, indicating that processes not modelled may be important drivers of the observed signal. Although the magnitude and timing of physical and biological changes can be simulated adequately at the seasonal time scale through calibration, time scale-specific dynamics, for example short-term cycles, were difficult to reproduce, and were relatively insensitive to the effects of varying parameters. The use of wavelet analysis is novel to aquatic ecosystem modeling, is complementary to traditional

goodness-of-fit metrics, and allows for assessment of variability at specific temporal scales. In this way, the effect of processes operating at distinct temporal scales can be isolated and better understood, both in situ and in silico. Wavelet transforms are particularly well suited for assessment of temporal and spatial heterogeneity when coupled to high-frequency data from automated in situ or remote sensing platforms.

3.2 Introduction

Anthropogenic activity has resulted in a globally pervasive degradation of freshwater ecosystem services, such as the availability and quality of water for consumption, irrigation, and recreation. In lakes with high nutrient loads from surrounding landscapes, eutrophication is one of the leading concerns. Eutrophic lakes are characterized by frequent phytoplankton blooms that affect the aesthetic nature of the lake, and may produce toxins that disrupt food webs and affect humans (Carmichael, 2002; Jonasson et al., 2010). Despite extensive research on phytoplankton dynamics, the frequency and timing of phytoplankton blooms remain elusive to accurate prediction (Arhonditsis and Brett, 2004; Flynn, 2005a).

Numerical simulations are often used to predict the impact of environmental changes, including those imposed by climate, land-use, nutrient loading, and groundwater, on aquatic ecosystems (e.g. Arhonditsis and Brett, 2005a, b; Gal et al., 2009; Markensten et al., 2010; Trolle et al., 2011; Trolle et al., 2008). Typically, models are calibrated to data from routine monitoring programs that sample the environment at fortnightly or monthly intervals, enabling simulations to reproduce seasonal and inter-annual variations. However, ecosystem phenomena relevant to water quality, such as phytoplankton succession and bloom formation, can occur over time scales of hours or days, and models calibrated exclusively to longer time scales may not provide

adequate insight into the causes and consequences of these phenomena (Harris, 1987) as even for the same state variable, different drivers may dominate variability at different timescales (Hanson et al., 2006).

Advection, light, nutrients, and predation are among the drivers of spatial and temporal heterogeneity of phytoplankton populations. Aquatic ecosystem models such as DYRESM-CAEDYM (Gal et al., 2009), ELCOM-CAEDYM (Romero et al., 2004), PROTECH (Elliott et al., 2007), and PCLake (Janse et al., 2010) are designed to represent these processes and predict outcomes on phytoplankton populations, but validation at the lower end of ecologically relevant time and space scales (e.g. hours to days and meters to tens of meters), is frequently limited by the resolution of observed data. Recently, the assessment of modelling accuracy of spatial heterogeneity in phytoplankton has been facilitated by the use of in situ and remote sensing technologies (e.g. Alexander and Imberger, 2009; Fragoso et al., 2008), but similar assessments of variations at short time intervals (e.g., hours to days) are rare, in part due to the cost and effort associated with making high-frequency observations using traditional, manual means. However, high-frequency water quality variables including temperature, dissolved oxygen, and phytoplankton pigment fluorescence data are available for many lakes via sensor networks (Porter et al., 2009). Here, we use both manual and high-frequency data to assess a model intended to capture the critical physical-biogeochemical interactions driving phytoplankton dynamics. We assess model predictions in the time and frequency domains using wavelet analysis; the application of this technique is novel for the assessment of aquatic ecosystem models, and allows exploration of how model setup, structure, and parameterization affect predictions of variability across a range of temporal scales. We demonstrate that the advent of high-frequency automated sensor data from in situ lake observatories presents new opportunities

and challenges for evaluating the predictive abilities of numerical simulations at temporal scales previously impossible.

3.3 Materials and methods

Lake Mendota, Wisconsin (WI) was chosen for this study because of its eutrophic status, extensive historical datasets, frequent manual water quality observations, and in situ sensor observatory. With some notable exceptions, summertime phytoplankton biomass in the lake is dominated by the Cyanobacteria genera *Microcystis* and *Aphanizomenon* (Brock, 1985; Carpenter et al., 2006). We chose to apply the model during this season (late June through late September 2008) because of availability of manual and high-frequency automated observations that could be used for comparative purposes with model simulation output.

The Dynamic Reservoir Simulation Model (DYRESM) was configured for Lake Mendota and coupled to the Computational Aquatic Ecosystem Dynamic Model (CAEDYM). DYRESM simulates the one-dimensional (1D) vertical structure of temperature, density, and salinity in a water body. CAEDYM is a process-based lake ecosystem model that simulates the time-varying distributions of carbon, nitrogen, phosphorus, dissolved oxygen, silica, phytoplankton and zooplankton. DYRESM and CAEDYM have been described elsewhere in detail (Gal et al., 2009; Imberger and Patterson, 1981).

3.3.1 Site description

Lake Mendota is located in Wisconsin, USA (43°06′24″N; 89°25′29″W) and has three main inflows, a single outflow, and a mean residence time of 4.5 years. The surface area is 39 km^2 and the mean and maximum depths are 12 and 25 m, respectively. The 686-km^2 watershed

is dominated by agriculture, which has contributed significantly to the eutrophic status of the lake (Brock, 1985). The onset of eutrophication is considered to have occurred in the mid-1800s (Stewart, 1976) and has been the focus of scientific study for more than a century, starting with the work of Birge and Juday (Birge, 1915; Birge and Juday, 1911; Juday, 1914). Lake Mendota has comprehensive historical datasets and is a site of continuing long-term study (Beckel, 1987; Brock, 1985; Magnuson et al., 2006).

3.3.2 Observed data

Data for model calibration and validation were obtained from the North Temperate Lakes Long Term Ecological Research (NTL LTER) program, the University of Wisconsin Space Science and Engineering Ground-Based Atmospheric Monitoring Instrument Suite Rooftop Instrument Group (SSEC GAMIS RIG, located 1.2 km from south shore of Lake Mendota and ~ 3 km from location of instrumented buoy), the United States Geological Survey (USGS) and an automated, instrumented buoy located near the center of the lake. We utilized these sources and historical publications to derive model forcing data and parameters for the simulations presented here.

Meteorological data at the hourly frequency were used to drive simulations. Wind speed, short-wave radiation, percent cloud cover, air temperature, vapor pressure, and precipitation were acquired from the SSEC GAMIS RIG. Hypsometric data input included area and volume at 1-m elevation intervals (Kamarainen et al., 2009). Volumetric flow rates and water temperature of three major inflows were acquired from USGS stream gage data at daily frequency.

Biweekly manual observations from the NTL LTER were used to prescribe initial conditions and for calibration of the model (NTL-LTER, 2011a, b, c). Data from 1995-2008

were used to assist with setting parameters for sediment nutrient fluxes and water column nitrogen transformations. The dataset included biweekly or monthly measurements of NO_3^--N (NO_3^- hereafter), NH_4^+-N (NH_4^- here after), PO_4^{3-}P (PO_4^{3-} hereafter), dissolved organic carbon (DOC), dissolved inorganic carbon (DIC), total nitrogen (TN), and total phosphorus (TP), at 0, 4, 8, 12, 16, and 20 m depths; temperature, pH, and dissolved oxygen (DO) every meter from 0-20 m; In 2008, weekly measurements of NO_3^-, PO_4^{3-}, TN, TP, DOC, DIC, and solvent-extracted chlorophyll-*a* (chl-*a*) at depths 0.5, 5, 10, 14, and 20 m were made. Depth integrated (0-8 m) samples were preserved biweekly and enumerated for phytoplankton cell counts by species and biovolume, and zooplankton counts by species and length. To align measurements of biomass of phytoplankton and zooplankton species with the partitioning in model simulations, phytoplankton and zooplankton counts were binned into one of four functional groups corresponding to groups of ecological coherence. For each sample, a minimum of 400 natural units per sample were counted and each sample was counted until the standard error of the mean of total cell counts was less than 10%. Phytoplankton biovolume and zooplankton mean lengths were converted to units of carbon concentration (g C m^{-3}) using conversion factors from the literature specific to functional groups (Table 3.1).

Automated high-frequency (min^{-1}) observations of temperature, DO, and chlorophyll fluorescence were made from an instrumented buoy platform at the deepest point in Lake Mendota (Figures 3.1 a, b, c, and 3.2a). A thermistor chain measured water temperature at 0.5 m increments from 0 to 2 m and 1 m increments from 2 to 20 m depths (Apprise Templine, Duluth, MN), which was used to prescribe initial conditions for model simulations and was used to evaluate model performance for water temperature simulations. Dissolved oxygen (D-Opto, Zebra-tech Ltd., Nelson, New Zealand) and fluorescence (Cyclops-7 Chlorophyll Fluorometer,

Turner Designs, Sunnyvale, CA) sensors were positioned at 0.5 m depth. After aggregation from min^{-1} to $hour^{-1}$ frequency to match model output, high-frequency temperature, DO, and chl-*a* fluorescence data were used for comparison against high-frequency model output of temperature, dissolved oxygen, and biomass expressed as chlorophyll-*a*. For chlorophyll fluorescence, the raw voltage output with the fluorometer default auto-gain was used; hereafter we refer to this measure as chl-*a* fluorescence in relative fluorescence units (RFU).

For each inflow, water samples were collected over the hydrograph to generate a total phosphorus (TP)-discharge relationship. Daily TP mass loading for 2008 was calculated using the USGS Graphical Constituent Loading Analysis System (GCLAS, Koltun et al., 2006). Average base-flow TP and dissolved inorganic phosphorus (PO_4^{3-}) concentrations specific to each inflow have been measured previously (Lathrop, 1979). We assumed the difference between TP and PO_4^{3-} concentrations was dominated by particulates (Lean, 1973a, b; Wetzel, 2001), and further specified to be organic in composition. A sensitivity analysis of chemical and biological response to the specific forms of P in hydrologic inflows was performed (e.g. the difference between TP and PO_4^{3-} defined as dissolved P, particulate P, particulate inorganic P, etc), and was found to have little effect on phytoplankton biomass and the chemical variables highlighted in this study, likely due to the small contribution of external TP loading to the in-lake P mass. We also tested the sensitivity of key state variables to both a range of historical P loading and a range of early summer PO_4^{3-} concentrations, and found phytoplankton biomass was very sensitive to in-lake PO_4^{3-} initial conditions, while effects of P external loading was negligible (results not shown). The inflow-specific proportions of PO_4^{3-} to particulate organic P were applied to TP loading estimated by GCLAS.

Nitrogen load data for the year 2008 was not available, thus TN load was estimated by assuming an approximately constant mass ratio of TN:TP in inflows as has been observed historically in inflows to this lake (Lathrop 1979). A range of annual TN load (520,000-1,150,000 kg N yr^{-1}) to Lake Mendota was estimated by Sonzogni and Lee (1974). We assumed the ratio of 2008 TN load to the historical maximum TN load (1,150,000 kg N yr^{-1}) in any single year was proportional to the ratio of 2008 TP load (50,700 kg P yr^{-1}) to the maximum recorded annual TP load since 1976 (1994: 67,000 kg P yr^{-1}; (Lathrop et al., 1999)). Thus, TN load for 2008 was estimated to be 522,000 kg N yr^{-1}. The ratio of total nitrogen, inorganic N (NO_3^- and NH_4^+), and organic N for each inflow have been measured previously (Lathrop, 1979) and we assumed that the same ratio amongst species existed in 2008. Similar to external P loading and in-lake initial conditions, we also tested sensitivity of key state variables to external TN loading and in-lake TN initial conditions and found initial conditions to be much more important for subsequent predictions of phytoplankton biomass and chlorophyll than external TN loading (results not shown).

3.3.3 Model Configuration

We initialized DYRESM-CAEDYM on day 179 of 2008 (June 27 2008) and simulated a 90 d period. Initial conditions for day 0 were based on observed data and exogenous drivers (e.g. prescribed daily meteorology, inflows and outflows) controlled subsequent dynamics. State variables were not reset to observed data at any time during the simulation. Minimum and maximum model vertical layer resolution was 0.5 and 2 m respectively, and the calculation and output time steps were 1 hour.

The CAEDYM model was configured with four functional groups of phytoplankton, four zooplankton groups, and one bacterial functional group. For phytoplankton and zooplankton, functional groups were chosen to represent broader taxonomical groups of the most abundant phytoplankton and zooplankton in Lake Mendota for the modelled season and these also largely correspond to groups of ecological coherence. For phytoplankton functional groups, we included a nitrogen-fixing cyanobacteria genus represented by *Aphanizomenon* sp. (A_{Aph}), a non nitrogen-fixing cyanobacteria genus represented by *Microcystis* sp. (A_{Mic}), chlorophytes and chrysophytes (A_{Chlor}), and diatoms (A_{Diat}). Four zooplankton groups were modelled: predatory zooplankton (e.g. copepods, Z_{Cop}), large zooplankton (e.g. daphnia, Z_{Daph}), small zooplankton (e.g. small cladocerans, Z_{Clad}), and micro-zooplankton (e.g. rotifers, Z_{Rot}). Phytoplankton were configured with fixed internal carbon concentration (*IC*) and fixed carbon to chlorophyll-*a* ratio. One bacterial functional group was activated in the biogeochemical model, configured to assimilate organic C, N, and P and release excess C, N, and P in inorganic forms.

3.3.4 Parameterization

Literature values, estimates from observed data, and user-defined values comprised the chemical and biological parameter set, specific to Lake Mendota, which was adapted for this system based on a parameter set used by Gal et al. (2009). Site-specific parameters were used when possible. When no site-specific parameters were available, we used values based on those from the literature. We summarize abbreviations, descriptions, values and sources for general parameters (Table 3.1a), bacteria (Table 3.1b), phytoplankton (Table 3.1c) and zooplankton (Table 3.1d). Zooplankton observed mean lengths from NTL LTER database were converted to dry weight using empirical relationships specific to the four defined functional groups (Culver et

al., 1985; McCauley, 1984; Ventura et al., 2000; Wiebe et al., 1975). Phytoplankton were parameterized with functional group-specific biomass to carbon ratios (Table 3.1c) while zooplankton was assumed to be 33% C by dry weight (Wiebe et al., 1975).

3.3.4.1 Light Attenuation

Modelled chemical and biological feedback to hydrodynamic driver variables includes light attenuation from pure water, phytoplankton, dissolved and particulate organic material, and suspended inorganic materials; these variables contribute to vertical attenuation as a function of their simulated concentrations at each model time step. We estimated coefficients for DOC extinction (K_{eDOC}) and phytoplankton groups (K_{eP}) from observed data, and assumed a negligible effect by other non-phytoplankton particulate material and dissolved inorganic materials. We assume a linear relationship between chromophoric dissolved organic matter (CDOM) and DOC.

Photosynthetically active radiation (PAR, 400-700nm) diffuse attenuation coefficients ($K_{d\,PAR}$) were calculated from observed Secchi disk depth (z_s) for the 2008 ice-free season. For each z_s, $K_{d\,PAR}$ was estimated (Kirk, 1994):

$$K_{d\,PAR} = 1.7 / z_s \qquad \text{Eq. 1}$$

We examined the linear relationship between phytoplankton functional group biomass (g C m^{-3}) and the estimated $K_{d\,PAR}$ (m^{-1}) for each observation, and differentiated the attenuation imparted by constituent materials. We tested for significance between phytoplankton functional group biomass (g C m^{-3}) and estimated $K_{d\,PAR}$ (m^{-1}) in order to assign a specific K_d for each phytoplankton functional group, using 13 observations from 2008. Only the N-fixing functional

group biomass showed a significant linear relationship (r^2=0.37, p<0.05) with $K_{d\ PAR.}$, but there was also a significant relationship between total phytoplankton biomass and $K_{d\ PAR}$ for the 2008 season (R^2 = 0.59, p<0.01). Therefore, we assumed the uniform $K_{d\ PAR}$ per unit total phytoplankton biomass applied to all four phytoplankton functional groups from the slope of this relationship (K_{eA}: 0.198 m^2 (mg Chl-*a*)$^{-1}$). We assumed that the y-intercept (0.454 m^{-1}) of the regression line fit to the data was an estimate of K_d for all light-attenuating materials in the water column other than phytoplankton (i.e. CDOM, inorganic constituents, and pure water). We assumed the attenuation of pure water to be 0.05 m^{-1} (Pope and Fry, 1997). The remaining attenuation (0.404 m^{-1}) was attributed to CDOM. Assuming a constant relationship between CDOM and DOC, we generated a K_{eDOC} per unit DOC based on the mean DOC concentration over the study period in Lake Mendota. The resulting K_{eDOC} estimate, (0.0072 m^2 (g DOC)$^{-1}$) is within the range of literature values for DOC-specific absorbance (Morris et al., 1995).

3.3.4.1 Water column nitrification rate

Simulated nitrification in the water column is modelled in CAEDYM as a function of a maximum temperature-referenced (20 ^oC) nitrification rate (μ_{NIT}) modified by temperature, concentrations of NH_4^+ and DO, and a half-saturation constant for the effect of oxygen on nitrification. To estimate the maximum nitrification rate, we applied the following relationship:

$$k_{nit} = [(\log C_2 - \log C_1) * 2.303] / (T_2 - T t_1) \quad \text{Eq. 2}$$

where k_{nit} is maximum nitrification rate when oxygen is saturated in the water at the mean of the observed temperatures, T_2 and T_1, and C_n is nitrate concentration at time t_n. Nitrification rate was corrected for temperature using an Arrhenius relationship:

$$k_{nit} = k_{nit\,20} \cdot \upsilon_{chem}^{(T_{avg} - 20)} \quad \text{Eq. 3}$$

where $k_{nit\,20}$ is the maximum nitrification rate under oxygen saturation at 20 ^{o}C, T_{avg} is the average of temperature, T, at t_1 and t_2, and υ_{chem} is the temperature multiplier (1.08; Jorgensen and Bendoricchio, 2001).

After fall turnover in Lake Mendota, a near-linear increase in NO_3^- concentrations initially occurs (t_1 through t_2; approximately day 265-335 in 2008) under saturated DO conditions. The source of the increase is presumably nitrification associated with oxidation of NH_4^+ to NO_3^-, as evidenced by a simultaneous decrease in NH_4^+. The half saturation constant for nitrification dependence on DO ($k_{DO\,nit}$) was estimated by visually inspecting a plot of NO_3^- versus DO concentration and identifying a step change in NO_3^- concentration as DO approaches zero; the DO concentration at this break was identified as the half-saturation constant. We investigated trends for all available years (1995-2008), and used 2008 estimates for parameter values; consistent patterns in DO, NO_3^-, and NH_4^+ were observed following fall mixis from 1995-2008.

3.3.4.3 Sediment nutrient flux

Fluxes of C, N, P, and O across the sediment-water boundary were simulated as a function of an assigned maximum rate referenced to a standard temperature (20 ^{o}C) and in turn

modified by temperature, pH and DO. We estimated maximum fluxes by assuming hypolimnetic accumulation or loss of the variable of interest during summer stratification reflected sediment release or uptake, respectively. Sediment fluxes of NO_3^-, NH_4^+, PO_4^{3-}, dissolved oxygen (i.e., sediment oxygen demand; SOD), DOC, dissolved organic nitrogen (DON), and dissolved organic phosphorus (DOP) were estimated in this manner. Hypolimnetic accumulation rate constants for these nutrients were estimated during summer stratification from 1995 to 2008 as:

$$R_{chem} = (C_2 - C_1) / (t_2 - t_1) \quad \text{Eq. 4}$$

Where R_{chem} is the maximum linear rate of hypolimnetic accumulation of the variable, calculated as the difference in concentration between C_1 and C_2 from time t_1 to t_2. The value of R_{chem} was normalized by volume to give a rate of change of concentration (g m^{-3} d^{-1}) and divided by mean hypolimnetic depth (fixed at 7.3m from seasonally average estimates) to yield the maximum sediment flux term, S_{chem} (g m^{-2} d^{-1}). Fluxes were corrected for temperature using an Arrhenius relationship analogous to Eq. 3. Observations made at the maximum routine sampling depth (20m) were used for this analysis, although hypolimnetic C, N, P, and O concentrations are not necessarily homogenous with depth. Rate of change for N, P, and O during summer stratification were greatest at 20m as compared to at other depths (data not shown), and thus represent maximum possible fluxes that could be derived from observational data. This simplifying assumption ignores the effect of spatial heterogeneity in sediment flux and the influence of biomass accumulation in the deepest part of the lake, both of which could be contributing to the most extreme flux rates in the deepest part of the lake, resulting in an overestimate of the maximum potential fluxes. The half saturation constant for maximum sediment nutrient flux

dependence on DO ($S_{DO\ chem}$) was estimated by visually inspecting a plot of the concentration of the relevant nutrient species versus DO concentration during summer stratification and identifying a step change in nutrient concentration as DO approached zero as described above for rates of nitrification. We investigated all available NTL LTER data and consistent patterns of hypolimnetic nutrient accumulation were observed during summer stratification from 1995-2008, but we used quantitative values for 2008 to define relevant sediment flux parameter values. Observation-based estimates and literature values specific to Lake Mendota were available for sediment oxygen demand (K_{SOD}) and sediment PO_4^{3-} flux (S_{PO4}). However, key state variables were highly sensitive to these parameters, and thus manual manipulation to minimize error was required.

For DOC from 1995-2008, we found no relationship between S_{DOC} and time or S_{DOC} and DO. Lake Mendota DOC is relatively low (mean hypolimnetic DOC 5.9 g m^{-3}, standard deviation 1.1 g m^{-3}) and has little temporal or spatial variation. Based on the DOC observations, and because of absence of DOP and DON measurements, we assumed no sediment flux of DOC and that DOP and DON sediment fluxes were likewise negligible, i.e., S_{DOC}, S_{DOP} , and S_{DON} were set to zero.

3.3.4.5 Calibration

With known inflows and water elevation, the water balance was closed by estimating outflow discharge that minimized the error in observed and predicted water level. The flux of water and energy from the lake via evaporation is included in DYRESM, and this process acts to concentrate solutes in the water column. We assumed that the evaporative fluxes were properly

parameterized by the wind-driven formulation in DYRESM, although we did not validate modeled evaporation rates.

Trial-and-error adjustments of sediment oxygen demand (k_{SOD}), maximum sediment flux of PO_4^{3-} (S_{PO4}), and phytoplankton settling velocity (v_{SA}), were made within the bounds of available published literature and system-specific field values (Table 3.1a) until satisfactory performance was achieved based on goodness-of-fit metrics pertaining to range and temporal pattern of DO, PO_4^{3-}, and phytoplankton biomass, respectively. These parameters were used for manual calibration because of the sensitivity of key state variables (DO, PO_4^{3-}, and phytoplankton biomass) to parameter values and because of the lack of agreement among literature and field-based values (see Table 3a for ranges from the literature and field).

3.3.4.6 Model evaluation

We used three statistical measures and wavelet analysis to evaluate model output against observational data (Table 3.2). Linear coefficient of determination, Spearman's rank correlation coefficient, and normalized mean absolute error were used for both manual measurements and for automated, high-frequency measurements of temperature, DO, and chl-*a* fluorescence. Wavelet analysis was used only for the high-frequency measurements of temperature, DO, and chl-*a* fluorescence, made at an instrumented platform at 0.5 m depth. Statistics were calculated for observed and predicted data at depths and times when observations were available. Observational data sampling frequency and statistical results are summarized in Table 3.2. All observations and predictions were compared directly, with the following exceptions: (1) all observed automated data (min^{-1}) were aggregated to hourly intervals to match the model output, (2) statistical calculations of observed chl-*a* fluorescence (RFU) and model output of chl-*a*

concentration (g m^{-3}) were made after standard normal transformation of data, such that chl-*a* RFU could be evaluated directly against model output, and (3) standard normal transform preceded wavelet analysis. Water temperature measurements were interrupted periodically from July 22 through August 9 2008 (day number 204-222); only available data were considered in evaluation.

Data were compared to model output using three well-accepted goodness-of-fit measures: coefficient of determination from linear regression (R^2) values, Spearman's rank correlation coefficient (Spearman's rho), and the normalized mean absolute error (NMAE, Alewell and Manderscheid, 1998):

$$NMAE = \frac{\sum_t^n \left(\left| S_t - O_t \right| \right)}{n\overline{O}}$$

Eq. 5

where *n* is number of observations, *O* is observed value, *S* is the simulated value, and *t* is time. NMAE provides a goodness-of-fit metric for state variables that do not cover strong gradients but whose mean values are important to reproduce. For example, epilimnetic soluble reactive phosphorus concentration can be very low during algal-dominated phases of the summer, and the observed values appear to fluctuate randomly around a low mean value quantitatively similar to analytical detection limits. In this case, it is important to reproduce the mean of the data, but not the random fluctuations, and the resultant NMAE coefficient would indicate the degree to which the mean is reproduced.

For the state variables for which high-frequency observations were available (temperature, DO, and chl-*a*), model performance was evaluated using wavelet transforms at

global and individual scales (Torrence and Compo, 1998). We performed wavelet analysis on several derived metabolic variables (whole water net primary productivity, gross primary productivity and respiration) to gain insight into phytoplankton dynamics, but had no observational data with which to compare those results. Wavelet analysis was also used to assess model sensitivity to variation in three CAEDYM parameters ($K_{d\,DOC}$, S_{PO4}, and Min_{res}); we considered simulated variables temperature, DO, and chl-a concentration for this analysis. The wavelet analysis software used to generate the results presented here can be downloaded at http://atoc.colorado.edu/research/wavelets/.

Global wavelet spectra represent the sum of variability of each time scale through time and can be plotted as a power spectrum. Visualizing observation and model data as power spectra provides a convenient means for determining whether model predictions apportion variability to time scales across the entire simulation in ways consistent with the observational data. Wavelet transforms at individual scales can be used to separate data by time scale (e.g., hour, day, week periods), while maintaining the time domain. When transforms are performed on both observed and modelled data, a direct comparison of scale-specific variation can be made through time. For example, we might expect a strong diel cycle in dissolved oxygen due to metabolism at times during the summer when phytoplankton biomass is high and days are sunny. However, the dissolved oxygen signal can be driven by processes at multiple scales, such as the aforementioned metabolism and changes in solubility driven by seasonal temperature cycles. Isolating the daily scale using wavelet transforms allows us to evaluate, e.g., daily dissolved oxygen cycles without the confounding effects of other scales. Wavelet transforms have been shown to be robust to modest deviations from stationarity, i.e. constant mean and variance

(Cazelles et al., 2008). Differences between the spectra of observed and modelled data may provide clues to processes missing or inappropriately represented in the model.

3.4 Results

3.4.1 Traditional goodness-of-fit

Surface water level at the outflow ranged 0.8 m in elevation through the simulation and was maintained within 4% of observed elevation. Water temperature and features of thermal stratification were reproduced well, including surface water temperature, metalimnetic depth, and hypolimnetic temperature (Figure 3.2a). Observed and predicted temperature (T_{obs} and T_{pred}) between 0 and 20 m were highly correlated (R^2=0.94, Rho=0.97, Table 3.2). The metalimnetic T_{obs} gradient was stronger than that of T_{pred}, but the observed seasonal hypolimnetic deepening by approximately 3 m was represented in the model output.

Over the duration of the simulation, the range and temporal variability of DO through the water column was well represented, though surface DO was under-predicted for most of the simulation (Figure 3.2b). Under-predictions of DO at the surface (0.5m) resulted in poorer goodness-of-fit metrics R^2 and Rho for high-frequency DO observations, but not for biweekly DO manual observations through the water column (R^2=0.79, Rho=0.87, Table 3.2). NMAE metrics for both high frequency and manual DO observations against simulated DO concentrations were both low (0.26 and 0.32, respectively). The predicted oxygen gradient reflected the predicted metalimnetic thermal gradient, which was similarly weaker than the observed gradient. Statistical analyses showed that the nutrients NO_3^-, NH_4^+, PO_4^{3-}, TP, and TN were generally well represented in the simulation (Table 3.2), though the metalimnetic gradients were weaker than those observed (Figures 3.2c and 3.2d). The model reproduced the trend of epilimnetic and hypolimnetic depletion of NO_3^- and simultaneous persistence of metalimnetic NO_3^- through ~ day 220 (Figure 3.2c). A decrease in simulated epilimnetic PO_4^{3-} from 0.030 g m^{-3} to <0.005 g m^{-3} from day 180 to 200, and accumulation of hypolimnetic PO_4^{3-} from 0.15 g m^-

^{3} to 0.25 g m^{-3} over the duration of the simulation are both consistent with observed data (Figure 3.2d, Table 3.2). Observed TN, TP, pH and DIC were significantly and positively correlated with model predictions (Table 3.2). Ammonium (NH_4^+) and DOC in general followed the seasonal pattern and magnitude of the observed data (Table 3.2). Both observed and predicted DOC had limited concentration range (~ 1 g m^{-3}) and no clear temporal pattern over the 90-day simulation, which resulted in poor R^2 and Spearman's rho terms, however the NMAE value was low (0.053), reflecting the small proportion of model residuals to mean observational values.

Surface (0.5m) and upper water column (0-8m) chl-*a* concentration were consistently higher in the modelled data than in observed in vitro chl-*a* concentrations from day number 180-230 by ~ 0.01-0.02 g m^{-3} (Figures 3.1d and 3.3a). Chlorophyll-*a* was over-predicted in the water column from day 0. The values of manual chl-*a* observations sometimes matched simulated chl-*a*, though shorter-term chl-*a* dynamics were not well captured, resulting in low correlation coefficients (R^2 = 0.074, Spearman's rho = 0.12). Model simulations reproduced the range of phytoplankton biomass although some temporal patterns were not reproduced (Figure 3.3b and 3.3c). The *Microcystis*-like functional group (A_{Mic}) biomass increased throughout the season and was similarly simulated, though a peak in observed biomass on day 231 was not predicted (Figure 3.3b). Both observed and simulated A_{Aph} biomass was lowest at the beginning and end of the simulated period, though the simulation did not predict two mid-season peaks in A_{Aph} on days 198 and 228 (Figure 3.3c). Observed and simulated A_{Chlor} and A_{Diat} biomass never exceeded 1% of total phytoplankton biomass in both simulated and measured data, but were included in model configuration to represent the two additional ecologically relevant groups.

In the time domain, goodness-of-fit metrics for high-frequency (h^{-1}) observations and predictions at 0.5 m indicated good model representation of temperature (R^2= 0.83, Rho=0.92,

and NMAE= 0.034), poorer representation of DO (R^2= 0.01, Rho=-0.04, NMAE=0.26), and moderate reproduction of chl-*a* concentration as compared to in situ chl-*a* fluorescence in RFU (R^2= 0.10, Rho=0.40, NMAE=1).

To assess the simulated zooplankton biomass, particularly for controls on phytoplankton biomass, we consider loss of phytoplankton biomass to zooplankton grazing, which represents <1% loss of standing biomass per day. Because we model the cyanobacterial-dominated phase in Lake Mendota, we expected zooplankton grazing to be low. Observed zooplankton standing biomass ranges from 0.01-0.06 g C m^{-3}, which is consistent with loss of ~ 0.001 g C m^{-3} d^{-1} of phytoplankton biomass due to grazing. Zooplankton speciation and abundance have remained remarkably stable over the past few decades, and our simulation of small loss of phytoplankton by zooplankton grazing is consistent with historical data (Brock, 1985).

3.4.3 Wavelet analysis

Water temperature spectra for observations and predictions had similar pattern across scales from hours to ~ 25 d, with spectral peaks at the 1 d and ~ 13 d scales (Figure 3.4a and 3.4b). Both T_{obs} and T_{pred} spectra had an increase in power at ~ 27 d and T_{obs} power exceeded T_{pred} at this scale. Observed DO (DO_{obs}) power spectra exceeded predicted DO (DO_{pred}) at all scales < 38 d, and both spectra had peaks at the 1 d scale, although the DO_{obs} spectra exceeded DO_{pred} spectra at that scale (Figure 3.4c and 3.4d). DO_{obs} spectrum also had peaks at ~ 5, 13, 18, and 33 d scales; DO_{pred} spectrum had peaks of much lower power at the 7, 10, and ~ 17 d scales.

Wavelet analysis of chl-*a* fluorescence spectra and simulated chl-*a* concentration (after standardization of both variables) indicated higher relative power in observed chl-*a* (chl-a_{obs}) fluorescence at time scales < 10 d (Figure 3.4e and 3.4f). Peaks were visible at the 3, 7, 9, and 18

d scale for chl-a_{obs} spectrum, with an average decrease in power at > 18 d scale. The predicted chl-*a* (chl-a_{pred}) spectrum exhibited peaks at the 1, 5, and 13 d scales, with large increase in power especially for > 20 d period.

Wavelet transforms shown for a single scale through time indicate the strength of variation at a particular frequency through time (Figure 3.5). Wavelet transform at the 1 d scale for T_{obs} showed higher amplitudes than the transform for T_{pred} (Figure 3.5a), but the amplitudes and phases at the 10 d scale were closely matched (Figure 3.5b). The single-scale 1 d wavelet transform for DO_{obs} had higher amplitude than DO_{pred} for most of the simulated period, particularly from day 195-205 (Figure 3.5c). The DO_{obs} 10 d scale had higher amplitude than DO_{pred} (Figure 3.5d). The chl-a_{obs} transform had higher amplitude than chl-a_{pred} at the 1 d scale, but not at the 10 d scale (Figure 3.5e and 3.5f). Observed and predicted chl-*a* transforms at the 10 d scale were out of phase through time.

Global wavelet analysis of simulated biomass, respiration, productivity, and net primary productivity (NPP) indicated strong diel signals for respiration, productivity, and NPP (Figure 3.6). The biomass spectrum has low power at shorter periods and higher power with longer period. Spectra of productivity, respiration, and NPP all contain peaks at the ~12 d period, and lesser peaks at the 5-6 d period.

3.5 Discussion

Aquatic ecosystem models are intended to reproduce the pattern, range, and timing of physico-chemical and biological variables driven by environmental change through time. The characteristic time scales at which environmental drivers operate (e.g. the life span of predators,

the occurrence of El Niño-Southern Oscillation, or annual hydraulic flushing) have been shown to control features of aquatic ecosystems (e.g. long term records of sedimented algal pigment, primary productivity, or water column transparency) independently at corresponding time scales, resulting in multiple scales of variation due to multiple drivers (Carpenter and Leavitt, 1991; Jassby et al., 1999; Jassby et al., 1990). Here, we use wavelets to analyze predictions from an aquatic ecosystem model in both the time and frequency domains, assessing variability across a range of temporal scales. This allows for the more focused examination of model performance across multiple timescales, potentially highlighting missing or mischaracterized mechanisms that dominate at different timescales. To our knowledge, this represents the first work evaluating coupled hydrodynamic-water quality model prediction of dissolved oxygen and chlorophyll at short (daily to sub-day) time scales. Understanding a model's ability to reproduce variability at characteristic timescales may highlight which processes contributing to overall variability are least understood.

Wavelet analysis has been used by others to assess observed temporal variability in lakes for long-term time series (e.g. Keitt and Fischer, 2006); short-term, high-frequency data (e.g. Langman et al., 2010); and plankton spatial heterogeneity (Blukacz et al., 2009). We demonstrate that this new and complementary approach is particularly powerful when environmental modelling predictions can be compared with the ever-increasing abundance of in situ data. The use of automated sensor data for validation of numerical ecosystem model predictions has been suggested as the next step in aquatic ecosystem modelling (Arhonditsis and Brett, 2004; Beck et al., 2009), and wavelet analysis offers a methodology for using the multi-scale data in calibration and validation.

We hypothesized that variation at characteristic time scales might provide insight into important processes, both observed and modelled. Some unexpected analytical results in the frequency domain led us to discuss the implications for model setup and configuration on time-scale predictions, and motivated a closer investigation into how model parameterization affects key predictions in both the time and frequency domains. Finally, our particular interest in short-term phytoplankton dynamics in this study necessitated scrutiny of the well-established biomass quantification methods and newer in situ fluorometric methods, and the challenges of making meaningful use of multiple phytoplankton data streams.

3.5.1 Time scale prediction

The model output re-created key spectral characteristics for temperature and in part for DO, but not for chl-*a*, suggesting other factors not modelled are relevant for high-frequency variables of interest at scales of hours to weeks. We were surprised to find the observed DO and chl-*a* signals to be decoupled, but we also found the predicted metabolic variables (NPP, GPP, R) were decoupled from the predicted DO signal. In general, predicted and observed spectra for all variables converged around the 7-10 d scale, while observations had more variability than predictions at scales of hours to ~ 1 week (Figure 3.4). It is notable that the DO_{obs} and chl-a_{obs} spectral signals were not closely coupled, particularly at lower scales around 1d, although they are linked physiologically through metabolism. In contrast, the spectra of DO_{pred} and chl-a_{pred} both had clear peaks at 7-10d and at 1d (Figures 3.4d and 3.4f). We also expected the global spectra for the predicted productivity, respiration, and NPP for phytoplankton to exhibit similar spectral characteristics as DO_{pred} and chl-a_{pred}. However, peaks at the daily scale and at the ~ 10-15 d scale for these metabolic variables occurred in the chl-a_{pred} spectrum, but not in the DO_{pred}

spectrum. De-coupling of closely related variables and processes in both predictions and observations in the frequency domain was unexpected and demands further investigation into drivers of variation in through time.

Wavelet transform of a single scale through time demonstrates how the scale-specific timing of model predictions may not match observations. The differences in amplitude of predictions and observations for DO and chl-*a* in the single-scale wavelet transforms were especially evident in the individual scale (1 d) plots (Figure 3.5). A large increase in the amplitude of the single scale DO_{obs} transform occurred from day 198-208. A similar increase in amplitude of chl-a_{obs} did not occur. The high amplitude of DO_{obs} during this period may be explained by physical changes related to a large precipitation event that occurred on day 194, where inflow volumes were approximately three times base-flow. The event resulted in observable disturbances in water temperature, DO, PO_4^{3-}, NO_3^-, (Figure 3.2), and NH_4^+ and DOC (not shown) around day 198. Water column chemical gradients for PO_4^{3-}, NO_3^-, NH_4^+, and DOC were also disrupted; hypolimnetic PO_4^{3-} fell to < 100 mg m^{-3} and upper water column (0-10m) NO_3^- increased by ~100 mg m^{-3}, while lower water column (10-20m) NO_3^- decreased by ~ 100 mg m^{-3}, possibly indicating the entrainment of hypolimnetic nutrients into the epilimnion. Even though daily inflow data, which included this disturbance event, were used to drive the model, we did not see the disturbance expressed in model predictions. We speculate that three-dimensional effects in the lake system that were not represented in the 1D model may explain this discrepancy between observations and predictions.

3.5.2 Model limitations

Ecosystem models are simplifications of the systems they represent, and cognizance of the limitations of a model permits the user to make more informed interpretation of model behavior. Some aspects of model setup and configuration that may contribute to the prediction accuracy of short-term phytoplankton dynamics in this study are explored below, and include spatial dimensionality, time step calculation, and representation of biological state variables.

Patterns detected by automated high-frequency observations and not reproduced in the 1D model - for example, the event beginning day 198- may represent spatial heterogeneity in the horizontal dimension (Fragoso et al., 2008; Platt et al., 1970; Steele and Henderson, 1992) or vertical dynamics not accounted for in the model (e.g. those described and modeled by Serizawa, et al. 2010). Hillmer et al. (2008) established an index for validation of the 1D assumption of horizontal homogeneity of phytoplankton:

$$L = (k/\mu)^{1/2} \qquad \text{Eq. 6}$$

where L is the characteristic length scale at which phytoplankton growth is offset by diffusion, k is horizontal diffusivity and μ is the net growth rate of phytoplankton. According to this index, phytoplankton patch size will exceed lake area when $k/\mu >>$ (basin scale)^2 and a 1D assumption of homogenous phytoplankton distribution is valid. When $k/\mu <<$ (basin scale)^2, patch size will be localized and the 1D assumption violated by horizontal concentration gradients (Hillmer et al., 2008). By bracketing potential horizontal diffusivity coefficients for Lake Mendota within ranges measured in systems of comparable area (0.02-0.3 m^2 s^{-1}, Peeters et al., 1996) and assuming net growth rate of 1.0 d^{-1}, a basin scale length of 6 km (Yuan, 2007), $L^2 >> k/\mu$, and the 1D assumption is not met. Thus, the variability in high-frequency observations we detected across some temporal scales may be in part due to horizontal heterogeneity, e.g. phytoplankton patchiness due to physical, chemical, or biological heterogeneity. When three dimensions are

collapsed into one, and a model is calibrated to 1D observational data, spatial heterogeneity is effectively subsumed into the mean seasonal value for the training period. As with other dynamic models, caution must be exercised when applying the calibrated parameters outside of the training period, as a new set of spatially heterogeneous conditions may subsequently be at play (Hillmer et al. 2008). Kamarainen et al. (2009) used a 3D hydrodynamic model for Lake Mendota to investigate the contribution to P loading of hypolimnetic entrainment; for that purpose, the authors found that single-location sampling to estimate average hypolimnetic P entrainment was sufficiently similar to multi-location sampling averages. For investigating the more complex processes of nutrient advection and biological response, a 3D modelling and sensing approach (as described by Vos et al. (2003)) would provide a powerful dataset for evaluating temporal and spatial predictions of a 3D model for the Lake Mendota system, but is nevertheless outside of the scope of this paper.

Likewise, the effects of the temporal resolution used in the model should be considered. The relationship between model calculation time step and prediction accuracy across time scales is unknown and deserves further investigation, particularly for short-term variation on the order of hours to days. Here, we used 1 h driver data and investigated predicted patterns at scales as short as 3 h. However, many high frequency environmental variables are measured at scales of seconds to tens of minutes on many platforms, which could provide a convenient test for time-step effects.

Surprising differences between predicted and observed chlorophyll *a* in the time and frequency domains motivated a closer inspection of the configuration of the biogeochemical model. Here, and typically among published studies of CAEDYM, the model was configured with static chlorophyll-*a*:C ratios (chl:C) and fixed internal C content for each phytoplankton

functional group. Under this configuration, predicted water column chl-*a* concentration is derived from predicted phytoplankton biomass and varies only as a function of functional group composition of biomass and total biomass. We used the long-term NTL LTER dataset to explore the validity of a static chl:C ratio assumption for this system (Figure 3.7). A range of two orders of magnitude of chl:C ratios was calculated for this system between 1999 and 2008. Predicted chl:C ratios are closer to the decadal median values than to those observed at the annual, seasonal, and daily scales. Although fixed chl:C ratios are used to derive chl-*a* concentration by the model, chl:C ratios are known to vary with cell age, across species, and with variations in temperature, nutrient, and light (Geider, 1987; Reynolds, 2006). For our simulations, chl-*a* concentration was overestimated by model output from the first day of the simulation; overestimates of chl:C ratio may explain some deviation of model fit with observations. But, had a fixed chl:C ratio been assigned to fit initial conditions of observed chl-*a,* it is likely that chl-*a* goodness-of-fit would be poor later in the simulation. Likewise, the poor correspondence of observed and predicted phytoplankton functional group biomass in units of carbon concentration could be due in part to the introduction of error and/or uncertainty in observation, introduced by the static configuration of chl:C ratios used for converting microscopic cell counts to carbon units (parameters shown in Table 3.1c), and the de-coupling of DO and chl-*a*. As suggested by Flynn (2005b), the use of dynamic chl:C ratios by aquatic ecosystem modelers may provide more realistic representations of chl-*a* concentrations, especially relevant to those using in situ, in vitro or in vivo chl-*a* measurements as a proxy for phytoplankton biomass, but is beyond the scope of this paper.

3.5.3 The challenges of multiple phytoplankton quantification methods

The challenges of mapping multiple types of observational data onto one or two state variables or derived variables in the model have been encountered by others (e.g. Rigosi et al., 2011 in press), and requires closer consideration of the relationship between observational data, model configuration and the use of multiple types of observational data (Flynn, 2005a). We focus here on model predictions of phytoplankton biomass and chl-*a* concentration, and compare them against three types of phytoplankton observations: (1) manual taxonomic identification to estimate biomass in units of carbon concentration [g C m^{-3}] and referred to as 'biomass' hereafter; (2) in vitro laboratory solvent extraction and spectrophotometric or fluorometric analysis of chl-*a* concentration, 'in vitro chl-*a*' hereafter; and (3) in situ optical chlorophyll fluorometry, 'in situ chl-*a*' hereafter. Each method has well-documented strengths and limitations (e.g. Gregor and Marsalek, 2004; Kepner and Pratt, 1994; Marra, 1997). We consider some challenges associated with the use of multiple methods for validation data in more detail below.

In vitro chl-*a*, in situ chl-*a* fluorescence, and biomass estimates from microscopy are all used routinely in comparison to model predictions, and we determined how these three variables linearly correlate to one another in this system. In Lake Mendota, long-term (1995-2008) biomass and in vitro chl-*a* concentration were positively and significantly correlated (R^2=0.400, n=195). The correlation coefficient between in situ chl-*a* RFU to manual in vitro chl-*a* concentration in 2008 between days 175 and 270 (where both were measured/collected at 0.5 m at the same location) was weak (R^2=0.06, n= 17, in situ fluorescence hourly average for the date and time corresponding to sample collection). These observations indicate that while biomass estimated from microscopy and in vitro chl-*a* concentrations are correlated, in situ chl-*a* fluorescence is not linearly correlated to in vitro chl-*a*. This is not surprising given the

documented methodological limitations of chl-*a* fluorescence (e.g. Fuchs et al., 2002; Heaney, 1978). Despite these limitations, fluorescence remains as one of the only practical methods of measuring short-term variability of chl-*a*. Our results further show that in vitro chl-*a* and in situ fluorescence are not interchangeable for Lake Mendota, and the use of one or another should be intentional.

Goodness-of-fit statistics indicated that model prediction of chl-*a* concentration was better represented by in situ chl-*a* fluorescence better than in vitro solvent-extracted chl-*a* measurements (Table 3.2). This finding is notable because in vitro chl-*a* concentration – as an estimate of pigment concentration – is conceptually more similar to model predictions of chl-*a* concentration than in situ chl-*a* fluorescence, which is a quantification of the emission intensity (and photosystem II photochemical efficiency) of chl-*a* within cells in whole water. Deriving more meaningful units of measure for in situ chl-*a* fluorescence data requires calibration of in situ data to in lab extracted in vitro chl-*a* concentration, but would also introduce assumptions about the relationship between in vivo and in situ chl-*a* (Falkowski and Kiefer, 1985). Gregor et al. (2005) suggested that in situ pigment fluorescence measurements should be the source of quantitative data and that taxonomic identification should be used to provide detailed taxonomic information about dominant phytoplankton taxa. In consideration of the frequency of manual sampling to inform automated data, or the use of automated high-frequency data at all, requirements for sample transport, analyst expertise, lab reagents and instruments must be balanced against the cost of sensors, platforms, and maintenance. Likewise, the optical properties of chl-*a* such as fluorescence yield, photo-adaptation and non-photochemical quenching must be acknowledged (Marra, 1997). Other types of automated sensing technologies (e.g. PHYTO-PAM, image-based monitoring and in situ flow cytometry) are being developed and in some

cases are available (Shade et al., 2009), and may fill a gap in high-frequency biological data in the future.

3.5.4 Improving model parameterization using wavelet analysis

A few important model parameters estimated from long-term observational data led to unrealistic lake chemical predictions. Observation-based estimation of two ecologically relevant parameters was unsuitable: sediment oxygen demand (K_{SOD}) and sediment PO_4^{-3} flux (S_{PO4}). Both estimates from field observations were too high for model use, as they caused excessive depletion of hypolimnetic DO and buildup of hypolimnetic PO_4^{-3}. Thus, these variables were manually calibrated: the final user-defined K_{SOD} value was 0.46 g m^{-2} d^{-1}, approximately half of that estimated by Brock (1985), and only 6% of the estimate from historical hypolimnetic DO data (Table 3.1a). The final user-defined S_{PO4} value was 0.0125 g m^{-2} d^{-1}; published laboratory estimates for S_{PO4} in Lake Mendota were approximately six-fold greater than this value (Holdren and Armstrong, 1980), and three-fold greater than our estimates from historical hypolimnetic PO_4^{3-} (Table 3.1a). These two processes are chemically and biologically relevant in a thermally stratified eutrophic lake and the inconsistency between observed rates from laboratory experiments or estimation from field observations and final model parameter values could be due to error derived from heterogeneous hypolimnetic nutrient concentrations or biomass accumulation in hypolimnetic waters. Alternatively, these parameters may be estimated correctly, but model processes (e.g. 1D layer averaging) may be flawed.

To investigate the effects of parameterization on wavelet spectra in the frequency domain, we altered the values of three CAEDYM parameters that have strong control over key physical, chemical and biological variables. Temperature, PO_4^{3-} concentration, and

phytoplankton biomass are sensitive to DOC-derived light attenuation ($K_{d\,DOC}$: standard value 0.15 g^{-1} m^3 m^{-1}, low 0.0075, high 0.03), sediment PO_4^{3-} flux (S_{PO4}: standard value 0.0125 g P m^{-2} d^{-1}, low 0.06, high 0.025), and Min_{res}, the minimum biomass below which zooplankton do not graze (standard value 0.01 g C m^{-3-}, low 0.0, high 1.0), respectively. Model output for temperature and DO were robust to changes in values (data not shown), but mean values of chl-*a* concentration was sensitive to a range of parameters tested (Figure 3.8). The sediment PO_4^{-3} flux term had the strongest effect on chl-*a* of the three parameters tested here, likely due to the limitation of phytoplankton growth by dissolved inorganic P. This observable relationship between parameter scaling and mean seasonal values in the prediction makes calibration of the model to long simulations of years to decades tractable. However, reproducing temporal dynamics, both in terms of the timing of critical peaks (e.g., phytoplankton blooms) and the sub-seasonal cycles of the ecosystem is much more challenging. For phytoplankton biomass, patterns of variation in the frequency domain did not respond substantially to parameter optimization (Figures 3.8a and 3.8b), in contrast to the average seasonal value, which was more sensitive to parameters values (Figure 3.8c). The frequency response may be a result of the configured model complexity (e.g., number of trophic levels used) or the design of the model (e.g., functional forms of the fluxes). For the sensitivity analysis of these three parameters, our preliminary results indicate differential response of state variables in the time versus frequency domains; wavelet analysis could be a tool complementary for calibration techniques such as those described by Makler-Pick et al. (2011) or Rigosi et al. (2011).

4.6 Conclusion

We used high-frequency water quality data to assess the prediction accuracy of an aquatic numerical model over multiple temporal scales using wavelet analysis. Traditional goodness-of-fit metrics indicated physical predictions were more accurate than chemical and biological variable predictions. Wavelet analysis confirmed these findings in the frequency domain and added information about the scales at which patterns were reproduced. Physical predictions were more accurate at all scales assessed, while chemical and biological patterns were reproduced over a smaller range of scales. Wavelet analysis of in situ data is particularly relevant for the assessment of short-term predictions such as phytoplankton bloom events, and represents a new domain within which numerical models can be calibrated and validated.

Consideration of spatial heterogeneity is important for interpretation of biological observations and predictions in this system and deserves further study. There are physical-chemical-biological interactions likely not well represented in our model, and identifying what these are and how they operate at the ecosystem scale over scales of hours to weeks is critical, especially when trying to reproduce ecosystem frequency response. Investigation of how variance scales with mean values of temperature, dissolved oxygen, pigment fluorescence, and other high-frequency variables measured by automated sensing platforms would increase understanding of model and system behavior and aid interpretation of results. A better understanding of automated sensing of biological variables and their relationship to model output will improve the utility of aquatic ecosystem models. Further research is required to understand how model complexity and predictive capability interact with the type and frequency of observed variables.

Our work highlights the challenges of reconciling multiple observational methods (e.g. phytoplankton biomass and various estimates of chlorophyll as a proxy for biomass) and we

show that results and subsequent interpretation may not be independent of commonly used methods. These differences reveal the need for a better understanding of how and why various methods diverge, and what useful information can be drawn from them.

Using data from sensor networks gave us a unique opportunity to evaluate the model at highly resolved time scales. For the aquatic modeling community, high-frequency sensing represents a step change for observational datasets with which to use for calibration and validation of aquatic ecological simulations. Most aquatic modelers use daily or sub-daily calculations, but predictions are usually presented at the frequency of observational data. The observational and analytical framework presented here sets the stage for future work that will doubtless include more high-frequency sensing data and, by necessity, involve a closer inspection of model behavior at high frequencies. Closer inspection will reveal surprises (e.g. the de-coupling of dissolved oxygen and primary productivity presented in this work), but we believe learning more about model behavior at all temporal scales of interest will advance the science of aquatic ecosystem simulations. Wavelet analysis allowed us to enter a new domain-frequency, leading to insight into the relationships between observations and model predictions. Now that such data are becoming more readily available, we anticipate new discovery of ecosystem processes that not only informs model development but also improves our prediction at scales pertinent to those of phytoplankton dynamics in eutrophic systems.

3.7 Acknowledgments

This work was funded in part by grants from the US National Science Foundation to the Global Lake Ecological Observatory Network (GLEON). ELK and KDM were supported by an NSF CAREER award (CBET 0738039) and the National Institute of Food and Agriculture,

United States Department of Agriculture (ID number WIS01516). This material is based upon NTL LTER work supported by the National Science Foundation under Cooperative Agreement #0822700. Wavelet software was provided by C. Torrence and G. Compo, and is available at URL: http://atoc.colorado.edu/research/wavelets/. We are grateful for the thoughtful comments of four anonymous reviewers.

3.8 References

Alewell, C., Manderscheid, B., 1998. Use of objective criteria for the assessment of biogeochemical ecosystem models. Ecological Modelling 107(2-3) 213-224.

Alexander, R., Imberger, J., 2009. Spatial distribution of motile phytoplankton in a stratified reservoir: the physical controls on patch formation. Journal of Plankton Research 31(1) 101-118.

Arhonditsis, G.B., Brett, M.T., 2004. Evaluation of the current state of mechanistic aquatic biogeochemical modeling. Marine Ecology-Progress Series 271 13-26.

Arhonditsis, G.B., Brett, M.T., 2005a. Eutrophication model for Lake Washington (USA) Part I. Model description and sensitivity analysis. Ecological Modelling 187(2-3) 140-178.

Arhonditsis, G.B., Brett, M.T., 2005b. Eutrophication model for Lake Washington (USA) Part II - model calibration and system dynamics analysis. Ecological Modelling 187(2-3) 179-200.

Beck, M.B., Gupta, H., Rastetter, E., Shoemaker, C., Tarboton, D., Butler, D., Edelson, D., Graber, H., Gross, L., Harmon, T., McLaughlin, D., Paola, C., Peters, D., Scavia, D., Schnoor, J.L.,
Weber, L., 2009. Grand challenges of the future for environmental modeling. Warnell School of Forestry and Natural Resources, University of Georgia, Arlington, VA.

Beckel, A.L., 1987. Breaking new waters: A century of limnology at the University of Wisconsin, Transaction of the Wisconsin Academy of Sciences, Arts, and Letters: Madison, WI.

Birge, E.A., 1915. The heat budgets of American and European Lakes, Transaction of the Wisconsin Academy of Sciences, Arts, and Letters: Madison, WI, pp. 116-213.

Birge, E.A., Juday, C., 1911. The inland lakes of Wisconsin: the dissolved gases of the water and their biological significance. Wisconsin Geological and Natural History Survey Bulletin 22 Scientific Series No. 7, Madison, WI.

Blukacz, E.A., Shuter, B.J., Sprules, W.G., 2009. Towards understanding the relationship between wind conditions and plankton patchiness. Limnology and Oceanography 54(5) 1530-1540.

Brock, T.D., 1985. A Eutrophic Lake, Lake Mendota, WI, 1st ed. Springer-Verlag, New York.

Carmichael, W.W., 2002. Health effects of toxin producing cyanobacteria: "The Cyanohabs", In: Melchiorre, S., Viaggiu, E., Bruno, M. (Eds.), Freshwater harmful algal blooms: health risk and control management Istituto Superiore di Sanità Istituto Superiore di Sanità. Rome, Italy pp. 70-80.

Carpenter, S.R., Lathrop, R.C., Nowak, P., Bennett, E.M., T., R., Soranno, P.A., 2006. The ongoing experiment: restoration of Lake Mendota and its watershed. Oxford University Press.

Carpenter, S.R., Leavitt, P.R., 1991. Temporal Variation in a Paleolimnological Record Arising from a Trophic Cascade. Ecology 72(1) 277-285.

Cazelles, B., Chavez, M., Berteaux, D., Menard, F., Vik, J.O., Jenouvrier, S., Stenseth, N.C., 2008. Wavelet analysis of ecological time series. Oecologia 156(2) 287-304.

Culver, D.A., Boucherle, M.M., Bean, D.J., Fletcher, J.W., 1985. Biomass of Freshwater Crustacean Zooplankton from Length‚ÄìWeight Regressions. Canadian Journal of Fisheries and Aquatic Sciences 42(8) 1380-1390.

Elliott, J.A., Persson, I., Thackeray, S.J., Blenckner, T., 2007. Phytoplankton modelling of Lake Erken, Sweden by linking the models PROBE and PROTECH. Ecological Modelling 202(3-4) 421-426.

Falkowski, P., Kiefer, D.A., 1985. Chlorophyll-a fluorescence in phytoplankton - relationship to photosynthesis and biomass Journal of Plankton Research 7(5) 715-731.

Flynn, K.J., 2005a. Castles built on sand: dysfunctionality in plankton models and the inadequacy of dialogue between biologists and modellers. Journal of Plankton Research 27(12) 1205-1210.

Flynn, K.J., 2005b. Modelling marine phytoplankton growth under eutrophic conditions. Journal of Sea Research 54(1) 92-103.

Fragoso, C.R., Marques, D., Collischonn, W., Tucci, C.E.M., van Nes, E.H., 2008. Modelling spatial heterogeneity of phytoplankton in Lake Mangueira, a large shallow subtropical lake in South Brazil. Ecological Modelling 219(1-2) 125-137.

Fuchs, E., Zimmerman, R.C., Jaffe, J.S., 2002. The effect of elevated levels of phaeophytin in natural water on variable fluorescence measured from phytoplankton. Journal of Plankton Research 24(11) 1221-1229.

Gal, G., Hipsey, M.R., Parparov, A., Wagner, U., Makler, V., Zohary, T., 2009. Implementation of ecological modeling as an effective management and investigation tool: Lake Kinneret as a case study. Ecological Modelling 220(13-14) 1697-1718.

Geider, R.J., 1987. Light and temperature dependence of the carbon to chlorophyll-a ratio in microalgae and cyanobacteria- implications for physiology and growth of phytoplankton New Phytologist 106(1) 1-34.

Gregor, J., Geris, R., Marsalek, B., Hetesa, J., Marvan, P., 2005. In situ quantification of phytoplankton in reservoirs using a submersible spectrofluorometer. Hydrobiologia 548 141-151.

Gregor, J., Marsalek, B., 2004. Freshwater phytoplankton quantification by chlorophyll alpha: a comparative study of in vitro, in vivo and in situ methods. Water Research 38(3) 517-522.

Hanson, P.C., Carpenter, S.R., Armstrong, D.E., Stanley, E.H., Kratz, T.K., 2006. Lake Dissolved Inorganic Carbon and Dissolved Oxygen: Changing Drivers from Days to Decades. Ecological Monographs 76(3) 343-363.

Harris, G.P., 1987. Time-series analysis of water-quality data from Lake Ontario- implications for the measurement of water-quality in large and small lakes Freshwater Biology 18(3) 389-403.

Heaney, S.I., 1978. Some observations on the use of the in vivo fluorescence technique to determine chlorophyll-a in natural populations and cultures of freshwater phytoplankton. Freshwater Biology 8(2) 115-126.

Hillmer, I., van Reenen, P., Imberger, J., Zohary, T., 2008. Phytoplankton patchiness and their role in the modelled productivity of a large, seasonally stratified lake. Ecological Modelling 218(1-2) 49-59.

Holdren, G.C., Armstrong, D.E., 1980. Factors affecting phosphorus release from intact lake sediment cores Environmental Science & Technology 14(1) 79-87.

Imberger, J., Patterson, J.C., 1981. A dynamic reservior simulation model- DYRESM 5, In: Fischer, H.B. (Ed.), Transport models for inland and coastal waters. Academic Press: New York.

Janse, J.H., Scheffer, M., Lijklema, L., Van Liere, L., Sloot, J.S., Mooij, W.M., 2010. Estimating the critical phosphorus loading of shallow lakes with the ecosystem model PCLake: Sensitivity, calibration and uncertainty. Ecological Modelling 221(4) 654-665.

Jassby, A.D., Goldman, C.R., Reuter, J.E., Richards, R.C., 1999. Origins and Scale Dependence of Temporal Variability in the Transparency of Lake Tahoe, California-Nevada. Limnology and Oceanography 44(2) 282-294.

Jassby, A.D., Powell, T.M., Goldman, C.R., 1990. Interannual Fluctuations in Primary Production: Direct Physical Effects and the Trophic Cascade at Castle Lake, California. Limnology and Oceanography 35(5) 1021-1038.

Jonasson, S., Eriksson, J., Berntzon, L., Spacil, Z., Ilag, L.L., Ronnevi, L.O., Rasmussen, U., Bergman, B., 2010. Transfer of a cyanobacterial neurotoxin within a temperate aquatic ecosystem suggests pathways for human exposure. Proceedings of the National Academy of Sciences of the United States of America 107(20) 9252-9257.

Jorgensen, S.E., Bendoricchio, G., 2001. Fundamentals of Ecological Modelling, 3rd ed. Elsevier Science Oxford, UK.

Juday, C., 1914. The inland waters of Wisconsin: the hydrography and morphometry of the lakes. Wisconsin Geological and Natural History Survey Bulletin 27 Scientific Series No. 9, Madison, WI.

Kamarainen, A.M., Yuan, H.L., Wu, C.H., Carpenter, S.R., 2009. Estimates of phosphorus entrainment in Lake Mendota: a comparison of one-dimensional and three-dimensional approaches. Limnology and Oceanography-Methods 7 553-567.

Keitt, T.H., Fischer, J., 2006. Detection of scale-specific community dynamics using wavelets. Ecology 87(11) 2895-2904.

Kepner, R.L., Pratt, J.R., 1994. Use of Fluorochromes for Direct Enumeration of Total Bacteria in Environmental-Samples - Past and Present. Microbiological Reviews 58(4) 603-615.

Kirk, J.T.O., 1994. Estimation of the absorption and the scattering coefficients of natural waters by use of underwater irradiance measurements. Applied Optics 33(15) 3276-3278.

Koltun, G.F., Eberle, M., Gray, J.R., Glysson, G.D., 2006. User's manual for the Graphical Constituent Loading Analysis System (GCLAS), In: Methods, U.T.a. (Ed.), p. 51.

Langman, O.C., Hanson, P.C., Carpenter, S.R., Hu, Y.H., 2010. Control of dissolved oxygen in northern temperate lakes over scales ranging from minutes to days. Aquatic Biology 9(2) 193-202.

Lathrop, R.C., 1979. Dane County water quality plan, In: Commission, D.C.R.P. (Ed.): Madison, WI.

Lathrop, R.C., Carpenter, S.R., Robertson, D.M., 1999. Summer water clarity responses to phosphorus, *Daphnia* grazing, and internal mixing in Lake Mendota. Limnology and Oceanography 44(1) 137-146.

Lean, D.R.S., 1973a. Movements of phosphorus between its biologically important forms in lake water. Journal of the Fisheries Research Board of Canada 30(10) 1525-1536.

Lean, D.R.S., 1973b. Phosphorus dynamics in lake water. Science 179(4074) 678-680.

Magnuson, J.J., Kratz, T.K., Benson, B.J., 2006. The Challenge of Time and Space in Ecology, In: Magnuson, J.J., Kratz, T.K., Benson, B.J. (Eds.), Long-term dynamics of lakes in the landscape: long-term ecological research on North Temperate Lakes. Oxford University Press, pp. 3-16.

Makler-Pick, V., Gal, G., Gorfine, M., Hipsey, M.R., Carmel, Y., 2011. Sensitivity analysis for complex ecological models - A new approach. Environmental Modelling & Software 26(2) 124-134.

Markensten, H., Moore, K., Persson, I., 2010. Simulated lake phytoplankton composition shifts toward cyanobacteria dominance in a future warmer climate. Ecological Applications 20(3) 752-767.

Marra, J., 1997. Analysis of diel variability in chlorophyll fluorescence. Journal of Marine Research 55(4) 767-784.

McCauley, E., 1984. A manual on methods for the assessment of secondary production in fresh waters. Blackwell Sci. Publ. , Oxford.

Morris, D.P., Zagarese, H., Williamson, C.E., Balseiro, E.G., Hargreaves, B.R., Modenutti, B., Moeller, R., Queimalinos, C., 1995. The attentuation of solar UV radiation in lakes and the role of dissolved organic carbon. Limnology and Oceanography 40(8) 1381-1391.

NTL-LTER, 2011a. Biological dataset: Madison, WI.

NTL-LTER, 2011b. Chemical Limnology dataset. North Temperate Lakes Long Term Ecological Research program, http://www.lternet.edu/sites/ntl/: Madison, WI.

NTL-LTER, 2011c. Physical Limnology dataset. North Temperate Lakes Long Term Ecological Research program, http://www.lternet.edu/sites/ntl/: Madison, WI.

Peeters, F., Wuest, A., Piepke, G., Imboden, D.M., 1996. Horizontal mixing in lakes. Journal of Geophysical Research-Oceans 101(C8) 18361-18375.

Platt, T., Dickie, L.M., Trites, R.W., 1970. Spatial heterogeneity of phytoplankton in a nearshore environment Journal of the Fisheries Research Board of Canada 27(8) 1453-&.

Pope, R.M., Fry, E.S., 1997. Absorption spectrum (380-700 nm) of pure water .2. Integrating cavity measurements. Applied Optics 36(33) 8710-8723.

Porter, J.H., Nagy, E., Kratz, T.K., Hanson, P., Collins, S.L., Arzberger, P., 2009. New Eyes on the World: Advanced Sensors for Ecology. Bioscience 59(5) 385-397.

Reynolds, C., 2006. The Ecology of Phytoplankton, 3rd ed. Cambridge University Press, New York.

Rigosi, A., MarcÈ, R., Escot, C., Rueda, F.J., 2011. A calibration strategy for dynamic succession models including several phytoplankton groups. Environmental Modelling & Software 26(6) 697-710.

Romero, J.R., Antenucci, J.P., Imberger, J., 2004. One- and three-dimensional biogeochemical simulations of two differing reservoirs. Ecological Modelling 174(1-2) 143-160.

Serizawa, H., Amemiya, T., Itoh, K., 2010. Effects of buoyancy, transparency and zooplankton feeding on surface maxima and deep maxima: Comprehensive mathematical model for vertical distribution in cyanobacterial biomass. Ecological Modelling 221(17) 2028-2037.

Shade, A., Carey, C.C., Kara, E., Bertilsson, S., McMahon, K.D., Smith, M.C., 2009. Can the black box be cracked? The augmentation of microbial ecology by high-resolution, automated sensing technologies. Isme Journal 3(8) 881-888.

Steele, J.H., Henderson, E.W., 1992. A simple model for plankton patchiness Journal of Plankton Research 14(10) 1397-1403.

Stewart, K.M., 1976. Oxygen Deficits, Clarity, and Eutrophication in some Madison Lakes. Int. Revue ges. Hydrobiol. Hydrogr. 61(5) 16.

Torrence, C., Compo, G.P., 1998. A practical guide to wavelet analysis. Bulletin of the American Meteorological Society 79(1) 61-78.

Trolle, D., Hamilton, D.P., Pilditch, C.A., Duggan, I.C., Jeppesen, E., 2011. Predicting the effects of climate change on trophic status of three morphologically varying lakes: Implications for lake restoration and management. Environmental Modelling & Software 26(4) 354-370.

Trolle, D., Skovgaard, H., Jeppesen, E., 2008. The Water Framework Directive: Setting the phosphorus loading target for a deep lake in Denmark using the 1D lake ecosystem model DYRESM-CAEDYM. Ecological Modelling 219(1-2) 138-152.

Ventura, M., Camarero, L., Buchcaca, T., Bartumeus, F., Livingstone, D.M., Catalan, J., 2000. The main features of seasonal variability in the external forcing and dynamics of a deep mountain lake (Redo, Pyrenees). J. Limnol. 59(1) 97-108.

Vos, R.J., Hakvoort, J.H.M., Jordans, R.W.J., Ibelings, B.W., 2003. Multiplatform optical monitoring of eutrophication in temporally and spatially variable lakes. Science of the Total Environment 312(1-3) 221-243.

Wetzel, R.G., 2001. Limnology: Lake and River Ecosystems, 3rd ed. Academic Press, San Diego.

Wiebe, P.H., Boyd, S., Cox, J.L., 1975. Relationships between zooplankton displacement volume, wet weight, dry weight, and carbon. Fishery Bulletin 73(4) 777-786.

Yuan, H.L., 2007. Development of a non-hydrostatic model and its application to two akes in Madison, WI, Civil and Environmental Engineering. University of Wisconsin-Madison: Madison, p. 232.

3.9 Tables

Table 3.1 General (a), bacterial (b), phytoplankton (c) and zooplankton (d) parameters used for the CAEDYM simulations, with modifications after Gal et al (2009).

Table 3.1a General parameters

Parameter	Description	Units	Assigned value	Values from field/literature
K_d	Light extinction coefficient of pure water	m^{-1}	0.25	
K_{PAR}	Fraction of incoming solar radiation which is photosynthetically active	-	0.45	
K_{eDOC}	Specific light attenuation coefficient due to the action of labile DOC	m^{-1} $(gC\ m^{-3})^{-1}$	0.02	0.02[a]
K_{eDOC}	Specific light attenuation coefficient due to the action of refractory DOC	m^{-1} $(gC\ m^{-3})^{-1}$	0.001	0.001[b]
K_{ePOC}	Specific light attenuation coefficient due to the action of labile POC	m^{-1} $(gC\ m^{-3})^{-1}$	0.01	0.01[a]
K_{ePOC}	Specific light attenuation coefficient due to the action of refractory POC	m^{-1} $(gC\ m^{-3})^{-1}$	0.02	
k_{SOD}	Maximum sediment oxygen demand (SOD) at 20°C	$g\ m^{-2}\ day^{-1}$	0.46	0.918[c], 7.97[d]
$k_{DO_{SOD}}$	Half saturation constant for DO effect on SOD	$g\ DO\ m^{-3}$	1.5	1.5[iv], 0.5[c]
ϑ_{SOD}	Temperature multiplier for SOD	-	1.08	1.02-1.14[e]
DO^{atm}	Equivalent DO at the air-water interface	$g\ DO\ m^{-3}$	Equation	$DO^{atm} = f(p,T,S)$[e]
k_{O_2}	Oxygen transfer coefficient dependent on wind speed	$m\ s^{-1}$	Equation	$k_{O_2} = f(u,T,S)$[e]
pCO_2^{atm}	Partial pressure of CO_2 at the air-water interface	atm	350×10^{-6}	
k_{pCO_2}	Gas transfer velocity for CO_2	$m\ s^{-1}$	Equation	$k_{pCO_2} = f(u,T,S)$[e]
K_w	Ion product of water		Equation	$K_w = f(T)$[f]
$K_{a1}; K_{a2}$	First and second acidity constants		Equation	$K_{a1,2} = f(T)$[f]
$Y_{O_2:C}$	Stoichiometric ratio of DO to C during photosynthesis and respiration	$g\ DO\ (g\ C)^{-1}$	2.67	Stoichiometric relationship
$Y_{O_2:N}$	Stoichiometric ratio of DO to N during nitrification	$g\ DO\ (g\ N)^{-1}$	3.43	Stoichiometric relationship
$V_{s_{POM}}$	Settling velocity of particulate detritus (POM), used for POC, PON, POP	$m\ s^{-1}$	Equation	Calculated from Stoke's Law: $V_{s_{POM}} = \frac{g d_{POM}^2}{18\nu}(\rho_{POM} - \rho_w)$
d_{POM}	Diameter of POM particles	m	8×10^{-5}	

ρ_{POM}	Density of POM particles	kg m^{-3}	1040	1070[g]
$\mu_{DEC\ POC}$	Maximum rate of POC decomposition to DOC at 20°C	day^{-1}	0.070	0.0187 (benthic) [h]
$\mu_{DEC\ POP}$	Maximum rate of POP decomposition to DOP at 20°C	day^{-1}	0.030	0.01-0.1[i]
$\mu_{DEC\ PON}$	Maximum rate of PON decomposition to DON at 20°C	day^{-1}	0.035	0.01-0.03[i]
k_{den}	Maximum denitrification rate under anoxia at 20°C	day^{-1}	0.05	0.1[i]
ϑ_{den}	Temperature multiplier for denitrification	-	1.05	1.045 [h]
K_{den}	Half saturation constant for denitrification dependence on oxygen	g DO m^{-3}	0.4	0.4[i]
k_{nit}	Maximum nitrification rate under oxygen saturation at 20°C	day^{-1}	0.106	0.106[d], 0.1-0.2[i]
ϑ_{nit}	Temperature multiplier for nitrification	-	1.08	1.08[i]
K_{nit}	Half saturation constant for nitrification dependence on oxygen	g DO m^{-3}	1.5	1.5[d]
ϑ_{S}	Temperature multiplier for sediment nutrient fluxes	-	1.08	
S_{FRP}	Maximum release rate of PO_4 from sediments at 20°C	g m^{-2} day^{-1}	0.0125	0.03[d], 0.065[j], 0.0008[k]
$K_{DO_{FRP}}$	Half saturation constant for sediment PO_4 release dependence on DO	g DO m^{-3}	2.0	2.0[d]
S_{NH_4}	Maximum release rate of NH_4 from sediments at 20°C	g m^{-2} day^{-1}	0.31	0.31[d]
$K_{DO_{NH4}}$	Half saturation constant for sediment NH_4 release dependence on DO	g DO m^{-3}	2.0	2.0 [d], 0.025[k]
S_{NO_3}	Maximum release rate of NO_3 from sediments at 20°C	g m^{-2} day^{-1}	-0.12	-0.12[d]
$K_{DO_{NO3}}$	Half saturation constant for sediment NH_4 release dependence on DO	g DO m^{-3}	50	50[d]
S_{DOC}	Maximum release rate of DOC from sediments at 20°C	g m^{-2} day^{-1}	0.0	0.0[d]
S_{DOC}	Maximum release rate of DOP from sediments at 20°C	g m^{-2} day^{-1}	0.0	0.0[d]
S_{DOC}	Maximum release rate of DON from sediments at 20°C	g m^{-2} day^{-1}	0.0	0.0[d]
$K_{DO_{DOC}}$	Half sat constant for sediment DOC release dependence on DO	g DO m^{-3}	0.5	0.5[d]

Source

[a] Kirk, J.T.O., 1994. Estimation of the absorption and the scattering coefficients of natural waters by use of underwater irradiance measurements. Applied Optics 33(15) 3276-3278.

[b] Morris, D.P., Zagarese, H., Williamson, C.E., Balseiro, E.G., Hargreaves, B.R., Modenutti, B., Moeller, R., Queimalinos, C., 1995. The attentuation of solar UV radiation in lakes and the role of dissolved organic carbon. Limnology and Oceanography 40(8) 1381-1391.

[c] Brock, T.D., 1985. A Eutrophic Lake, Lake Mendota, WI, 1st ed. Springer-Verlag, New York.

[d] Derived from NTL LTER data specific to Lake Mendota.

[e] Wanninkhof, R., 1992. Relationship between wind-spped and gas-exchange over the ocean. Journal of Geophysical Research-Oceans 97(C5) 7373-7382.
[f] Butler, J.N., 1982. Carbon dioxide equilibria and their applications. Addison-Wesley.
[g] Degobbis, D., Gilmartin, M., 1990. Nitrogen, phosphorus, and biogenic silicon budgets for the northern Adriatic Sea. Oceanologica Acta 13(1) 31-45.
[h] Sinsabaugh, R.L., Findlay, S., 1995. Microbial production, enzyme activity, and carbon turnover in surface sediments of the Hudson River estuary. Microbial Ecology 30(2) 127-141.
[i] Jorgensen, S.E., Bendoricchio, G., 2001. Fundamentals of Ecological Modelling, 3rd ed. Elsevier Science Oxford, UK.
[j] Holdren, G.C., Armstrong, D.E., 1980. Factors affecting phosphorus release from intact lake sediment cores Environmental Science & Technology 14(1) 79-87.
[k] Serruya, C., Edelstein, M., Pollingher, U., Serruya, S., 1974. Lake Kinneret sediments: nutrient composition of the pore water and mud water exchanges. Limnology and Oceanography 19(3) 489-508.

Table 3.1b Bacterial parameters				
Parameter	**Description**	**Units**	**Assigned values**	**Values from field/literature**
ϑ_B	Temperature multiplier for growth	-	1.08	
T_{STD_B}	Standard temperature	°C	20	
T_{OPT_B}	Optimum temperature	°C	30	30[l]
T_{MAX_B}	Maximum temperature	°C	38	38[l]
K_{DO_B}	Half saturation constant for dependence of POM/DOM decomposition on DO	g DO m^{-3}	1.5	
f_{An_B}	Aerobic/anaerobic factor	-	0.8	
ϑ_{Br}	Temperature multiplier for loss	-	1.08	
k_{Br}	Bacterial respiration rate at 20°C	day^{-1}	0.12	
k_{Be}	DOC Excretion	-	0.7	
K_B	Half saturation constant for bacteria function	g C m^{-3}	0.01	
$\mu_{DEC\ DOC}$	Maximum bacterial DOC uptake rate	day^{-1}	0.05	
k_{BIN}	Internal C:N ratio of bacteria	g N $(g\ C)^{-1}$	0.16	0.16[m]
k_{BIP}	Internal C:P ratio of bacteria	g P $(g\ C)^{-1}$	0.04	0.04[m]

Sources

[l] Lovell, C.R., Konopka, A., 1985. The effects of temperature on bacterial production in a dimictic eutrophic lake. FEMS Microbiology Ecology 31(3) 135-140.
[m] Makino, W., Cotner, J.B., 2004. Elemental stoichiometry of a heterotrophic bacterial community in a freshwater lake: implications for growth- and resource-dependent variations. Aquatic Microbial Ecology 34(1) 33-41.

Table 3.1c Phytoplankton parameters

Parameter	Description	Units	Assigned values				Values from field/literature			
			A_{Mic}: *Microcystis*	A_{Aph}: *Aphanizomenon/ Anabaena*	A_{Chlor}: *Chlorophytes/ Chrysophytes*	A_{Diat}: *Diatoms*	A_{Mic}: *Microcystis*	A_{Aph}: *Aphanizomenon/ Anabaena*	A_{Chlor}: *Chlorophytes/ Chrysophytes*	A_{Diat}: *Diatoms*
μ_{MAX}	Maximum potential growth rate	day^{-1}	0.6	0.48	0.2	1.25	0.048-1.11[n]	0.27-0.98[o] 0.27-1.56[p]	2.4-8.57[q] 0.62-2.91[n] 0.33-0.55[r]	1.7[s]
I_s	Light saturation for maximum production	$\mu mol\ m^{-2}s^{-1}$	250	220	170	20			75[a]	
K_{eA}	Specific attenuation coefficient	$m^{-1}\ (gC\ m^{-3})^{-1}$	0.198	0.198	0.198	0.198				0.448[t]
K_P	Half saturation constant for phosphorus uptake	$g\ P\ m^{-3}$	0.0018	0.0012	0.01	0.005			0.0011[u] 0.001[v]	0.0028-0.0111[u]
K_N	Half saturation constant for nitrogen uptake	$g\ N\ m^{-3}$	0.02	0.001	0.030	0.060				
IN_{MIN}	Minimum internal N ratio	$g\ N\ (g\ C)^{-1}$	0.070	0.070	0.090	0.090	0.163[n]	0.163[n]	0.034[n]	0.125[u]
IN_{MAX}	Maximum internal N ratio	$g\ N\ (g\ C)^{-1}$	0.24	0.16	0.14	0.15	0.239[n]	0.239[n]	0.135[n]	0.146[u]
UN_{MAX}	Maximum rate of nitrogen uptake	$g\ N\ (g\ C)^{-1}\ day^{-1}$	0.08	0.12	0.060	0.15				
IP_{MIN}	Minimum internal P ratio	$g\ P\ (g\ C)^{-1}$	0.002	0.005	0.006	0.021	0.014[n]	0.014[n]	0.021[n]	0.0119[u]
IP_{MAX}	Maximum internal P ratio	$g\ P\ (g\ C)^{-1}$	0.023	0.023	0.059	0.085	0.023[n]	0.023[n]	0.059[n]	0.085[u]
UP_{MAX}	Maximum rate of phosphorus uptake	$g\ P\ (g\ C)^{-1}\ day^{-1}$	0.01	0.01	0.007	0.018	0.01[w]		0.0074[u]	0.0031-0.0187[u]
k_{NF}	N fixation rate	$g\ N\ (g\ C)^{-1}\ day^{-1}$	0	0.15	0	0	0	0.140[x]	0	0
f_{NF}	Growth reduction under N_2 fixation	-	1.00	0.67	1.00	1.00				
ϑ_{Ag}	Temperature multiplier for growth	-	1.07	1.10	1.08	1.08	1.075[y]		1.075[y]	
T_{STD_A}	Standard temperature	°C	19	24	20	19				
T_{OPT_A}	Optimum temperature	°C	30	30	21	17	20-30[u] 29-34[z]	25[n]	14-28[aa] 14-25[oo], 20[bb]	16-17[u]
T_{MAX_A}	Maximum temperature	°C	40	40	35	22	35[z]	30[n]	29-35[aa], >35[u]	26-27[u]

k_r	Metabolic loss rate coefficient	day^{-1}	0.05	0.05	0.05	0.05	0.08[cc]		0.07[qq]	0.039-0.051[u] 0.01[qq]
ϑ_{Ar}	Temperature multiplier for metabolic loss	-	1.10	1.09	1.06	1.08			1.05[y]	
k_{pr}	Rate of photorespiration (day^{-1})	-	0.014	0.014	0.014	0.014				
f_{res}	Fraction of respiration relative to total metabolic loss	-	0.8	0.8	0.8	0.5				
f_{DOM}	Fraction of metabolic loss rate that goes to DOM	-	0.3	0.1	0.1	0.5				
d_A	Cell diameter	m	$1x10^{-5}$	$1x10^{-7}$	$1x10^{-5}$	$1x10^{-5}$				
V_{S_A}	Settling velocity	$m\ s^{-1}$	$3.6x10^{-5}$	$-5.1x10^{-7}$	$1.2x10^{-6}$	-0.057				$7x10^{-6}$-$1.2x10^{-5}$[u]
Y_{ChlC}	Chlorophyll:C ratio	-	50	100	40	40				
$Y_{CBiovol}$	Carbon:biovolume ratio (used for estimating algal biomass gC/m^3)	$pg\ C\ \mu m^{-3}$	0.127	0.127	0.198	0.199	0.127[n]	0.127[n]	0.198[n]	0.199[n]

Sources

[n] Reynolds, C., 2006. The Ecology of Phytoplankton, 3rd ed. Cambridge University Press, New York.

[o] Foy, R.H., Gibson, C.E., Smith, R.V., 1976. The influence of daylength, light intensity, and temperature on the growth rates of planktonic blue-green algae. British Phycological Journal 11(2) 151-163.

[p] Fogg, G.E., 1949. Growth and heterocycst production in Anabena cylindrica Lemm II. in relation to carbon and nitrogen metabolism Ann. Botany London 13 241-259.

[q] Pollingher, U., Berman, T., 1982. Relative contributions of net and nanno phytoplankton to primary production in Lake Kinneret (Israel) Archiv. fur Hydrobiologie 96(1) 33-46.

[r] Sandgren, C., 1988. Growth and Reproductive Strategies of Freshwater Phytoplankton. Cambridge University Press.

[s] Butterwick, C., Heaney, S.I., Talling, J.F., 2005. Diversity in the influence of temperature on the growth rates of freshwater algae, and its ecological relevance. Freshwater Biology 50(2) 291-300.

[t] Kirk, J.T.O., 1994. Estimation of the absorption and the scattering coefficients of natural waters by use of underwater irradiance measurements. Applied Optics 33(15) 3276-3278.

[u] Zohary, unpublished data (after Gal et al., 2009)

[v] Sandgren, C., 1988. Growth and Reproductive Strategies of Freshwater Phytoplankton. Cambridge University Press.

[w] Healey, F.P., Hendzel, L.L., 1979. Indicators of phosphorus and nitrogen deficiency in 5 algae in cultures. Journal of the Fisheries Research Board of Canada 36(11) 1364-1369.

[x] Dugdale, V.A., Dugdale, R.C., 1962. Nitrogen metabolism in lakes. II. role of nitrogen fixation in sanctuary Lake Pennsylvania. Limnology and Oceanography 7(2) 170-177.

[y] Hipsey et al. in preparation

[z] Imai, H., Chang, K.H., Kusaba, M., Nakano, S., 2009. Temperature-dependent dominance of Microcystis (Cyanophyceae) species: M. aeruginosa and M. wesenbergii. Journal of Plankton Research 31(2) 171-178.
[aa] Ukeles, R., 1961. The Effect of Temperature on the Growth and Survival of Several Marine Algal Species. Biological Bulletin 120(2) 255-264.
[bb] Sandgren, 1995. Chrysophyte Algae: Ecology, Phylogeny, and Development. Cambridge University Press.
[cc] Robson, B.J., Hamilton, D.P., 2004. Three-dimensional modelling of a Microcystis bloom event in the Swan River estuary, Western Australia. Ecological Modelling 174(1-2) 203-222.

Table 3.1d Zooplankton parameters

Parameter	Description	Units	Assigned values				Values from field/literature			
			Z_1: Predatory	***Z_2: Macro-large***	***Z_3: Macro-small***	***Z_4: Micro***	***Z_1: Predatory***	***Z_2: Macro-large***	***Z_3: Macro-small***	***Z_4: Micro***
g_{MAX}	Grazing rate	gC m^{-3} $(g\ Z\ m^{-3})^{-1}$ day^{-1}	1	0.75	0.3	0.5	1[dd]	0.75[ee] 1.67[ff]	0.3[ee]	
k_{mf}	Grazing efficiency	-	0.8	0.7	0.8	0.85				
k_{Zr}	Respiration rate coefficient	day^{-1}	0.1	0.2	0.075	0.025	0.32[dd]	0.12[ff] 0.195[gg]	0.06[hh]	
k_{Zm}	Mortality rate coefficient	day^{-1}	0.02	0.04	0.015	0.005				
k_{Zf}	Fecal pellet fraction of grazing	day^{-1}	0.025	0.05	0.02	0.007				
k_{Ze}	Excretion fraction of grazing	day^{-1}	0.1	0.1	0.1	0.1	0.13[dd]	0.11[ff]		
$f_{f_{SED}}$	Fecal pellet fraction that sinks directly to sediments	-	0.7	0.1	0.1	0.1				
ϑ_{Zg}	Temperature multiplier for growth	-	1.07	1.07	1.07	1.07	1.1[dd]	1.15[ff]		
T_{STD_Z}	Standard temperature	°C	20	20	20	20	20[dd]	20[ff]	20[dd]	20[ii]
T_{OPT_Z}	Optimum temperature	°C	19	20	18	24	29[dd] 11[ij]	28[ff] 17[jj]	17[jj]	25[ii]
T_{MAX_Z}	Maximum temperature	°C	35	35	35	35	34[dd]	34[ff]		
ϑ_{Zr}	Respiration temperature dependence	-	1.11	1.15	1.06	1.06	1.1[dd]	1.15[ff]		
K_Z	Half saturation constant for grazing	g C m^{-3}	2	2	2	2	0.14[kk]	0.54[ll]		0.164[mm]
k_{ZIN}	Internal ratio of nitrogen to carbon.	g N $(g\ C)^{-1}$	0.18	0.18	0.16	0.15	0.184[nn] 0.18[oo]	0.18[oo]	0.161[pp] 0.114[oo]	0.149[qq]

k_{ZIP}	Internal ratio of phosphorus to carbon	g P (g C)$^{-1}$	0.0045	0.0125	0.006	0.03	0.005[nn] 0.004[oo]	0.012[nn] 0.0125[oo]	0.0083[pp] 0.0066[oo]	0.0212[qq]
P_{zk_1}	Preference of zooplankton for predatory zooplankton	-	0.15	0	0	0	0.1[rr]	0[rr, ss]	0[ss]	0[ss]
P_{zk_2}	Preference of zooplankton for macro- large zooplankton	-	0.15	0	0	0	0.6[rr,ss]	0[rr,ss]	0[ss]	0[ss]
P_{zk_3}	Preference of zooplankton for macro-small zooplankton	-	0.15	0	0	0	0.15[rr,ss]	0[ss]	0[p]	0[ss]
P_{za_4}	Preference of zooplankton for micro zooplankton	-	0.15	0	0	0	0.15[rr,ss]	0[rr,ss]	0[ss]	0[ss]
P_{zp}	Preference of zooplankton for POC	-	0	0.1	0.098	0.05	0[ss]	0.1[tt]	0.098[uu]	
P_{zb}	Preference of zooplankton for Bacteria	-	0	0.6	0.06	0.06	0[ss]	0.15[uu]	0.6[uu]	0.05[uu]
$P_{A\ Mic}$	Preference of zooplankton for *Microcystis*-like phyto	-	0	0.01	0.001	0.05	0[ss]	0.01[vv]	0.001[uu]	0.05[s]
$P_{A\ Aph}$	Preference of zooplankton for *Aphaniazomenon*-like phyto	-	0	0.01	0.001	0.05	0[ss]	0.01[ww]	0.001[uu]	0.05[vv]
$P_{A\ Chlor}$	Preference of zooplankton for Chloro/chryso-like phyto	-	0	0.15	0.075	0.05	0[ss]	0.15[ww]	0.075[uu]	0.05[ww]
$P_{A\ Diat}$	Preference of zooplankton for diatom-like phyto	-	0	0.18	0.075	0.05	0[ss]	0.18[ww]	0.075[uu]	0.05[xx]
Min_{res}	Minimum phytoplankton biomass below which zooplankton will not graze	g C m^{-3}	0.01	0.03	0.8	0.05				

Sources

[dd] Gophen, M., 1976a. Temperature effect on lifespan, metabolism, and development time of *Mesocyclops-leuckarti*. Oecologia 25(3) 271-277.

[ee] Demott, W.R., 1982. Feeding selectivities and relative ingestion rates of Daphnia and Bosmina. Limnology and Oceanography 27(3) 518-527.

[ff] Gophen, M., 1976b. Temperature-dependence of food-intake, ammonia excretion and respiration in Ceriodaphnia-reticulata (Lake Kinneret, Israel) Freshwater Biology 6(5) 451-455.

[gg] Lampert, W., 1986. Respons of the respiratory rate of Daphnia-magna to changing food conditions Oecologia 70(4) 495-501.

[hh] Urabe, J., Watanabe, Y., 1990. Influence of food density on respiration rate of 2 crustacean plankters, Daphnia galeata and Bosmina longirostris. Oecologia 82(3) 362-368.

[ii] Galkovskaja, G.A., 1987. Planktonic rotifers and temperature Hydrobiologia 147 307-317.

[jj] Bertilsson, J., Berzins, B., Pejler, B., 1995. The occurrence of limnic microcrustaceans in relation to temperature and oxygen Hydrobiologia 299(2) 163-167.

[kk] Landry, M., Hassett, R., 1985. Time scales in behavioral, biochemical, and energetic adaptations to food-limiting conditions. Archiv. fur Hydrobiologie(21) 209-211.

[ll] Haney, J., Trout, M., 1985. Size selective grazing by zooplankton in Lake Titicaca. Archiv fuer Hydrobiologie(21) 147-160.

[mm] Stemberger, R.S., Gilbert, J.J., 1985. Body size, food concentration, and population growth in planktonic rotifers. Ecology 66(4) 1151-1159.

[nn] Andersen, T., Hessen, D.O., 1991. Carbon, nitrogen and phosphorus content of freshwater zooplankton. Limnology and Oceanography 36(4) 807-814.

[oo] Sterner, R.W., Hessen, D.O., 1994. Algal nutrient limitation and the nutrition of aquatic herbivores. Annual Review of Ecology and Systematics 25 1-29.

[pp] Dobberfuhl, D.R., Elser, J.J., 2000. Elemental stoichiometry of lower food web components in arctic and temperate lakes. Journal of Plankton Research 22(7) 1341-1354.

[qq] Jensen, T.C., Verschoor, A.M., 2004. Effects of food quality on life history of the rotifer Brachionus calyciflorus Pallas. Freshwater Biology 49(9) 1138-1151.

[rr] Gophen, M., Azoulay, B., 2002. The trophic status of zooplankton communities in Lake Kinneret (Israel). Verh. Internat. Verein. Limnol. 28 836-839.

[ss] Lampert, W., 2007. Limnoecology. Oxford University Press Inc.

[tt] Lampert, W., 1974. Method for determining food selection by zooplankton Limnology and Oceanography 19(6) 995-998.

Table 3.2 Coefficient of determination (R^2) from linear regression, Spearman's rank correlation coefficient (Spearman's rho), and NMAE value for key state variables and observed data. Number of observation indicates number of values used in analyses after outlier removal and aggregation. Depth range of 0-20 indicates discrete sampling depths detailed in Methods.

State Variable	Frequency of Observation (aggregated frequency, when applicable)	Depth or depth range (no. of discrete depths)	Number of observations	R^2	Spearman's rho	NMAE	Wavelet analysis
Temperature	min^{-1} (hr^{-1})	0.5 (1)	1488	0.83	0.92	0.034	x
Temperature	min^{-1} (2 hr^{-1})	0-20 (24)	21,230	0.94	0.97	0.047	
DO	min^{-1} (hr^{-1})	0.5 (1)	1777	0.01	-0.04	0.26	x
DO	2 $week^{-1}$	0-20 (24)	178	0.79	0.87	0.32	
Chl-*a* (in situ fluorescence)	min^{-1} (hr^{-1})	0.5(1)	1777	0.10	0.40	1	x
Chl-*a* (extracted, g m^{-3})	$week^{-1}$	0-20 (5)	130	0.07	0.12	1.2	
DIC	$month^{-1}$	0-20 (11)	25	0.84	0.96	0.053	
pH	$week^{-1}$	0-20 (20)	39	0.91	093	0.020	
NH_4^+	$week^{-1}$	0-20 (5)	190	0.11	0.26	1.8	
NO_3^-	$week^{-1}$	0-20 (5)	190	0.75	0.88	0.28	
PO_4^{3-}	$week^{-1}$	0-20 (5)	189	0.33	0.39	1.6	
TN	$week^{-1}$	0-20 (5)	190	0.28	0.65	0.41	
TP	$week^{-1}$	0-20 (5)	173	0.21	0.51	0.35	
DOC	$week^{-1}$	0-20 (5)	189	0	-0.02	0.053	
A_{Aph}	2 $week^{-1}$	0-8 (integrated)	7	0.08	0.70	0.51	
A_{Mic}	2 $week^{-1}$	0-8 (integrated)	7	0.01	-0.20	0.96	
Predicted phytoplankton biomass, respiration, NPP, and GPP	n/a	n/a	2160 (for all variables)	n/a	n/a	n/a	x

3.10 Figures

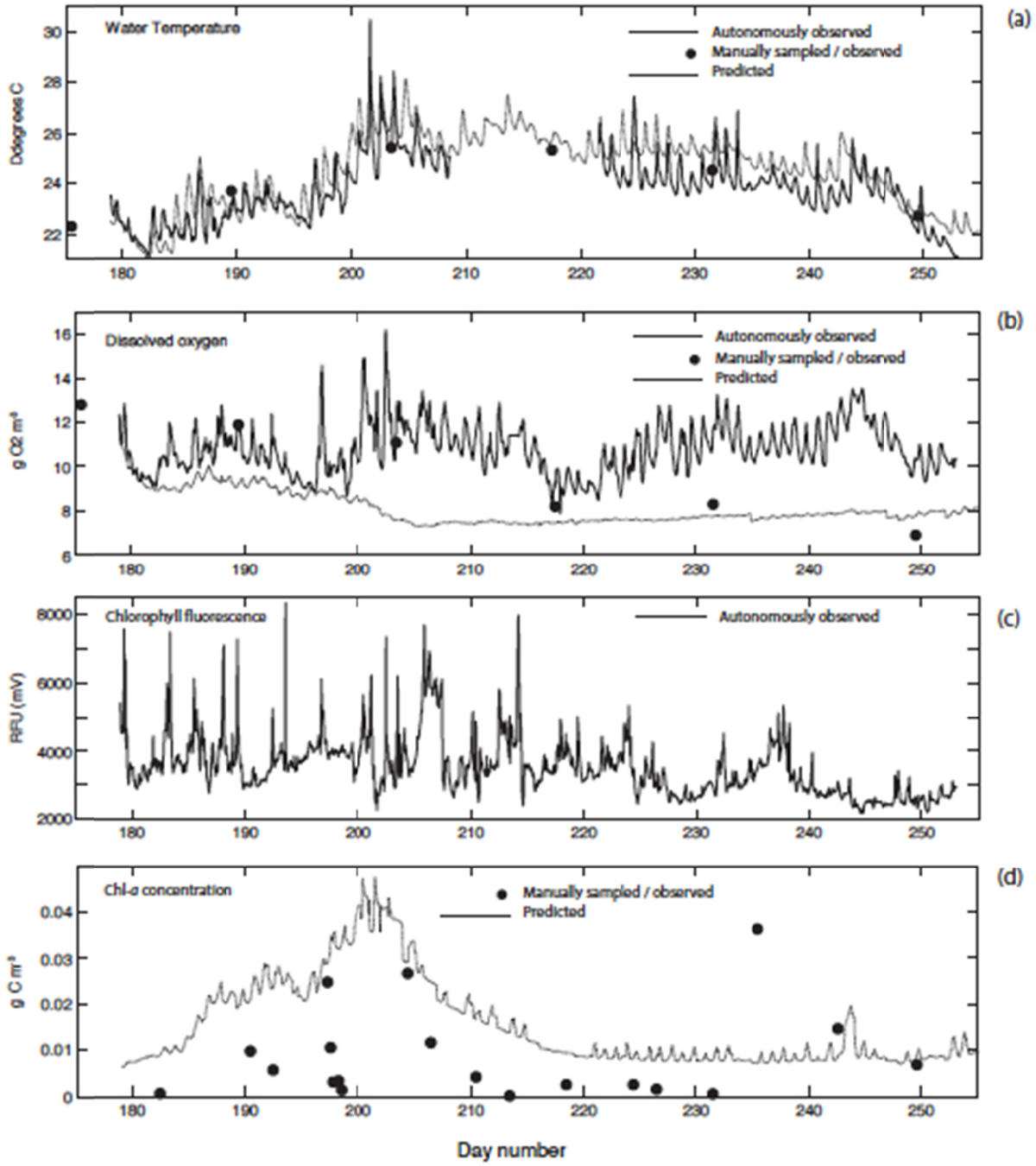

Figure 3.1 High-frequency observed (solid) and predicted (dashed) temperature (a), dissolved oxygen (b) and chl-*a* fluorescence (c) and concentration (d). Predicted values were from the 0.5 m depth layer of the simulation. High frequency observations (a, b, and c) were collected at an instrumented buoy (0.5 m depth) located near the center of Lake Mendota, WI from day number 180 to 270, 2008. Manual temperature, DO, and in vitro solvent –extracted chl-*a* measurements are overlaid as solid circles.

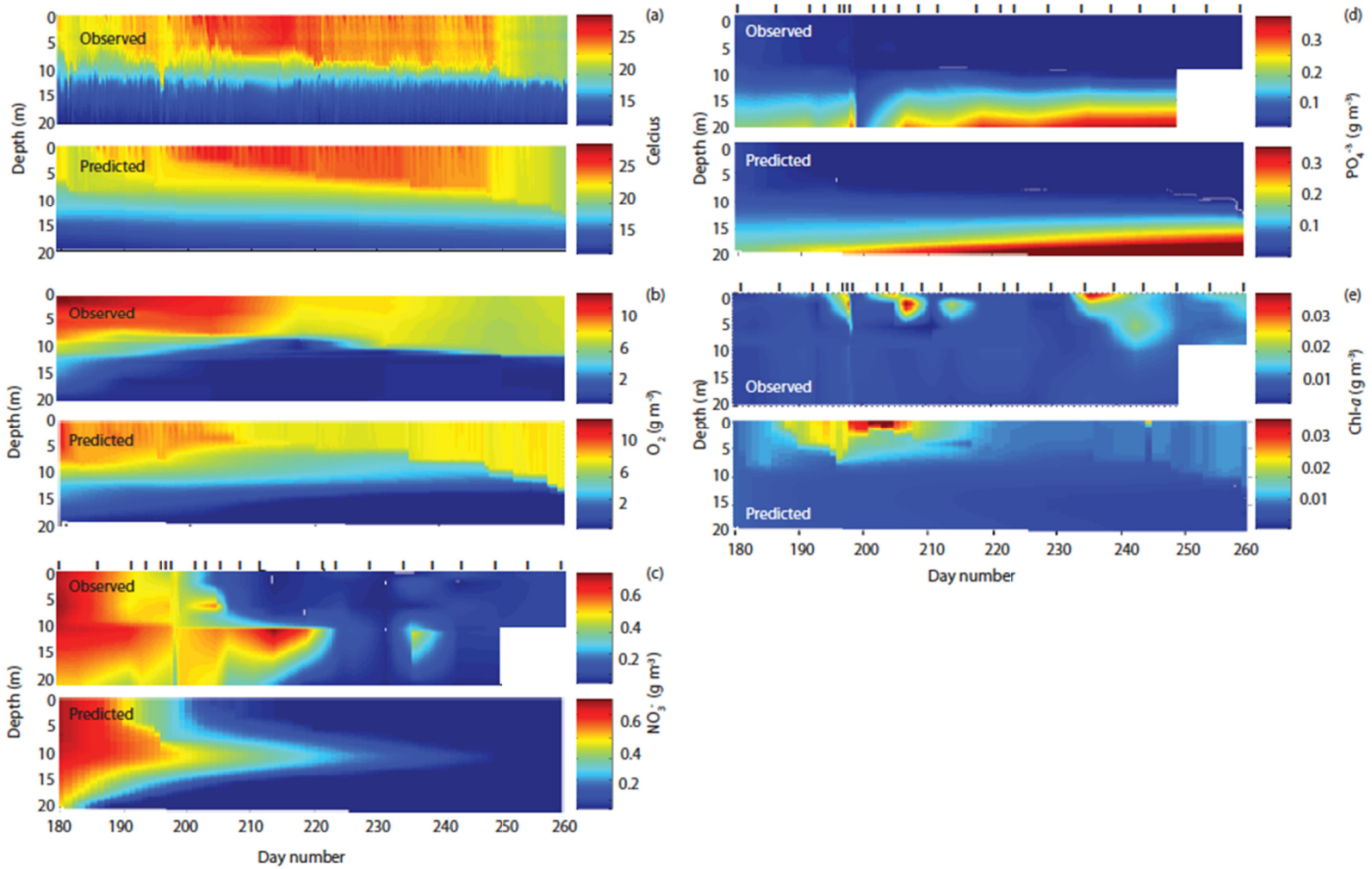

Figure 3.2 Interpolated observed (upper) and predicted (lower) temperature (a), DO (b), NO_3^- (c), PO_4^{3-} (d), and chl-*a* (d). Observed temperature data (hr^{-1}) from automated thermister chain positioned at least every 1m from 0-20m (a), PO_4^{3-} (b), NO_3^- (c), and laboratory-extracted manual chl-*a* (d). Phosphate, NO_3^- and laboratory-extracted manual chl-*a* were sampled at 5 discrete depths from 0-20 m; vertical lines above observed plots c, d, and e indicate occurrence of manual sampling.

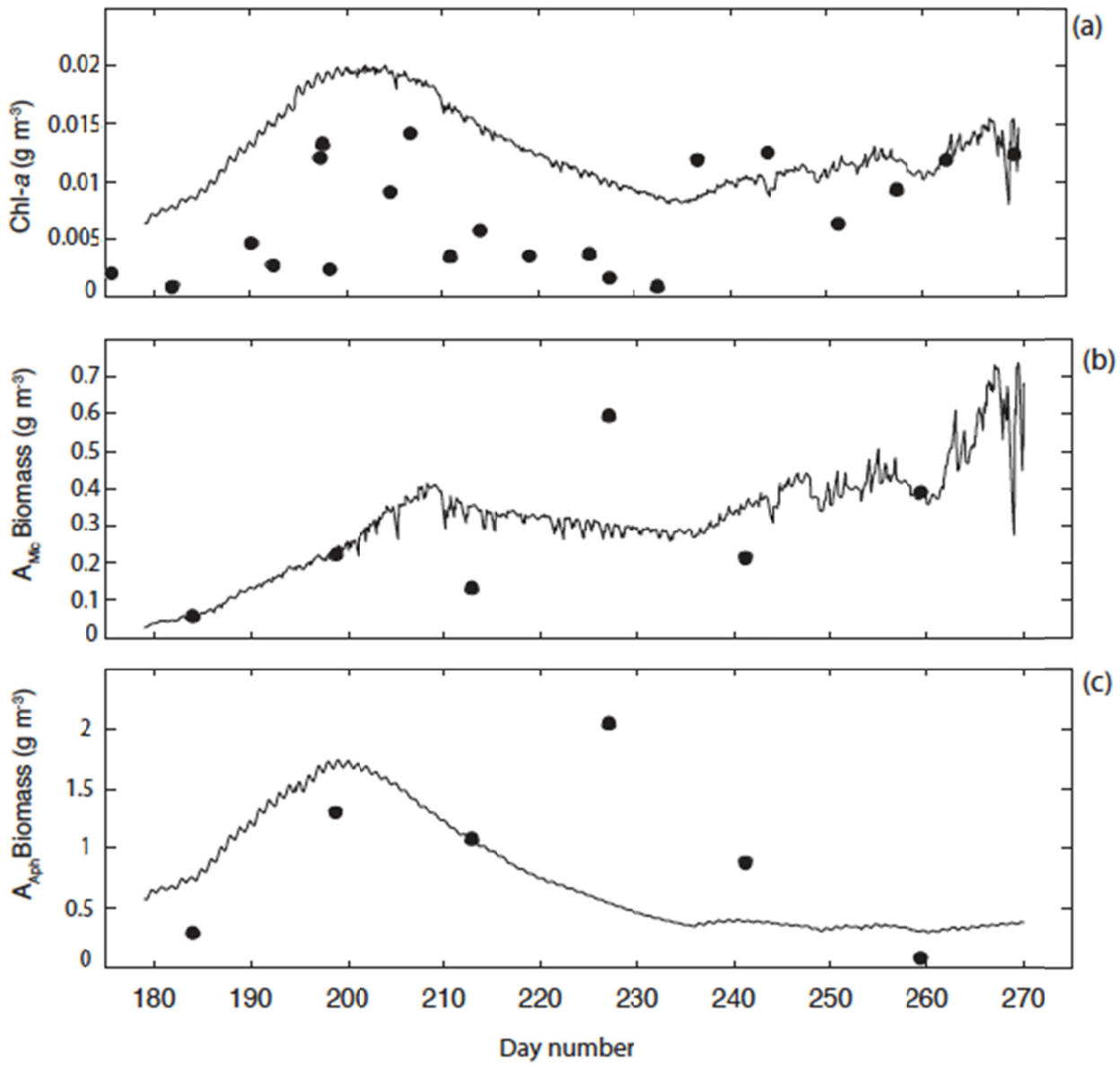

Figure 3.3 Observed (solid circles) and predicted (solid line) total chlorophyll-*a* concentration (a), the Microcystis-like functional group (A_{Mic}) biomass (b) and the Aphanizomenon-like functional group (A_{Aph}) biomass (c) vertically averaged over 0-8 m depth. Predicted and observed values from 0-8 m vertically averaged (depth integrated) range.

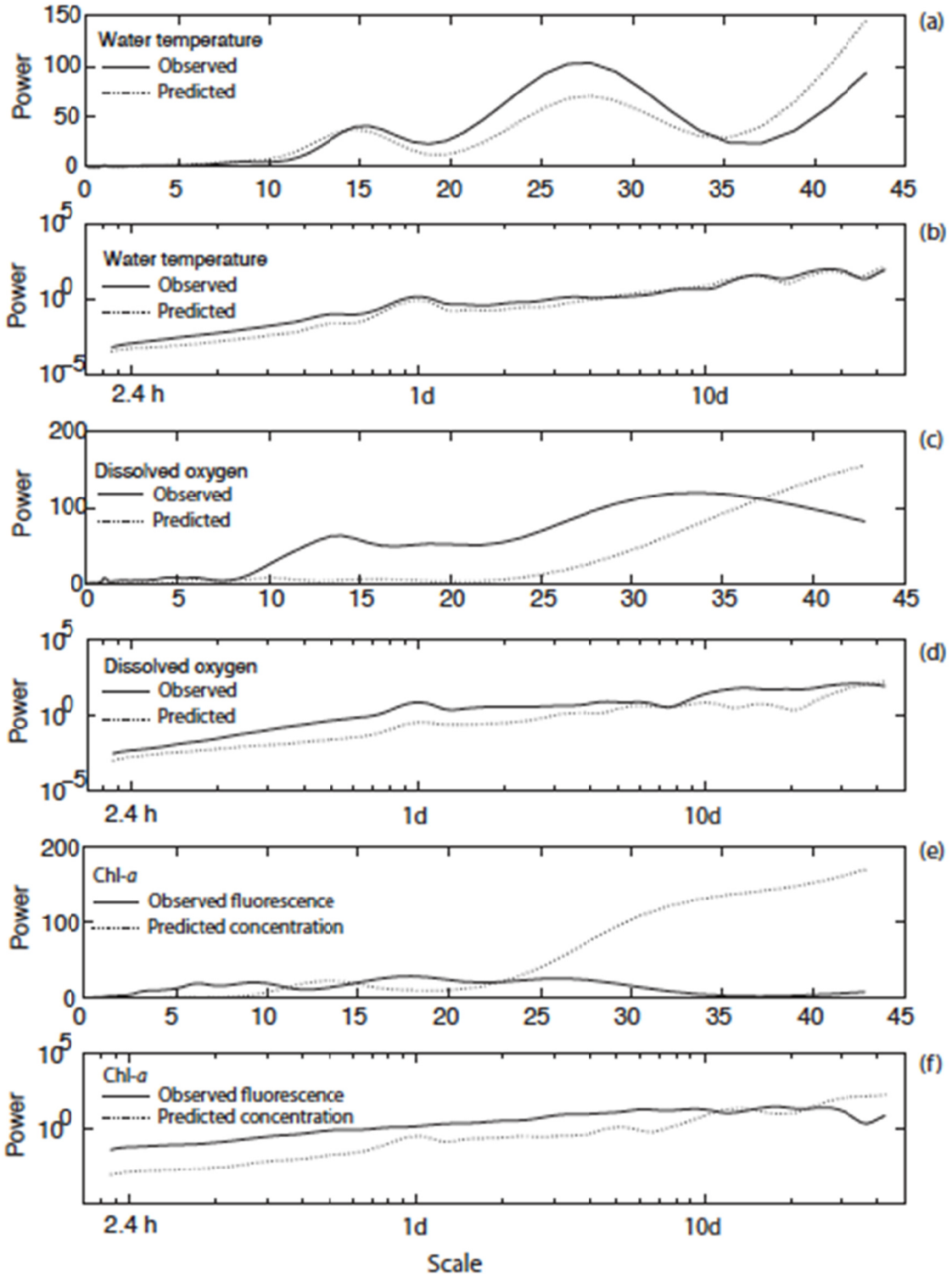

Figure 3.4 Global wavelet analysis of high-frequency (hr^{-1}) temperature (a, b), dissolved oxygen (c, d) and chlorophyll-*a* (e, f) observations (black) and predictions (dashed). Global wavelet transforms are plotted on linear (a, c, and e) and logarithmic (b, d, and f) axes.

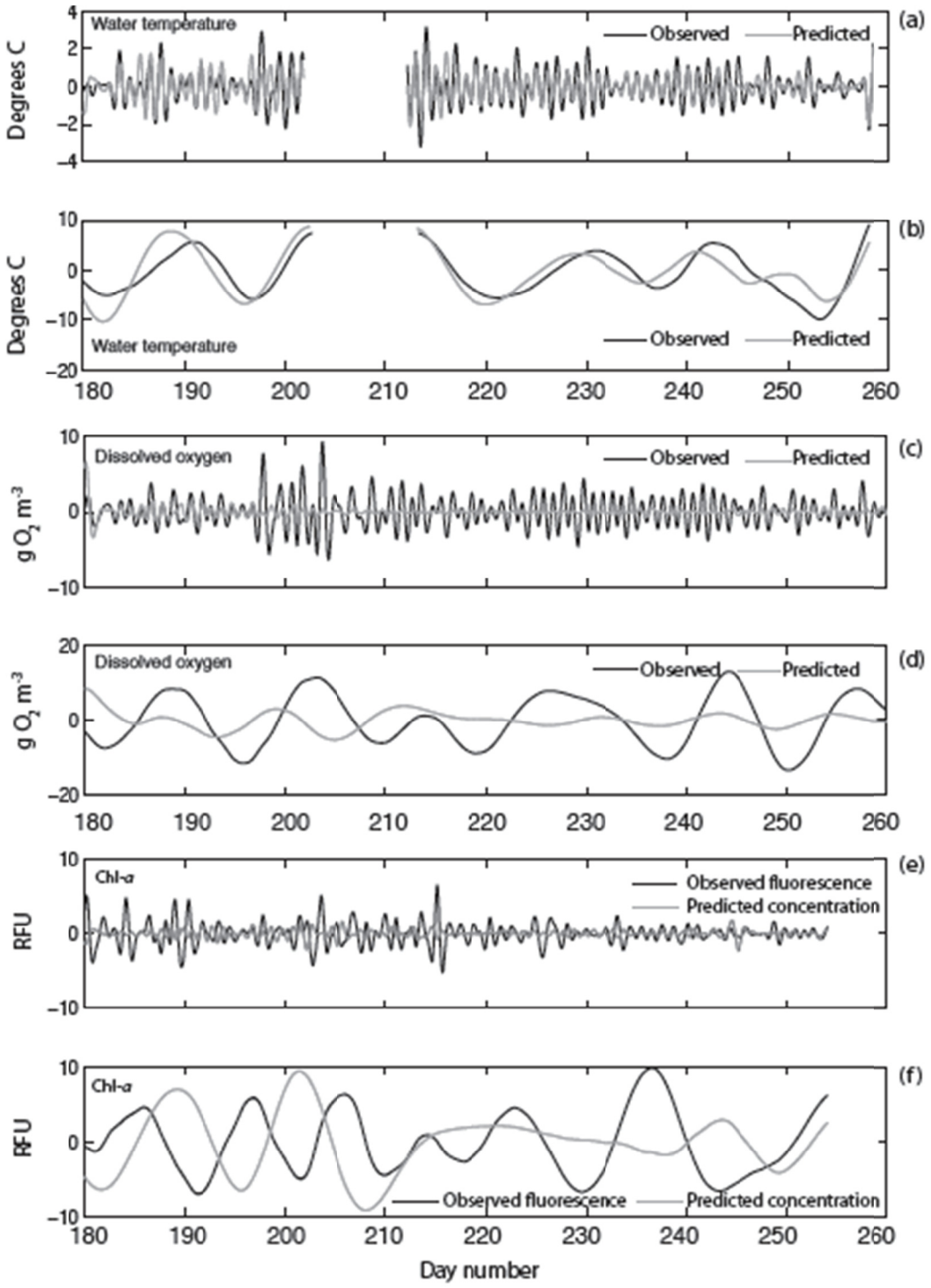

Figure 3.5 Single-scale wavelet transforms of temperature (a, b), dissolved oxygen, (c, d), and chl-*a* fluorescence (e, f) at the 1 d (a, c, and f) and 10 d scale (b, d, and f). Observed data indicated with solid lines and predicted data indicated with dashed lines. Missing temperature data from day 208-218 were removed for the analysis and the two sets of adjacent data were made consecutive so that the analysis was run on a continuous time series. Single scale transform shown here was separated after analysis to indicate missing data.

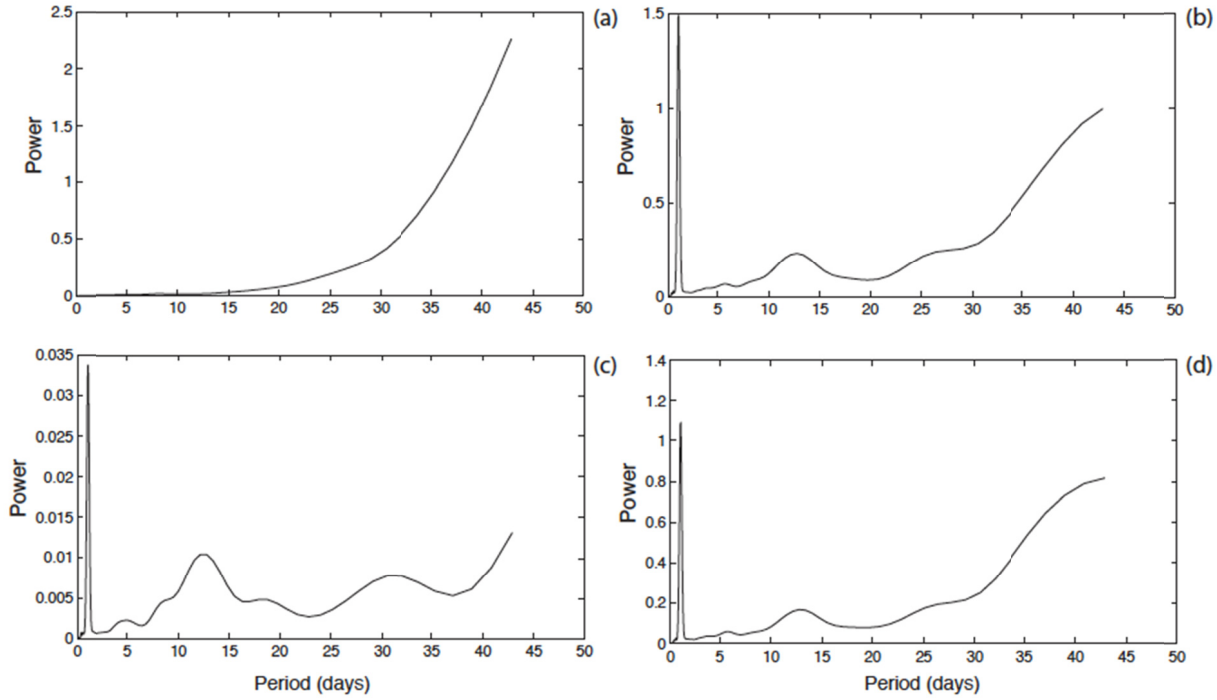

Figure 3.6 Spectral analysis of biomass (a), gross primary productivity (b), respiration (c) and net primary productivity (d) for 2008 from model output.

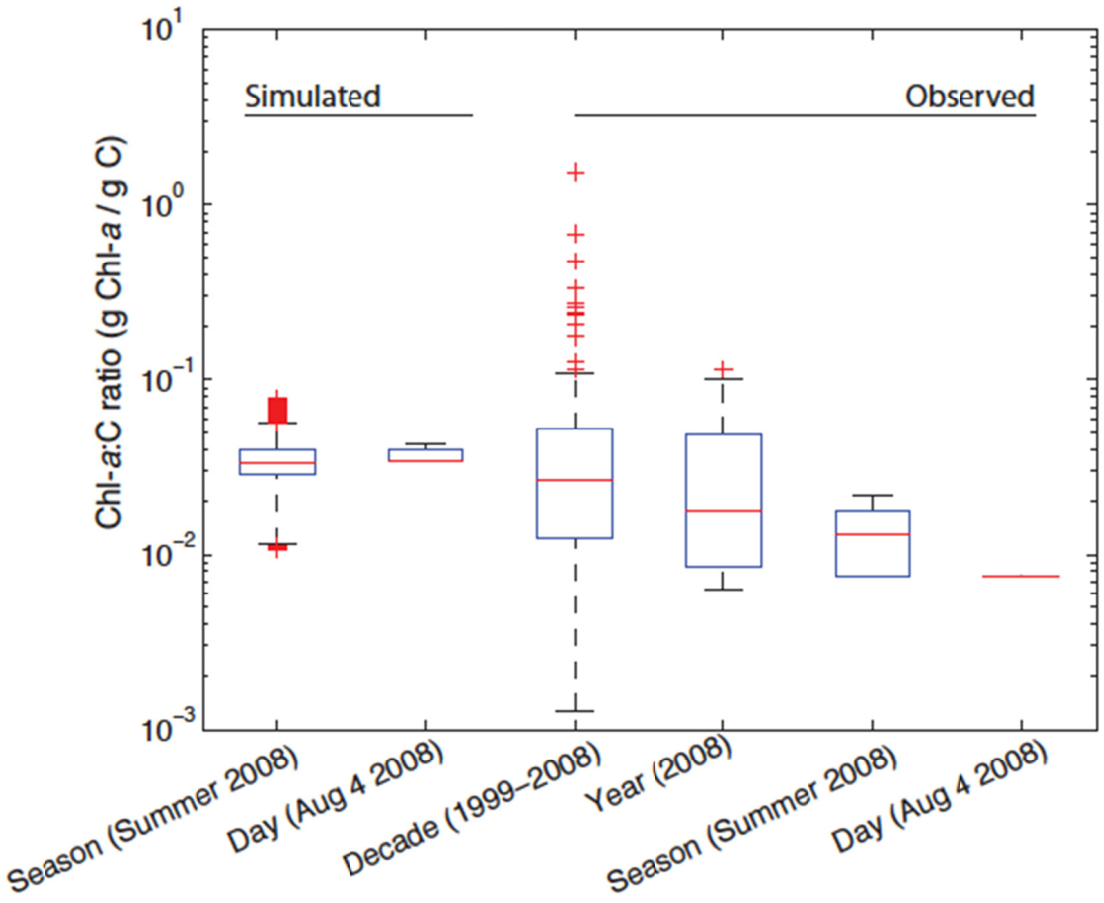

Figure 3.7 Simulated and observed chlorophyll-to-carbon (Chl:C) ratios over a range of time scales. Chl:C for Aug 4 2008 is a mean of hourly values for the simulation and a single combined observation of biomass and chl-*a*.

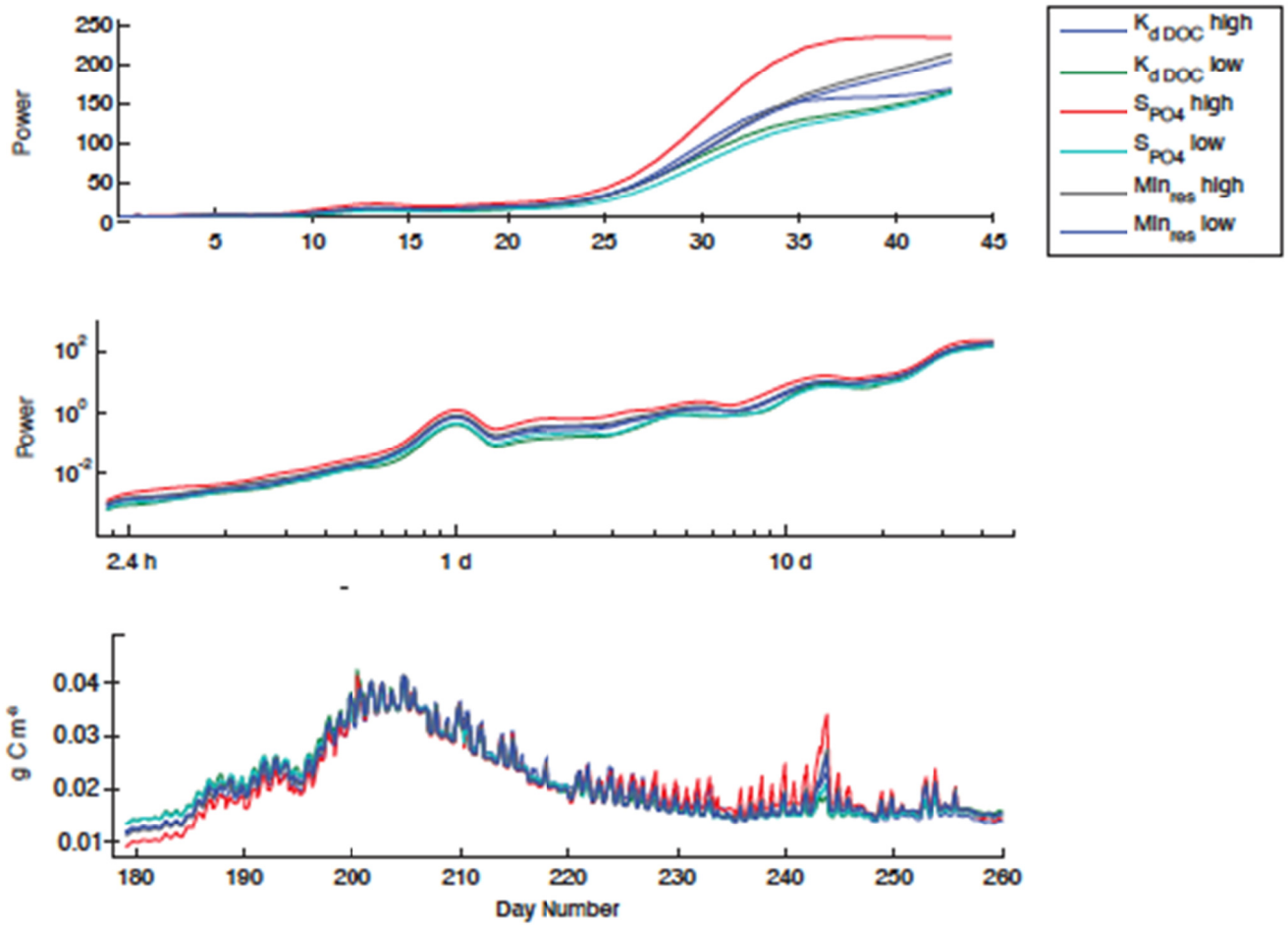

Figure 3.8 The effect of modifying key CAEDYM parameters in the time and frequency domains on simulated variables temperature (a), dissolved oxygen (b), and chl-a (in units of g C m^{-3}) (c) as assessed by global wavelet analysis.

Chapter 4 - The role of exogenous drivers on water quality in hydrodynamic-biogeochemical simulations of a eutrophic lake

Emily L. Kara, Paul C. Hanson, and Katherine D. McMahon

4.1 Abstract

To determine the influence of exogenous drivers and starting conditions associated with regional climate change on the water quality of a eutrophic temperate lake, we simulated the response of key variables (phytoplankton biomass, net and gross primary productivity, and phytoplankton respiration) to different nutrient and water temperature scenarios. Nutrient and temperature scenarios were bounded by observed historical extremes in nutrient and temperature conditions, with the year 2008 as a nominally average year, in a 3x3 factorial design. The initial conditions of water column phosphorus concentration were more important to the timing and magnitude phytoplankton response than nitrogen concentration or initial water column temperature. The magnitude of phytoplankton biomass responded to changes in initial conditions and nutrient loading, but the temporal dynamics did not. Our results indicate that phosphorus has an overall more significant effect on phytoplankton biomass than nitrogen and temperature, but we recommend that more accurate scenarios of changing climate be used in conjunction with nutrient scenarios to better understand the importance of future climate change.

4.2 Introduction

Lakes are sensitive indicators of surrounding environmental change (Williamson et al., 2009). Degraded surface water quality due to anthropogenic eutrophication is prevalent worldwide, and Wisconsin's Yahara lakes have received excessive nutrient loading for more than 150 years. As early as the 1906 and yet today, the most upstream of the Yahara chain of

lakes, Lake Mendota, displays characteristic signs of eutrophication: increased primary productivity dominated by *Cyanobacteria* species, decreased water clarity, and longer and more prevalent hypolimnetic anoxia (Brock, 1985; Kara et al., 2012). Although targeted management of non-point source nutrient inputs to increase water quality has been in effect in the Mendota watershed for many decades, with renewed effort since 1997, significant external nutrient loading occurs in Lake Mendota (Kara et al., 2011; Lathrop, 2007), and water quality remains degraded (Carpenter et al., 2007). Lake Mendota water quality reflects short term variation in regional drivers, e.g. such as the improved quality of surface water during drought years (Lathrop, 2007), but also remains degraded due to historical and continued nutrient loading from the watershed that contributes to significant sediment nutrient content and internal loading (Soranno et al., 1997), even in drought years.

For south central Wisconsin, regional trends in climate over more than five decades reveal significant increases in winter and spring warming, increased nighttime temperatures, increasing precipitation, and an overall longer growing season (Kucharik et al., 2010). The impact of changing regional climate on water quality of the Yahara chain of lakes is unknown, but, in general, a warming climate has been putatively associated with environmental factors relevant to water quality, and particularly for already-impaired waters: increased nutrient loading (Trolle et al., 2011), increased *Cyanobacterial* dominance (Paerl & Huisman, 2008), and longer summertime stratification (Sahoo et al., 2010), which has implications for hypolimnetic release of sediment nutrients. Mechanistic water quality simulations show differential predicted responses to a warmer climate depending on the lake mixing status and the composition of nutrient loading (Gal et al., 2009; Trolle et al., 2008). Overall, the expected response of water

quality to changing climate is of increased degradation due to a synergy of processes and positive feedbacks, within lakes and through the global carbon cycle (Moss et al., 2011).

Here, we use a coupled hydrodynamic-biogeochemical model previously calibrated and validated for Lake Mendota, Wisconsin, to test the effects of a range of temperature and nutrient scenarios on key water quality variables. We focus on phytoplankton biomass, net and gross primary productivity, and respiration. We aimed to assess how Lake Mendota water quality variables respond to the single and additive effects of temperature and nutrients, which could be informative to regional water quality managers and legislators.

4.3 Methods

Lake Mendota, Wisconsin is located in south central Wisconsin and has been described in detail elsewhere (Brock, 1985; Carpenter et al., 2007; Kara et al., 2012; Lathrop, 2007). To predict the effect of temperature and nutrient conditions on water quality variables, we used a one-dimensional hydrodynamic model (the Dynamic Reservoir Simulation Model [DYRESM]), dynamically coupled to a biogeochemical model (Computational Aquatic Ecosystem Dynamics Model [CAEDYM]). Model configuration, parameterization, calibration, and validation were described previously (Kara et al., 2012). We relied on a long term water quality record, from the North Temperate Lakes Long Term Ecological Research program for physical, chemical, and biological initial conditions and observations for calibration and validation (NTL-LTER, 2011a, 2011b, 2011c)

We tested the sensitivity of the model to initial conditions and external drivers hypothesized to play a role in the timing and magnitude of biomass, net primary productivity (NPP), respiration, and gross primary productivity (GPP) of phytoplankton. The effects of initial

water column temperature, external nutrient loading, and initial water column nutrient concentrations were examined in 18 scenarios.

Initial conditions were identified from historical observations. The 2008 simulation started at the onset of a *Cyanobacteria*-dominated biomass phase, which typically occurs in mid- to late-June following a clear-water phase in Lake Mendota. To determine the historical variation in temperature and water column chemistry at the onset of *Cyanobacterial* dominance when z_s was first < 3m, we used NTL LTER observations and identified minimum and maximum upper water column (0-10m vertically averaged) temperature, PO_4^{3-}, and NO_3^-, which defined initial conditions for scenarios. Minimum and maximum upper water column PO_4^{3-} observed at the end of the clear water phase between 1995-2008 corresponds to 46% and 230% of mean 2008 upper water column PO_4^{3-} (0.032 g P m^{-3}). Minimum and maximum upper water column NO_3^- observed at the end of the clear water phase corresponds to 50% and 124% of mean 2008 upper water column NO_3^- (0.734 g N m^{-3}). Similarly, "high T", "low T", and "2008 T" represented historical maximum and minimum upper water column temperatures and observed initial water column temperatures in 2008; mean minimum and maximum 0-10m vertically averaged surface temperatures were 78% and 110% of 2008 temperature.

Scenarios also used different external driver data; simulations included external loads that ranged from 43% to 200% of 2008 load (50,700 kg P yr^{-1}) for TP (2008 TP loading from Koltun et al., 2006; historical TP range after Lathrop et al., 1999) and from 11% to 130% of 2008 load (522,000 kg N yr^{-1}) for TN (Sonzogni & Lee, 1974). Chemical speciation of the external P and N loads (i.e. inorganic, organic, and particulate organic nutrients) was scaled proportionately to mass of total loading, as described by Kara et al. (2012). Nine phosphorus-temperature scenarios and nine nitrogen-temperature scenarios were simulated, comprised of all combinations of three

temperature and three nutrient scenarios each, in two 3 x 3 matrices (Table 4.1). “High P” was a simulation of the maximum loading and maximum initial water column concentrations, “2008 P” represented conditions observed in 2008, and “low P” represented a combination of the lowest loading and initial water column P concentrations in the historical dataset and likewise for nitrogen scenarios.

4.4 Results

We tested the sensitivity of key state variables associated with phytoplankton biomass to initial conditions and exogenous drivers associated with regional climate change, and assessed the contribution to the timing and magnitude of phytoplankton dynamics. Phosphorus initial conditions and external loading had the most significant effect on phytoplankton biomass of scenarios tested. Minimum historical surface P (46% of 2008 mean epilimnetic PO_4^{3-} concentration) and external loading (43% of 2008 TP loading) resulted in an approximate 25% reduction in maximum phytoplankton biomass as compared to 2008. Maximum historical surface P (230% of 2008 mean epilimnetic PO_4^{3-}) and external loading (200% of 2008 external P loading) resulted in an approximate 25% increase in maximum phytoplankton biomass. Seasonal phytoplankton maximum biomass responded positively to the magnitude of water column P initial conditions and external P loading rates; higher P corresponded to greater biomass (Figure 4.1a). The timing of maximum biomass was also related to the magnitude of P in the water column at the start of the simulation and external loading during the simulation. Maximum historical P in the system extended growth and persistence of phytoplankton biomass, resulting in the timing of maximum phytoplankton biomass to occur 10 d later than the 2008 scenario, and minimum historical water column P reduced the maximum biomass, and resulted

in earlier peak biomass, ~ 10 d earlier than the 2008 scenario. Initial water column temperature (0-10 m vertically averaged minimum and maximum surface temperatures were 78% and 110% of 2008 temperature) also had a secondary effect on biomass. Temperature scenarios within high, low, and 2008 P scenarios grouped together tightly according to P conditions, and differentiation within a given set of P conditions occurred in response to temperature effects. For a given P scenario, the highest temperature scenarios had the highest biomass during the time period when total biomass was increasing. None of the scenarios appeared to alter the periodicity of dynamics in biomass, respiration, and productivity (Figure 4.1 and 4.2).

The magnitude of the response of phytoplankton biomass to historical minimum and maximum temperature, initial N conditions and external N loading scenarios was much less than the response to P scenarios; total biomass for all scenarios varied by < 5% from biomass of the 2008 scenarios (data not shown).

4.5 Discussion

The differential responses of phytoplankton to nutrient and temperature conditions were consistent with our expectations for the system: the scenarios predicted phosphorus conditions to control phytoplankton biomass, a relationship that is well supported by the literature (e.g. Schindler, 1978; Vollenweider, 1976). Likewise, the effects of initial conditions and loading of N on phytoplankton biomass were less important than effects due to P, as has also been demonstrated experimentally in temperate lakes. Inter-annual variations in Lake Mendota water clarity have been attributed to difference in springtime P concentration and external P loading (Lathrop et al., 1999) further supporting the outcomes of the scenarios.

We were interested in the ability of the model to predict temporal dynamics of phytoplankton for 2008 and the effects of physico-chemical drivers on temporal patterns. With phytoplankton initial conditions held constant, biomass for the 'low P' scenarios diverged from the 2008 scenario after 7 days and biomass for the 'high P' scenario diverged after 14 days (Figure 4.1). Likewise, surface (0-10 m) PO_4^{-3} was predicted to remain above 0.005 g m^{-3} for 7 days into the simulation for 'low P', and for 14 days for the 'high P' scenario. From a management perspective, the prediction of the timing of PO_4^{-3} reduction below the limit of detection and the resulting phytoplankton response could be used to predict the onset of *Cyanobacterial* dominance.

Assuming the predicted system response is characteristic of real system behavior, initial conditions might be used to forecast the timing and magnitude of phytoplankton biomass, similar to the work of Lathrop and others for water clarity (Lathrop et al., 1999). Multi-year simulations compared to the rich historical dataset could be useful for testing the efficacy of the model for this use. Phosphorus initial conditions and loading affected the timing and magnitude of peak biomass, but did not change the dynamics of phytoplankton functional groups through time. Brock (1985) speculated that the quality (e.g. dissolved, particulate, organic, inorganic) and quantity of springtime P loading might be important for structuring phytoplankton succession. It is also likely that significant variation in phytoplankton community dynamics under these scenarios was not well predicted because of the identical initial conditions used for phytoplankton functional group biomass; inclusion of variation in functional group initial conditions, as is indicated by the NTL LTER record, may result in more dynamic patterns simulated among functional groups. Results of the N scenarios indicated this nutrient to be less important for timing and magnitude of phytoplankton biomass. Because of the dominance of N_2-

fixing *Cyanobacteria* in the system and the complexity of the N cycle, these scenarios and parameterization of the nitrogen-fixing *Cyanobacterial* functional group deserve closer attention in future work. A robust assessment of the prediction abilities of the model under historical conditions would also ideally model the system from the date of ice-off, to test the ability of the model to predict early biomass dominance by diatoms and succession by the dominant *Cyanobacteria*.

Seasonal phytoplankton biomass and productivity were influenced by initial P conditions more than by initial water temperature over the ranges tested; direct effects of P initial conditions and temperature on respiration, GPP, and NPP were more difficult to interpret (Figure 4.1b and 4.2). The results suggest that indirect changes to nutrient conditions due to changing climate, e.g. impacts on P cycle from hydrology (Lathrop, 2007) or thermal stability (Soranno et al., 1997), may have a greater effect on phytoplankton biomass than direct temperature effects on algal physiology. Though we simulate an average increase or decrease in water column temperatures, climate change will entail more complex effects (Trolle et al., 2011), which should be investigated with scenarios including regional climate change effects and increased likelihood of higher severe storm frequency that might deliver large pulses of nutrients. For Lake Mendota, drought years have been associated with reduced nutrient loading and increased water quality (Lathrop, 2007).

In comparison to similar studies in other systems, our findings are distinct, and point to the understanding that lakes respond differently to drivers such as temperature and nutrient loading, and that generalization about lake response to changing drivers are difficult to make. Trolle et al 2011 found external loading to have less effect on water quality variables than temperature for three morphologically distinct New Zealand lakes. Gal and colleagues found

external P loading to have minimal effect on internal TP concentration in Lake Kinneret, Israel, but external N loading did have an effect on internal TN loading (Gal et al., 2009). Lake Kinneret was also more sensitive to winter-spring loading than to summer-fall nutrient loading, indicating that the intra-annual timing of loading has important implications for water quality. The interaction of external nutrients, internal loading, morphometry, mixing regime, and meteorology all contribute water quality responses; the combination of these factors is unique for most lakes, causing generalizations to be difficult to make across a limited number of systems.

4.6 Conclusions and next steps

For lake Mendota, Wisconsin, we found in lake P concentrations at the beginning of simulations was more important to subsequent phytoplankton biomass than in-lake nitrogen concentrations or water temperature. The magnitude and timing of blooms was most sensitive to in lake P initial conditions, but the pattern of biomass over the 90 day scenario was not. To compare our findings against numerous years of observational data from this lake is beyond the scope of this work, but could used to further confirm these results or to identify additional important variables.

Parameterization, calibration, and validation of aquatic ecosystem models is time consuming, but the more sets of data we have to work with, the closer we might move to understanding how lakes across many gradients and across the landscape may respond to changing hydrologic, meteorological, and nutrient regimes.

4.7 Acknowledgements

Thanks to Dale Robertson for preparation of meteorological driver data. Thanks to

Yvonne Hsieh, Chin Wu, Jordan Read, Luke Winslow, Kevin Rose, Evelyn Gaiser, Matt Hipsey, David Hamilton, Tim Kratz, Cayelan Carey, Lucas Beversdorf, Todd Miller, Stefan Bertillson, David da Motta Marques, and John Dedrick for assistance with the initial setup of simulations.

4.8 References

Brock, T. D. (1985). *A Eutrophic Lake: Lake Mendota, Wisconsin* (p. 308). Springer Verlag.

Carpenter, S. R., Benson, B., Biggs, R., Chipman, J. W., Foley, J. A., Golding, S. A., Hammer, R. B., et al. (2007). Understanding Regional Change : A Comparison of Two Lake Districts. *BioScience*, *57*(4), 323-335.

Gal, G., Hipsey, M. R., Parparov, a., Wagner, U., Makler, V., & Zohary, T. (2009). Implementation of ecological modeling as an effective management and investigation tool: Lake Kinneret as a case study. *Ecological Modelling*, *220*(13-14), 1697-1718. doi:10.1016/j.ecolmodel.2009.04.010

Kara, E. L., Hanson, P. C., Hamilton, D. P., Hipsey, M. R., McMahon, K. D., Read, J. S., Winslow, L., et al. (2012). Time-scale dependence in numerical simulations: Assessment of physical, chemical, and biological predictions in a stratified lake at temporal scales of hours to months. *Environmental Modelling & Software*, *35*, 104-121. Elsevier Ltd. doi:10.1016/j.envsoft.2012.02.014

Kara, E. L., Heimerl, C., Killpack, T., Bogert, M. C., Yoshida, H., & Carpenter, S. R. (2011). Assessing a decade of phosphorus management in the Lake Mendota, Wisconsin watershed and scenarios for enhanced phosphorus management. *Aquatic Sciences*, *74*(2), 241-253. doi:10.1007/s00027-011-0215-6

Koltun, G., Eberle, M., Gray, J., & Glysson, G. (2006). User's manual for the Graphical Constituent Loading Analysis System (GCLAS). *US Geological Survey Techniques of Water Resources-Investigations Book 4* (p. 51).

Kucharik, C. J., Serbin, S. P., Vavrus, S., Hopkins, E. J., & Motew, M. M. (2010). Patterns of Climate Change Across Wisconsin From 1950 to 2006. *Physical Geography*, *31*(1), 1-28. doi:10.2747/0272-3646.31.1.1

Lathrop, R. (2007). Perspectives on the eutrophication of the Yahara lakes. *Lake and Reservoir Management*, *23*(4), 345-365. doi:10.1080/07438140709354023

Lathrop, R., Carpenter, S. R., & Robertson, D. (1999). Water clarity responses to phosphorus, Daphnia grazing, and internal mixing in Lake Mendota. *Limnology and Oceanography*, *44*(1), 137-146.

Magnuson, J., Robertson, D., Benson, B., Wynne, R., Livingstone, D., Arai, T., Assel, R., et al. (2000). Historical trends in lake and river ice cover in the northern hemisphere. *Science*, *289*, 1743-1746.

Moss, B., Kosten, S., Meerhoff, M., Battarbee, R. W., Jeppesen, E., Mazzeo, N., Havens, K. E., et al. (2011). Allied attack : climate change and eutrophication. *Limnology*, 101-105. doi:10.5268/IW-1.2.359

NTL-LTER. (2011a). Physical Limnology Dataset. *North Temperate Lakes Long Term Ecological Research Program*. Madison, WI.

NTL-LTER. (2011b). Chemical Limnology Dataset. *North Temperate Lakes Long Term Ecological Research Program*. Madison, WI. Retrieved from http://www.lternet.edu/sites/ntl/

NTL-LTER. (2011c). Biological Limnology Dataset. *North Temperate Lakes Long Term Ecological Research Program*. Madison, WI.

Paerl, H. W., & Huisman, J. (2008). Blooms Like It Hot. *Science*, *320*, 57-58.

Sahoo, G. B., Schladow, S. G., Reuter, J. E., & Coats, R. (2010). Effects of climate change on thermal properties of lakes and reservoirs, and possible implications. *Stochastic Environmental Research and Risk Assessment*, *25*(4), 445-456. doi:10.1007/s00477-010-0414-z

Schindler, D. (1978). Factors regulating phytoplankton production and standing crop in the world's freshwaters. *Limnology and Oceanography*, *23*(3), 478-486.

Sonzogni, W., & Lee, G. (1974). Nutrient sources for Lake Mendota. *Transactions of the Wisconsin Academy of Sciences, Arts, and Letters*.

Soranno, P., Carpenter, S. R., & Lathrop, R. (1997). Internal phosphorus loading in Lake Mendota : response to external loads and weather. *Methods*, *1893*, 1883-1893.

Trolle, D, Skovgaard, H., & Jeppesen, E. (2008). The Water Framework Directive: Setting the phosphorus loading target for a deep lake in Denmark using the 1D lake ecosystem model DYRESM–CAEDYM. *Ecological Modelling*, *219*(1-2), 138-152. doi:10.1016/j.ecolmodel.2008.08.005

Trolle, Dennis, Hamilton, D. P., Pilditch, C. A., Duggan, I. C., & Jeppesen, E. (2011). Environmental Modelling & Software Predicting the effects of climate change on trophic status of three morphologically varying lakes : Implications for lake restoration and management. *Environmental Modelling and Software*, *26*(4), 354-370. Elsevier Ltd. doi:10.1016/j.envsoft.2010.08.009

Vollenweider, A. (1976). Advances in defining critical loading levels for phosphorus in lake eutrophication, 53-83.

Williamson, C. E., Saros, J. E., Vincent, W. F., & Smol, J. P. (2009). Lakes and reservoirs as sentinels , integrators , and regulators of climate change. *Arctic*, *54*, 2273-2282.

4.9 Figures

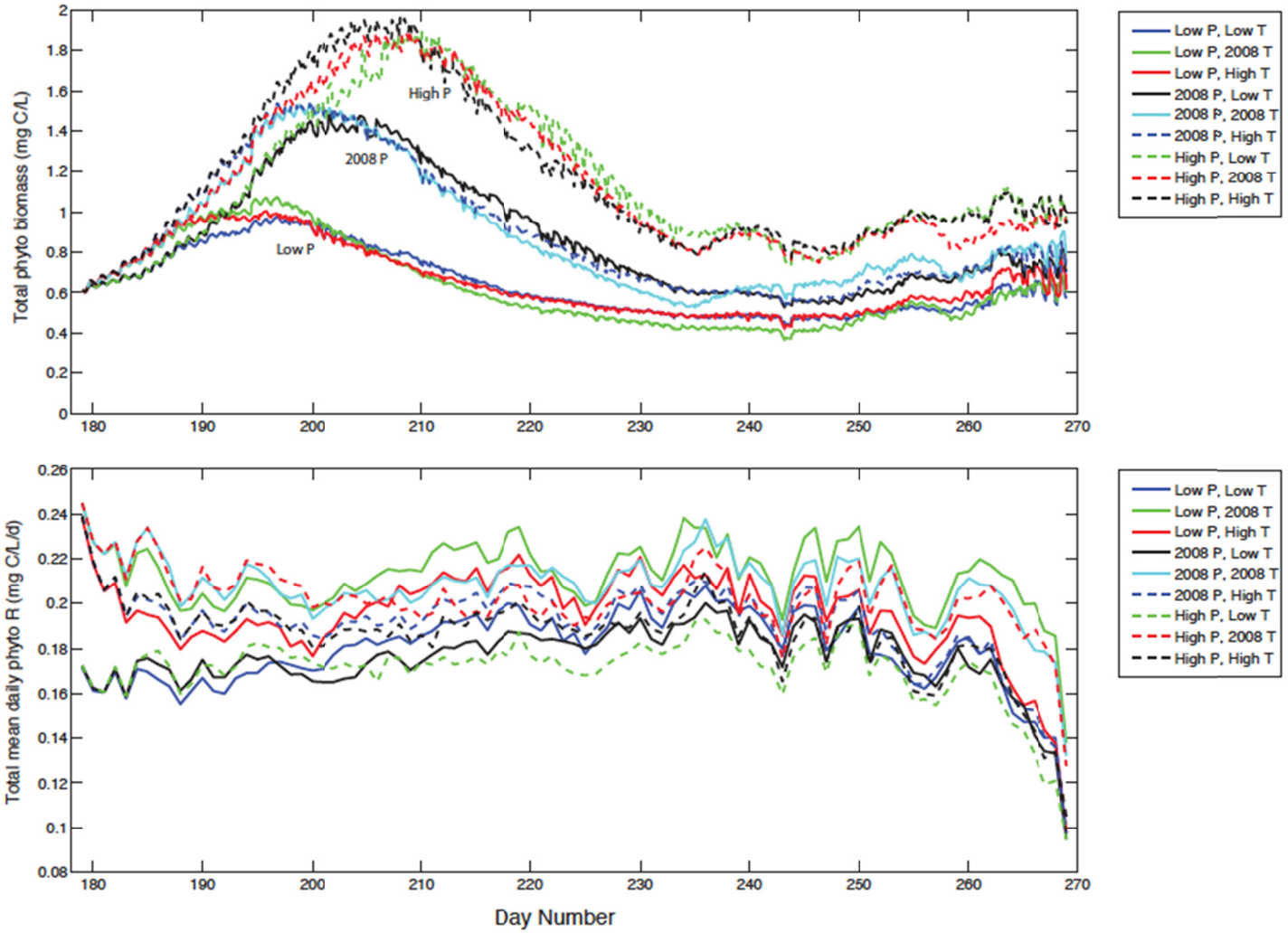

Figure 4.1 Nine temperature and phosphorus scenarios showing (a) simulated total phytoplankton biomass (top panel) and (b) gross primary productivity (bottom panel) for upper (0-8m) water column of Lake Mendota, WI.

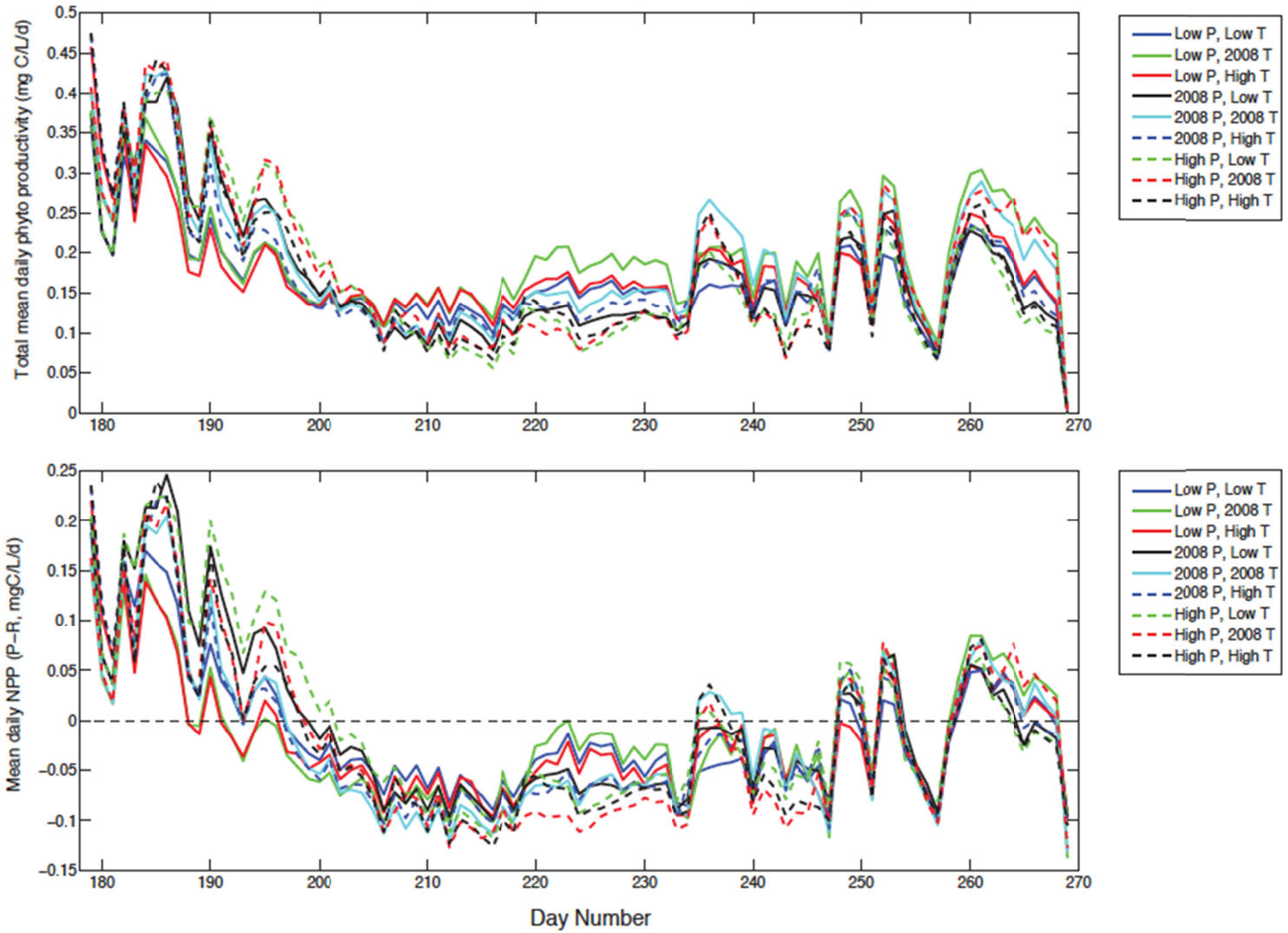

Figure 4.2 Nine temperature and phosphorus scenarios showing (a) simulated respiration (top panel) and (b) net primary productivity (bottom panel) for upper (0-8m) water column of Lake Mendota, WI.

4.10 Tables

	Low temperature 78% nominal	**2008 nominal temperature**	**High temperature** 110% nominal
Low phosphorus 46% nominal SRP 43% nominal loading	1. Low phosphorus Low temperature	2. Low phosphorus 2008 temperature	3. Low phosphorus High temperature
2008 nominal SRP and loading	4. 2008 phosphorus Low temperature	5. 2008 phosphorus 2008 temperature	6. 2008 phosphorus High temperature
High phosphorus 230% nominal SRP 200% nominal loading	7. High phosphorus Low temperature	8. High phosphorus 2008 temperature	9. High phosphorus High temperature

Table 4.1 Summary of temperature and phosphorus scenarios. High and low conditions were bounded by historical extremes observed in Lake Mendota. Percent difference from nominal (2008) conditions are given for epilimnetic (0-12m) SRP and surface (0-5m) temperature conditions. Source: NTL LTER (historical water column SRP and temperature data) and Lathrop et al. 1998 (external P loading data).

Chapter 5 - A decade of seasonal dynamics and interactions within freshwater bacterioplankton communities from eutrophic Lake Mendota, Wisconsin, USA

Emily L. Kara, Paul C. Hanson, Yu Hen Hu, Luke Winslow, Katherine D. McMahon

5.1 Abstract

With an unprecedented decade-long time series from a temperate eutrophic lake, we analyzed bacterial and environmental co-occurrence networks to gain insight into dynamics at the community level. We found that (1) bacterial co-occurrence network were non-random, (2) season explained network complexity, and (3) community complexity was negatively correlated with underlying community diversity across different seasons. Network complexity was not related to habitat heterogeneity of associated environmental variables. Primary productivity may drive seasonal changes in diversity and network complexity in an additive manner, whereby diversity increases and interaction network complexity decreases during the ice-free period on an annual basis. While the implications of bacterioplankton network structure on ecosystem function are still largely unknown, network analysis, in conjunction with traditional multivariate techniques, continues to increase our understanding of bacterioplankton temporal dynamics.

5.2 Body

The central role of seasonal cycles in the temporal dynamics of aquatic microbial communities has been highlighted in river, lake, and marine systems by the use of ordination, analysis of community similarity, diversity, and the abundance of individual taxa (Crump & Hobbie, 2005; Fuhrman et al., 2006; Gilbert et al., 2012; Shade et al., 2007; Wu & Hahn, 2006), and bacterioplankton have been linked to the seasonal succession of other planktonic organisms

(Gasol et al., 1992; Graham et al., 2004; Kent et al., 2007; Maurice et al., 2010). As the size and extent of biological data sets grow, scientists turn to new techniques, such as network analysis, to understand biological complexity over large scales (e.g. Barberán et al., 2012). Here we use an unprecedented decade-long time series of freshwater bacterioplankton community observations to test the hypotheses: (1) community co-occurrence networks from this sample set are non-random, (2) season explains the organization and complexity of co-occurrence networks, and (3) community richness and diversity correlate to co-occurrence network complexity.

Surface water samples were collected from Lake Mendota, Wisconsin, USA, and analyzed by automated ribosomal intergenic spacer analysis as described previously (Shade et al., 2007; see Supplemental Materials). From 2000 to 2009, a total of 34 spring, 53 summer, and 34 autumn observations were made (Table S1). Thirty-two environmental variables were collected at the same location by the North Temperate Lakes Long Term Ecological Research program (lter.limnology.wisc.edu, Table S1).

We quantified the richness, evenness, and diversity of the underlying communities, and the properties of spring, summer, and autumn bacterioplankton community and biogeochemical co-occurrence networks. To characterize underlying bacterial communities, richness (*R*, number of operational taxonomic units observed) and Shannon evenness and diversity (Magurran, 2011) were calculated for each season. Using local similarity analysis, co-occurrence networks (*networks* hereafter) were generated from interactions with local similarity scores (R) > 0.3, P-value < 0.001, false discovery rate <0.05, and no time lag (Ruan et al., 2006). Erdős-Rényi (E-R) random networks were generated for comparison to empirical networks, where for every empirical network with n nodes and m edges, a random network with n nodes and m edges was generated, where every edge had an equal probability of being assigned to any node (Newman,

2003). Network comparisons were made using connectance (edges (L) per node (S)^2), characteristic path length (D, average shortest path length between nodes), and clustering coefficient (Cl, of node u: $Cl(u) = 2L_u / ((deg(u))*(deg(u)-1))$ where L_u is the number of edges between neighbors of u and deg is degree, the number of edges per node) (Kuchaiev et al., 2011). The properties S, L, Cl, and D were calculated for real and random networks using GraphCrunch2 software (Kuchaiev et al., 2011), and networks were visualized using Cytoscape (Smoot et al., 2011).

Network properties depended upon the number of observations included in the analysis, similar to the effect of sampling effort on network properties described by (Martinez et al., 1999). To correct for unequal sampling efforts between seasons, we performed Monte Carlo simulations of 1000 observation-normalized networks for each season, where each network was comprised of 30 randomly selected observational dates within a season. For each Monte Carlo simulation, an E-R random graph was generated. For the networks comprised of all observations, 1000 E-R random graphs were generated and median values for network properties of these random graphs are reported (Table 5.1). Differences between median values for distributions of randomized networks were made using the Wilcoxon rank sum test.

From spring to autumn, network complexity decreased, as indicated by decreasing Cl and increasing D (Figure 5.1a). Trends were robust to normalizing for the number of observations made: median values of observation-normalized network properties L, S, Cl, and D significantly varied across season (Figure 5.1b, α=0.005), consistent with trends shown in Figure 1a. The spring network had 7 high-degree nodes (> 15 edges/node), while summer and autumn networks had 5 and 1, respectively (Figure 5.1a). The underlying communities' richness and diversity increased (Figure 5.1a) and were significantly different (Figure 5.1b, α=0.005), while community

evenness did not differ significantly across seasons (data not shown). Network properties *L*, *S*, *Cl*, and *D* of Monte Carlo distributions of real networks were significantly different than those of corresponding distributions of random networks (α=0.005).

Our results indicate (1) non-random bacterioplankton co-occurrence networks and (2) an inverse relationship between network complexity and diversity and richness of the underlying communities for this system. Springtime conditions were favorable to fewer taxa (lower richness), but resulted in overall more interactions between taxa, and more complex interactions, especially between the most abundant taxa (Figure 5.1). Barberán et al. (2011) hypothesized that soil microbial co-occurrence network complexity was inversely related to habitat heterogeneity across broad spatial scales. In contrast, we found that network complexity was not related to heterogeneity of community habitat, as estimated by the variance of 32 physical, chemical, and biological variables across seasons, or to the complexity of co-occurrence networks of environmental variables for each season (Figure S1). Increases in bacterioplankton community diversity and richness over the open water season may be due to changes in day length, and concomitant trends in water temperature and primary productivity, which lag insolation by ~ 7 weeks in this system (Brock, 1985). We found correlations (edges) between temperature, day length, and dissolved oxygen and bacterial taxa were more frequent than those between taxa and other variables (Figure 5.1a). Negative diversity-latitude (Shurin et al., 2007) and positive diversity-productivity (Ptacnik et al., 2008) relationships have been observed for other aquatic organisms; here, diversity increased after ice off as summer succeeded spring. Primary productivity through time may have an additive effect on diversity during the ice-free season until primary productivity is limited by reduced insolation and by ice cover, after which diversity

decreases. Uneven temporal sampling limited our ability to test this hypothesis across years, but cross-system comparisons over a gradient of productivity could be used to do so.

The robust recurrent patterns in diversity and co-occurrence networks are especially compelling in light of the magnitude of microbial turnover rates (10-60% removal of standing bacterial biomass per day) measured in this system and others (Brock, 1985; Hahn et al., 2012). Although a vast and diverse persistent seed bank likely underlies the observed communities (Caporaso et al., 2011; Lennon & Jones, 2011), the most abundant taxa recur and interact in repeatable pattern in spite of constant removal by planktonic grazers and other loss factors [e.g. viral lysis (Maurice et al., 2010)]. The maintenance and recurrence of the most abundant members of the community may be determined by environmental cues that trigger growth under more favorable conditions (Jones & Lennon, 2010).

In macro-scale ecology, high diversity-low interaction communities, like those represented by the autumnal co-occurrence networks, have been observed and associated with greater stability (McCann, 2000); while food web robustness has also been shown to correspond to higher complexity of food web networks (Dunne et al., 2002). In this early stage of the application of network analysis to microbial observations, the implications of interaction network structure on the functioning of ecosystems and engineered systems are unknown. But, the possibilities of testing hypotheses such as this in systems that are more easily or stochastically perturbed (e.g. microbially-mediated wastewater treatment processes or human gut microbial communities) are numerous, and, due to the availability of economical and high-through put next-generation sequencing technologies, are within reach for experimental ecology.

Table 5.1. Summary of co-occurrence network properties. Regular type indicates a single value calculated and reported, while boldface type indicates the median value reported from an analysis including 1000 Monte Carlo simulations. Top panel: network properties calculated from networks generated from all observations (*n*) made for spring (*n*=34), summer (*n*=53), and autumn (*n*=34) seasons. For networks generated from all observations, 1000 E-R

random graphs were generated with an equal number of nodes (*S*) and edges (*L*) as the corresponding original network but distinct characteristic path length (*D*) and clustering coefficient (*Cl*); we report the median values of random graph populations, indicated in bold (D_{rand} and Cl_{rand}). Bottom panel: network properties from observation-normalized Monte Carlo simulations (*n*=30 x 1000 simulations) and E-R random graphs generated from each Monte Carlo simulation. As above, E-R random graphs had equal *L* and *S* but significant differences between *D* and D_{rand} and *Cl* and Cl_{rand}.

	Nodes (*S*)	Edges (*L*)	*L*/*S*	L/S^2	*D*	D_{rand}	*Cl*	Cl_{rand}	Cl/Cl_{rand}
All observations									
Spring	91	202	2.22	0.0244	3.27	**3.41**	0.248	**0.045**	5.57
Summer	88	182	2.07	0.0235	3.54	**3.83**	0.236	**0.043**	5.55
Autumn	84	131	1.56	0.0186	3.59	**3.82**	0.217	**0.029**	7.43
Sampling effort-normalized median values from Monte Carlo simulations									
Spring	**84**	**167**	**1.99**	**0.0237**	**3.47**	**3.66**	**0.256**	**0.043**	**5.90**
Summer	**86**	**143**	**1.66**	**0.0193**	**3.83**	**4.13**	**0.188**	**0.032**	**5.81**
Autumn	**79**	**108**	**1.37**	**0.0173**	**3.88**	**4.18**	**0.167**	**0.026**	**6.56**

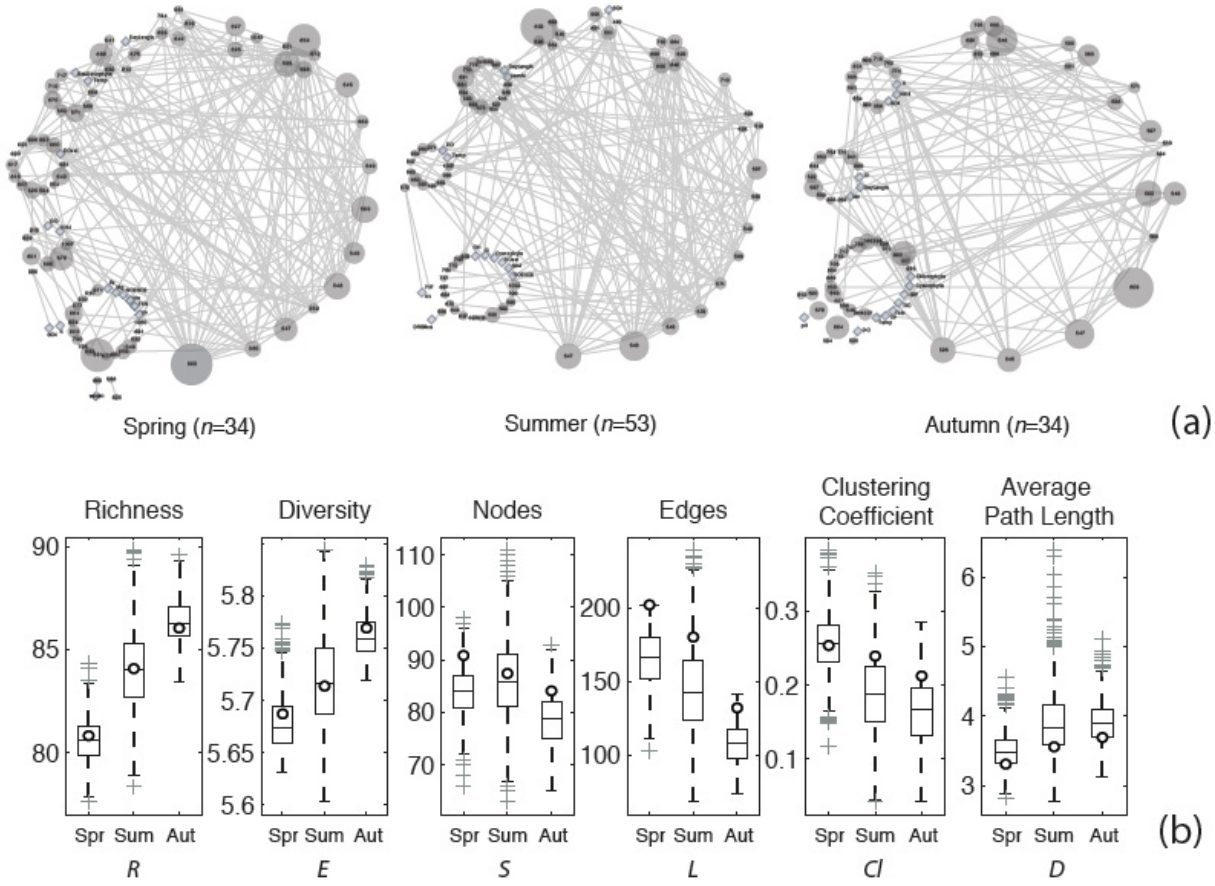

Figure 5.1. Co-occurrence network visualization (a) and properties (b) for a ten-year time series of bacterioplankton communities in Lake Mendota, WI, USA. From spring to autumn, diversity (*E*) and richness (*S*) increased while network complexity decreased. The spring season network had more nodes,

edges, and high-degree nodes than summer or autumn (a). Network visualizations (a) are comprised of all significant (LSA $R > 0.3$, $p < 0.001$, no time lag) interactions between OTUs and environmental variables, by season, for all observations. The number of total observations (n) for each season are indicated in parentheses below networks. Nodes are labeled with OTU fragment length or environmental variable name. For OTUs, node area is proportional to average relative abundance for the season indicated. Diamonds indicate all environmental variable nodes. Nodes are grouped according to degree (edges/node), with highest degree node at the bottom of the network and nodes of decreasing degree placed sequentially, counter-clockwise, such that lowest-degree nodes (1 edge/node) are grouped to the immediate left of the highest-degree node. Network complexity decreased across seasons while richness and diversity increased, and trends in all network properties, diversity and richness were robust to normalizing for the number of observations made (b). Network properties (number of nodes (S), edges (L), clustering coefficient (Cl), and characteristic path length (D)) are shown in (b). Open circles indicate properties calculated for networks shown in (a), which included all observations for a given season. Boxplots represent observation-normalized results: we performed LSA (LSA $R > 0.3$, $p < 0.001$, no time lag) and network analysis on networks generated from Monte Carlo simulations of 30 randomly drawn observations from each season. Results of 1000 simulations for each season were aggregated and compared to test the effect on network properties of the number of observations included in the analysis. Boxes represent inter-quartile range and whiskers indicate 10th and 90th percentiles, plus symbols indicate outliers.. Significant differences exist between observation-normalized distributions of network properties from each season, for all properties (Wilcoxon rank sum test: $\alpha=0.01$, $p<0.0001$).

5.3 Acknowledgements

ELK and KDM were supported by an NSF CAREER award (CBET 0738039) and the National Institute of Food and Agriculture, United States Department of Agriculture (ID number WIS01516). This material is based upon NTL LTER work supported by the National Science Foundation under Cooperative Agreement #0822700. Thanks to Jack A. Gilbert, Alex Eiler and Hannes Peter for thoughtful discussion. Parallelized analysis was run with the assistance of UW Condor high throughput computing system (http://research.cs.wisc.edu/condor/)

5.4 References

Barberán, A., Bates, S. T., Casamayor, E. O., & Fierer, N. (2011). Using network analysis to explore co-occurrence patterns in soil microbial communities. *The ISME journal*, *6*(2), 343-51. doi:10.1038/ismej.2011.119

Brock, T. D. (1985). *A Eutrophic Lake: Lake Mendota, Wisconsin* (p. 308). Springer Verlag.

Caporaso, J. G., Paszkiewicz, K., Field, D., Knight, R., & Gilbert, J. a. (2011). The Western English Channel contains a persistent microbial seed bank. *The ISME journal*, 1-5. Nature Publishing Group. doi:10.1038/ismej.2011.162

Crump, B. C., & Hobbie, J. E. (2005). Synchrony and seasonality in bacterioplankton communities of two temperate rivers, *50*(6), 1718-1729.

Dunne, J. A., Williams, R. J., Martinez, N. D., & Fe, S. (2002). Network topology and biodiversity loss in food webs: Robustness increases with connectance. *Ecology Letters*, *5*(4), 558-567. doi:10.1046/j.1461-0248.2002.00354.x

Fuhrman, J. A., Hewson, I., Schwalbach, M. S., Steele, J. a, Brown, M. V., & Naeem, S. (2006). Annually reoccurring bacterial communities are predictable from ocean conditions. *Proceedings of the National Academy of Sciences of the United States of America*, *103*(35), 13104-9. doi:10.1073/pnas.0602399103

Gasol, J., Peters, F., Guerrero, R., & Pedrós-Alió, C. (1992). Community structure in Lake Ciso: Biomass allocation to trophic groups and differing patterns of seasonal succession in the meta- and epilimnion. *Arch. Hydrobiol.*, 275-303.

Gilbert, J. a, Steele, J. a, Caporaso, J. G., Steinbrück, L., Reeder, J., Temperton, B., Huse, S., et al. (2012). Defining seasonal marine microbial community dynamics. *The ISME Journal*, 298-308. doi:10.1038/ismej.2011.107

Graham, J. M., Kent, a D., Lauster, G. H., Yannarell, a C., Graham, L. E., & Triplett, E. W. (2004). Seasonal dynamics of phytoplankton and planktonic protozoan communities in a northern temperate humic lake: diversity in a dinoflagellate dominated system. *Microbial ecology*, *48*(4), 528-40. doi:10.1007/s00248-004-0223-3

Hahn, M. W., Scheuerl, T., Jezberová, J., Koll, U., Jezbera, J., Šimek, K., Vannini, C., et al. (2012). The Passive Yet Successful Way of Planktonic Life: Genomic and Experimental Analysis of the Ecology of a Free-Living Polynucleobacter Population. (J. H. Badger, Ed.)*PLoS ONE*, *7*(3), e32772: 1-17. doi:10.1371/journal.pone.0032772

Jones, S. E., & Lennon, J. T. (2010). Dormancy contributes to the maintenance of microbial diversity. *Proceedings of the National Academy of Sciences of the United States of America*, *107*(13), 5881-5886. doi:10.1073/pnas.0912765107

Kent, A. D., Yannarell, A. C., Rusak, J. A., Triplett, E. W., & Mcmahon, K. D. (2007). Synchrony in aquatic microbial community dynamics. *Microbial Ecology*, 38-47. doi:10.1038/ismej.2007.6

Kuchaiev, O., Stevanović, A., Hayes, W., & Pržulj, N. (2011). GraphCrunch 2: Software tool for network modeling, alignment and clustering. *BMC bioinformatics*, *12*(1), 24. BioMed Central Ltd. doi:10.1186/1471-2105-12-24

Lennon, J. T., & Jones, S. E. (2011). Microbial seed banks: the ecological and evolutionary implications of dormancy. *Nature reviews. Microbiology*, *9*(2), 119-30. Nature Publishing Group. doi:10.1038/nrmicro2504

Magurran, A. (2011). *Biological diversity: Frontiers in measurement and assessment*. (A. E. Magurran & B. J. McGill, Eds.) (p. 345). New York: Oxford University Press.

Martinez, N. D., Hawkins, B. A., Dawah, H. A., & Feifarek, B. P. (1999). Effects of sampling effort on characterization of food-web structure. *Ecology*, *80*(3), 1044-1055.

Maurice, C. F., Bouvier, T., Comte, J., Guillemette, F., & Del Giorgio, P. a. (2010). Seasonal variations of phage life strategies and bacterial physiological states in three northern temperate lakes. *Environmental microbiology*, *12*(3), 628-41. doi:10.1111/j.1462-2920.2009.02103.x

McCann, K. S. (2000). The diversity-stability debate. *Nature*, *405*(6783), 228-33. doi:10.1038/35012234

Newman, M. E. J. (2003). The structure and function of complex networks. *SIAM Review*, *45*(2), 167-256.

Ptacnik, R., Solimini, A. G., Andersen, T., Tamminen, T., Brettum, P., Lepistö, L., Willén, E., et al. (2008). Diversity predicts stability and resource use efficiency in natural phytoplankton communities. *Proceedings of the National Academy of Sciences of the United States of America*, *105*(13), 5134-8. doi:10.1073/pnas.0708328105

Ruan, Q., Steele, J. a, Schwalbach, M. S., Fuhrman, J. A., & Sun, F. (2006). A dynamic programming algorithm for binning microbial community profiles. *Bioinformatics (Oxford, England)*, *22*(12), 1508-14. doi:10.1093/bioinformatics/btl114

Shade, A., Kent, A. D., Jones, S. E., Newton, R. J., Triplett, E. W., & McMahon, K. D. (2007). Interannual dynamics and phenology of bacterial communities in a eutrophic lake. *Limnology and Oceanography*, *52*(2), 487-494. doi:10.4319/lo.2007.52.2.0487

Shurin, J. B., Arnott, S. E., Hillebrand, H., Longmuir, A., Pinel-Alloul, B., Winder, M., & Yan, N. D. (2007). Diversity-stability relationship varies with latitude in zooplankton. *Ecology letters*, *10*(2), 127-34. doi:10.1111/j.1461-0248.2006.01009.x

Smoot, M., Ono, K., Ruscheinski, J., Wang, P., & Ideker, T. (2011). Cytoscape 2.8: new features for data integration and network visualization. *Bioinformatics (Oxford, England)*, *27*(3), 431-432.

Wu, Q. L., & Hahn, M. W. (2006). High predictability of the seasonal dynamics of a species-like Polynucleobacter population in a freshwater lake. *Environmental microbiology*, *8*(9), 1660-6. doi:10.1111/j.1462-2920.2006.01049.x

5.7 Supplementary Materials

Bacterioplankton community sampling and fingerprinting

121 bacterioplankton community (BC) samples were collected from the integrated upper water column (0-12m) on monthly- to twice-monthly basis from 2000-2009 under ice-free conditions on Lake Mendota, Wisconsin, USA. Sample dates are listed in Supplementary Table 1 (S1). Samples were collected from the location of maximum depth in Lake Mendota at 43° 06′ N, 89° 24′W, 327 m.s.l. Seasons were defined by the astronomical March and September equinox and the June solstice.

Samples were filtered (0.2 μm Pall Supor filters) and stored at -80 C until subsequent processing. Deoxyribonucleic acid (DNA) was extracted with QBiogene Bio101 FastDNA extraction kit and modifications to manufacturer's protocol described previously (Yannarell et al., 2003; Yannarell & Triplett, 2005), and followed by amplification by polymerase chain reaction and automated ribosomal intergenic spacer analysis (ARISA) as described by Shade and colleagues (Shade et al., 2007). ARISA profiles were analyzed using Genemarker v 1.5 software (SoftGenetics, LLC) and a custom R script developed in the R statistics package (R Development Core Team, 2011) to aid in high-throughput 'binning' of peaks, as previously described (Jones & McMahon, 2009).

Environmental variables

Thirty-three physical, chemical and biological water quality parameters were collected at biweekly frequency during ice-free seasons by the North Temperate Lakes Long Term Ecological Research (NTL LTER) program at the same location as microbial sample collection; a complete listing of variables, protocols, and observational data is available at

www.lter.limnology.wisc.edu and variables and abbreviations are listed in Supplementary Table 1 (S1) (NTL-LTER, 2011a, 2011b, 2011c). Data underwent quality control as described in NTL LTER protocols, all flagged data were removed, and replicates averaged. Phytoplankton samples were collected across a vertically averaged integrated depth 0-8m and biomass was summed at the division level for functional groups *Cyanophyta*, *Bacillariophyta*, and *Chlorophyta*. For zooplankton, organism density was used. For all other variables, discrete depth measurements were typically made every 1-4 m from 0-20 m depth; all variables measured between 0-12m depths were vertically-averaged.

When NTL LTER observations did not co-occur with microbial sampling, time-weighted averages of observations within +/- 17 days were assigned to microbial observations. For >90% of samples, LTER environmental observations occurred within 7 days of bacterioplankton sampling. For time-weighted interpolation, nearby observations were averaged after being weighted by a value inversely proportional the absolute value of the number of days between water quality observations and microbial observations:

$$Y_{int} = [\sum^{n}_{i=1} w_i * y_i] / \sum^{n}_{i=1} w_i$$

$$w_i = 17 - |x_i - x_0|$$

Where Y_{int} is the interpolated value used in subsequent analyses for microbial samples corresponding to day of year x_0, n is the number of observations made within +/- 17 days of x_0 for any given year, x_i is day of year that variable y_i was collected on. w_i is the 'weighted' factor which is proportional to the temporal proximity of the water quality observation to the microbial observation. For example: a microbial sample was collected on day 50 ($x_0 = 50$), and NTL LTER

water quality samples were collected on day 40 (x_1) and 54 (x_2). If temperature is unknown on day 50, but had values of 15 (y_1) and 18 (y_2),

$$Y_{int} = [((17-|40-50|)*15)+ ((17-|54-50|)*18)] / ((17-|40-50|) +(17-|54-50|)) = 17.0$$

Supplementary Table 1. Bacterioplankton community sampling dates, environmental variables, and abbreviations.

Microbial sampling dates (mm/dd/yy)				**Environmental variables**	**Abbreviation**
3/15/00	8/29/02	8/2/05	7/22/08	Month	Month
3/30/00	9/12/02	8/19/05	8/7/08	Year	Year
4/14/00	9/24/02	8/31/05	8/22/08	Day of year	Day of year
4/27/00	10/8/02	9/18/05	9/5/08	Day length	Day Length
5/11/00	10/22/02	10/10/05	9/15/08	Alkalinity	Alk
6/6/00	11/7/02	11/8/05	10/2/08	Calcium	Ca
6/20/00	11/20/02	4/6/06	10/17/08	Chlorophyll-a	Chl
7/17/00	5/13/03	4/21/06	2/24/09	Chloride	Cl
8/1/00	5/28/03	5/4/06	4/29/09	Dissolved inorganic carbon	DIC
8/17/00	6/9/03	5/15/06	6/9/09	Dissolved oxygen	DO
9/12/00	6/27/03	6/9/06	6/18/09	Dissolved organic carbon	DOC
9/26/00	7/23/03	7/13/06	6/26/09	Dissolved oxygen percent saturation	DOsat
10/10/00	8/7/03	7/17/06	7/7/09	Dissolved reactive silica	DRSilica
10/24/00	9/8/03	8/3/06	7/30/09	Iron	Fe
11/28/00	9/22/03	8/22/06	8/10/09	Potassium	K
3/13/01	10/15/03	9/8/06	8/26/09	Magnesium	Mg
4/23/01	11/11/03	10/6/06	9/13/09	Manganese	Mn
5/21/01	5/19/04	10/20/06	9/27/09	Ammonium	NH4
6/4/01	5/26/04	11/3/06	10/9/09	Nitrate+ nitrite	NO3NO2
7/2/01	6/11/04	11/16/06	10/26/09	Sodium	Na
7/5/01	6/25/04	5/11/07	11/14/09	Sulfate	So4
7/16/01	7/8/04	5/29/07	12/4/09	Soluble reactive phosphorus	SRP
7/30/01	7/22/04	6/11/07		Total inorganic carbon	TIC
8/13/01	9/2/04	7/23/07		Total kjeldhal nitrogen	TKN
8/28/01	9/16/04	8/6/07		Total organic carbon	TOC
9/10/01	9/30/04	8/20/07		Total phosphorus	TP
9/26/01	10/12/04	9/27/07		Temperature	Temp
10/20/01	9/16/04	10/12/07		Zooplankton density	Zoop

11/6/01	9/30/04	11/1/07	pH	pH
11/26/01	10/12/04	5/10/08	Secchi depth	Secchi
5/24/02	4/11/05	6/5/08	Bacillariophyta biomass	Bacillarophyta
7/1/02	5/25/05	6/25/08	Chlorophyta biomass	Chlorophyta
8/1/02	6/22/05	7/11/08	Cyanophyta biomass	Cyanophyta

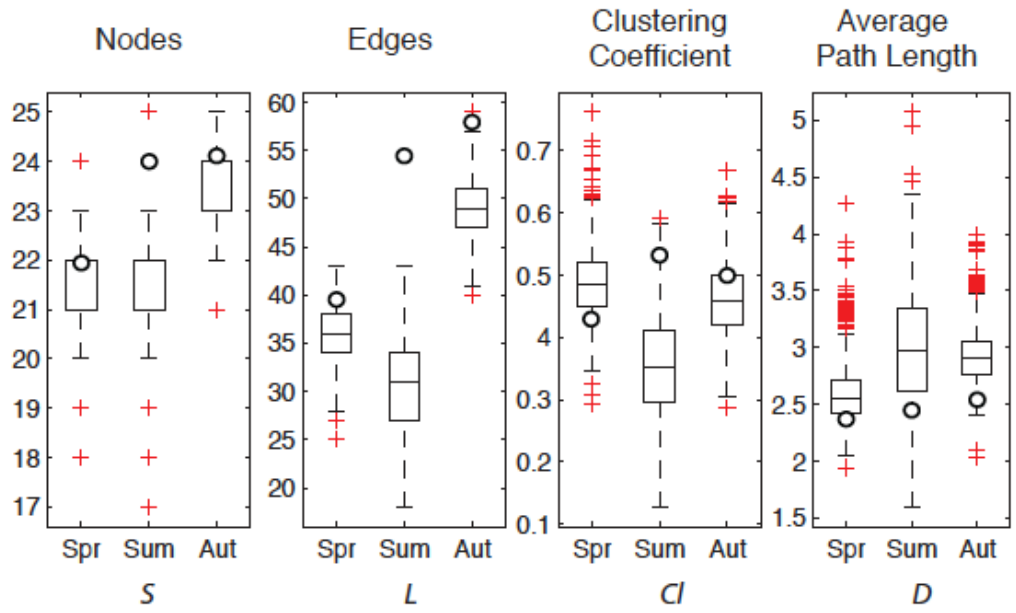

Figure S1 Co-occurrence network properties for a ten-year time series of environmental variables in Lake Mendota, WI, USA (number of nodes (*S*), edges (*L*), clustering coefficient (*Cl*), and characteristic path length (*D*)). Open circles indicate properties calculated for networks that include all observations for a given season. Boxplots represent observation-normalized results: we performed LSA (LSA $R > 0.3$, $p < 0.001$, no time lag) and network analysis on networks generated from Monte Carlo simulations of 30 randomly drawn observations from each season. Results of 1000 simulations for each season were aggregated and compared to test the effect on network properties of the number of observations included in the analysis. Boxes represent inter-quartile range and whiskers indicate 10th and 90th percentiles, red pluses indicate outliers. Significant differences exist between observation-normalized distributions of network properties from each season, for all properties (Wilcoxon rank sum test: $\alpha=0.01$, $p<0.0001$).

References

Jones, S. E., & McMahon, K. D. (2009). Species-sorting may explain an apparent minimal effect of immigration on freshwater bacterial community dynamics. *Environmental microbiology*, *11*(4), 905-13. doi:10.1111/j.1462-2920.2008.01814.x

NTL-LTER. (2011a). Physical Limnology Dataset. *North Temperate Lakes Long Term Ecological Research Program*. Madison, WI.

NTL-LTER. (2011b). Chemical Limnology Dataset. *North Temperate Lakes Long Term Ecological Research Program*. Madison, WI. Retrieved from http://www.lternet.edu/sites/ntl/

NTL-LTER. (2011c). Biological Limnology Dataset. *North Temperate Lakes Long Term Ecological Research Program*. Madison, WI.

Shade, A., Kent, A. D., Jones, S. E., Newton, R. J., Triplett, E. W., & McMahon, K. D. (2007). Interannual dynamics and phenology of bacterial communities in a eutrophic lake. *Limnology and Oceanography*, *52*(2), 487-494. doi:10.4319/lo.2007.52.2.0487

R Core Development Team. (2011). R: A Language and Environment for Statistical Computing. Retrieved from http://www.r-project.org

Yannarell, a C., Kent, a D., Lauster, G. H., Kratz, T. K., & Triplett, E. W. (2003). Temporal patterns in bacterial communities in three temperate lakes of different trophic status. *Microbial ecology*, *46*(4), 391-405. doi:10.1007/s00248-003-1008-9

Yannarell, A. C., & Triplett, E. W. (2005). Geographic and Environmental Sources of Variation in Lake Bacterial Community Composition. *Applied and environmental microbiology*, *71*(1), 227-239. doi:10.1128/AEM.71.1.227

Chapter 6 - Organic phosphorus speciation in a eutrophic lake

Emily L. Kara, Monika Ivancic, Barbara Cade-Menun, and Katherine D. McMahon

6.1 Abstract

We used ^{31}phosphorus nuclear magnetic resonance spectroscopy (^{31}P NMR) to characterize particulate and dissolved phosphorus from a eutrophic lake over five months, from summer stratification through fall mixis. We characterized P structure and speciation from the surface and hypolimnion of Lake Mendota, Wisconsin. We found orthophosphate, monoesters, diesters, pyrophosphate, polyphosphate and phosphonates in both particulate and dissolved phosphorus samples. For particulate samples, phosphonates, polyphosphate, and pyrophosphate consistently increased in relative proportion from late spring through early fall, until fall mixis. Hypolimnetic particulate phosphorus samples were much more variable in composition, as were both dissolved epilimnetic and hypolimnetic samples compared to epilimnetic particulate samples. Consistent phosphonate observed in both epilimnetic and hypolimnetic samples may be due to the recalcitrance of this organic P compound. Dissolved P samples were mainly comprised of orthophosphate, but occasionally contained monoesters, diester, polyphosphate, pyrophosphate, and phosphonate. When dissolved reactive phosphorus and total dissolved phosphorus were below the limit of detection by colorimetry, we typically saw no signal in ^{31}P NMR results.

The hydrological inflows to the lake were sampled on three dates characterizing low flow, high flow, and spring runoff. Particulate river samples were similar in compound diversity to lake particulate samples, but generally contained more orthophosphate and monesters than lake samples.

6.2 Introduction

Over the past century, anthropogenic activities have increased the flux of carbon (C), nitrogen (N), and phosphorus (P) into global cycles by 13, 108, and 400%, respectively (Falkowski et al., 2000). These increases have resulted in discernable and, in some cases, severe effects, including global climate change, acidification, and eutrophication of marine and fresh waters. Due to human activities including watershed deforestation agricultural runoff, and urban development, Lake Mendota, Wisconsin, has been eutrophic for more than 150 years. Mitigation of water quality degradation by reduction of P-loading is a known solution (Jeppesen et al., 2005), but has not been implemented sufficiently to improve water quality in this watershed (Carpenter et al., 2007). Nutrient management has been in place in the Mendota watershed for more than a century, and although in-lake P concentrations were significantly reduced as a result of management of nutrient loading in the 1950's (Lathrop et al., 1998), continued reduction of loading and in-lake P levels after that period has not occurred, despite prominent pubic and political focus on water quality, especially over the past two decades (Jones, 2010).

By mass, phosphorus is the least abundant of the major nutrients required for primary production (i.e. algal and *Cyanobacterial* growth), but unlike carbon and nitrogen, P has no significant atmospheric source. P enters Lake Mendota by external loading- mainly by hydrologic inputs from the surrounding watershed and atmospheric deposition- and by internal loading from the lake's anoxic hypolimnion and sediment. Significant springtime precipitation events, variations in spring mixis temperatures, and strength of thermal structure during summer stratification can determine on a year-to-year basis whether internal or external P sources dominate total loading rates (Soranno et al., 1997). The effect of the chemical nature of these

sources (sediment and hypolimnion versus overland surface flow) and their contribution P pool is unknown.

Orthophosphate (PO_4), is the preferred P substrate for both phytoplankton and bacterioplankton in aquatic systems (Rigler, 1956; Wetzel, 2001). In temperate, stratified, eutrophic lakes, dissolved reactive phosphorus (DRP) concentrations decrease after ice off and spring mixing, and eventually are reduced to low levels (<10 μg/L), annually. In eutrophic Lake Mendota, Wisconsin, this period of low DRP typically begins around the end of June (~ day 175), ends at fall lake turnover around October (~ day 270), and is typified by high primary productivity and phytoplankton biomass is dominated by *Cyanobacteria* species. During this period, of the main nutrients required for primary production, P is likely most limiting in the epilimnion of Lake Mendota (Brock, 1985).

Early work on the speciation and transformation of P in aquatic systems depended on gel filtration chromatography, which allows for separation by molecular weight, and colorimetric determination. It was previously assumed that the compounds included in the DNRP were dissolved organic P (e.g. Lean, 1973), although it is now know that this fraction can encompass both organic and inorganic P forms (Turner et al., 2006). Using colorimetric and gel filtration techniques, detailed characterization of the structure and environmental importance of the DNRP pool is not possible. Over the past two decades, the use of phosphorus-31 nuclear magnetic resonance spectroscopy (^{31}P NMR) has become available for the characterization of phosphorus-containing molecular structures from environmental samples (Cade-Menun, 2005). ^{31}P NMR has been used extensively to characterize aquatic sediments (Hupfer et al., 2004; Reitzel et al., 2007), but similar studies on aquatic freshwater systems have been limited in scope (but see Cade-Menun et al., 2006; Nanny & Minear, 1997; Reitzel et al., 2006). The studies that have

been undertaken have assessed only limited spatial and temporal variability in systems, likely in part due to the effort required to collect, prepare, and analyze samples using ^{31}P NMR spectroscopy. Although the work of Lean, Minear, Paerl and Downes, and White and Payne in the ‘60s through ‘80s elucidated many important details of phosphorus cycling in lakes, the classes of compounds described in those works are now considered to be inaccurate, but have yet to be characterized using modern techniques. The spatial and temporal dynamics of phosphorus speciation in lakes is poorly described, particularly in light of the extensive research done in marine waters and lake, river, and marine sediments (Cade-Menun, 2005).

6.2.1 Terminology

In order to continue a review of the literature in the context of the current research, a clarification of terms used to describe various forms and fractions of phosphorus is required. A proxy for dissolved orthophosphate is commonly estimated following filtration of surface waters by an ammonium-molybdate reaction and colorimetric determination (Murphy & Riley, 1962). For accuracy, we will define and refer to molybdate colorimetric determination of dissolved phosphorus as DRP- but we caution this is just a proxy for orthophosphate concentration, and that not all phosphate may react with molybdate under the acid condition required for this determination. Acid-labile organic and condensed P species may be falsely detected as orthophosphate (Worsfold et al., 2005), while orthophosphate associated with humic and fulvic acids may evade detection using this technique (Turner et al., 2006). Forms of phosphorus that react with molybdate only after acid digestion are referred to as DNRP. The sum of DRP and DNRP together will be referred to as TDP- or the total dissolved phosphorus detected using a molybdate reaction and colorimetry following acid digestion for filtered water samples. Total

phosphorus (TP) is determined following acid digestion and analysis by colorimetry or inductively coupled optical emission spectroscopy (ICP OES). Total particulate phosphorus (TPP) is likewise the acid-digested particulate-only (in this study includes solids collected on 0.45 μm filter) fraction of P, also assessed by colorimetry or ICP OES. Some techniques do allow direct measurement of orthophosphate; when indicating direct detection of orthophosphate (e.g. by 31-phosphorus nuclear magnetic resonance spectroscopy) we will refer to it as orthophosphate, or as PO_4, in addition to when referring to the substrate in general. For historical works that use alternative or outmoded vocabulary for specific fractions of P, we use language consistent with those studies, but include parenthetical remarks to indicate relationships to the definitions described above.

6.2.2 Early characterization of environmental phosphorus and its biological availability

The recognition of the importance of phosphorus for water quality and eutrophication in the early 1970s (e.g. Dillon & Rigler, 1974), was accompanied by an effort to characterize the molecular forms phosphorus found in the environment in order to understand if and how the fates of distinct structures differed in aquatic systems. Techniques to assess P included traditional colorimetric determination using an ammonium molybdate method on unprocessed or acid-hydrolyzed whole- or filtered-water samples. Further discrimination was made using gel filtration (e.g. Sephadex and Sepharose) chromatography to characterize molecular weight, enzyme assays to determine bio-availability or to confirm structural assignment, and fluorescence to confirm molecular composition utilizing known excitation and emission wavelengths of target compounds. Deoxyribonucleic acid, for example, can be confirmed by all

of these techniques. Early in the field of study, molecular weight was most frequently used to distinguish forms of DNRP.

Minear investigated aquatic organic P (DNRP) in the early 1970s, first by synthesizing soluble organic P from algal cultures to establish protocols (1972). Techniques of concentration and characterization were then applied to lake water samples. From three lakes in Washington state, 20% of the soluble organic P was determined to be high molecular weight (molar weight > 50,000), and was speculated to be deoxyribonucleic acid (DNA), based on by fluorometry and enzyme assays (Minear, 1972).

Using gel filtration combined with radiolabeled P substrates ($[^{32}P]$-PO_4), Lean (1973) carried out several experiments that allowed rate constants between particulate, organic (DNRP), and inorganic P (DRP) to be estimated for the transformation of phosphorus forms from small, eutrophic Heart Lake, Ontario. His work showed that two dissolved organic P pools- high molecular weight 'colloidal P' (HMW DNRP) and a smaller molecular weight 'excretion' product (LWM DNRP)- interacted with P flows in lake systems, and showed the exchange mechanisms between the pools, which mainly flows from particulate P (mainly comprised of phytoplankton in that system) to excreted dissolved organic P or PO_4, and the excreted organic P can flow to colloidal P, or directly to PO_4. Colloidal P was permanently stored in an unreactive form or was mineralized to PO_4. Particulate P by far accounted for the largest pool of P (98.5%), with colloidal P (1.2%), PO_4 (0.2%), and excreted organic P (0.1%) accounting for the remaining P. The largest exchange rates under steady state conditions occurred between particulate P and PO_4. Lean's experiments also confirmed that organic P (LWM DNRP) excretion products from live phytoplankton was a significant source of organic P, and that this excretion took place at the time of maximum biomass production (Lean, 1973).

Paerl and Downes showed that P-starved algal cultures could utilize high molecular weight (>5000) acid-hydrolysable organic P substrates (gel-filtered HMW DRP), but did not grow as rapidly on high molecular weight P as on orthophosphate (Paerl & Downes, 1978). White and Payne (1980) went on to show that high molecular weight acid-hydrolysable P from different New Zealand lakes was taken up at different rates by an axenic *Chlorella* culture, indicating that not all high molecular weight organic P compounds were equally bioavailable (White & Payne, 1980).

The sources of DNRP in natural waters are from live phytoplankton (Kuenzler, 1970), zooplankton, (Peters & Lean, 1973), or fish (Schaus et al., 1997). During in-lake decomposition of allochthonous and autochthonous organisms, cellular components undergo abiotic (mechanical and photo-oxidative) and biotic (mediated be bacteria and fungi) degradation, and organic P may be released. Using 8 axenic marine phytoplankton cultures, Kuenzler showed dissolved organic P production and uptake that was dependent on environmental conditions including light, P limitation, and nitrogen limitation (1970). The experiments showed that excretion and uptake both occurred by phytoplankton, but that uptake was sometimes limited by lack of alkaline phosphatase activity (Kuenzler, 1970). Eisenreich and Armstrong showed the proportion of dissolved inositol phosphates (monoesters) to total dissolved phosphorus was significant, ranging from 19-26 percent of lake water and surface foam in Lake Mendota, Wisconsin (Eisenreich & Armstrong, 1977). Inositol phosphates (IP) typically originate in soils, where they are accumulated from buildup of plant derived organic matter. Plants store phosphate intracellularly as inositol hexaphosphate (IHP), much like bacterial store polyphosphate. However, there is also evidence for algal-derived IP, particularly when present in lower ester forms. The author suggest that soil inputs of IP account for ~ 20,000 kg IP/year loading to the

lake, while algal-derived IP accounts for 17,000 kg IP/year. In the context of mean loading rate of P to Lake Mendota of 34,000 kg P/ year (Lathrop, 2007), these loading estimates represent significant fractions of the in-lake P budget.

6.2.3 Characterization of environmental phosphorus using ^{31}P nuclear magnetic resonance spectroscopy

It was not until the mid-1990s that solution ^{31}P nuclear magnetic resonance (NMR) spectroscopy became available for the assignment of molecular formulas and structures to phosphorus-containing compounds, and at this time there was a renewal of research activity around organic P in lakes. NMR spectroscopy is possible due to the emission of electromagnetic radiation of atomic nuclei with an odd number of protons or neutrons upon perturbation with electromagnetic radiation. ^{31}P is one such isotope, and is present at 100% natural abundance, making it ideal for NMR spectroscopy, unlike some other isotopes present in many natural systems and organisms (e.g. ^{1}H, ^{15}N, or ^{17}O) at less than 100% abundance. In NMR, nuclei of non-zero spin (odd number of protons or neutrons) are aligned under a constant magnetic field, perturbed by a radio frequency (RF) pulse equal to the difference between the nuclei spin states, and then allowed to 'relax' and return to thermodynamic equilibrium. As they relax, nuclei emit energy that is a function of the bonds associated with the give isotope. The emission energy signal resulting only from non-equilibrium (non-zero spin) nuclear spin magnetism is known as the free induction decay (FID). The number of pulses (or 'scans') repeated depends on the concentration of target nuclei in the sample, such that more scans are required to detect lower concentration compounds. For ^{31}P NMR spectroscopy of environmental samples, the uses of hundreds to tens of thousands of scans have been reported. Digitized FID data are processed

using Fourier transform, typically with a software package. The resulting output data can be compared across samples, experimental parameters, and magnets, based on the chemical shift (in units of parts per million, ppm). Processed sample spectra contain peaks at specific chemical shifts that correspond to distinct molecular structures (Figure 6.1). Environmental phosphorus compounds have a well-established record of shift assignments e.g. see (Cade-Menun, 2005), which allows for relatively unambiguous assessment of specific compounds (e.g. DNA or polyphosphate) from samples. NMR has benefits over other analytical tools in that all compounds can be analyzed simultaneously in a single solution and the technique is non-destructive for samples.

NMR can be used for both solid (*solid-state* NMR) and liquid (*solution* NMR) samples. The benefits and drawbacks of both types of NMR for environmental ^{31}P studies are described elsewhere (Cade-Menun, 2005). For this work, and for many environmental samples from lakes, rivers, and marine water and sediment samples, solution state NMR is preferred, particularly because of the higher resolution of Fourier-transformed data for peak assignment and for higher diversity of resolved peaks.

Other ^{31}P NMR spectroscopy experimental parameters of relevance include extraction and concentration technique, re-suspension solvent, spin-lattice (referred to as T_1) relaxation time, pulse angle, number of scan, probe size, and external standardization. Sample processing, including concentration, extraction, and sample preparation, are discussed in greater detail below in section 6.3.3. ^{31}P NMR spectroscopy experimental parameters are generally chosen to maximize signal-to-noise ratio while minimizing the total length of the experiment, due to the cost associated with instrument time and the potential for sample degradation during long experiments.

Spin-lattice relaxation time, or T_1 relaxation time, refers to the delay time given for nuclei to relax prior to another RF pulse. As nuclei relax, energy is dissipated to the surrounding environment and to the surrounding nuclei; spin-spin (T_2) relaxation is a negligible process compared to spin lattice relaxation (McDowell et al., 2006). T_1 relaxation time, however, if not long enough, can result saturated nuclei that have poorer spectral resolution than nuclei that are allowed to fully relax, and subsequent lower signal to noise ratios. T_1 can also vary with extractants (Cade-Menun et al., 2002) and with the concentration of paramagentic ions, which also must be present, but not at too high concentrations (Ding et al., 2010; McDowell et al., 2006). Spectral quality may be sacrificed if T_1 time is non-optimal.

Signal strength is also a function of the number of scans used in an experiment. Additional scans yields higher resolution and diversity of peaks. Typically, due to cost of instrument time and the potential of degradation of certain P species during the experiment (typically controlled to be at or around 20C), the minimum number of scans is used. For samples containing lower concentration of nuclei, more scans are required to achieve adequate signal to noise. Likewise, probe size is proportional to signal, such that the limit of detection is proportional to the square of the probe diameter. External standards are required to zero spectra, which can vary due to pH and concentration of other dissolved solutes. Typically, samples will be spiked with H_3PO_4 just prior to the end of the experiment, and the resultant peak is set to 6ppm. Standardizing with D_2O, added to allow 'locking' can also be done and results in very close match with standardization of external source. External standards of other compounds of interest can also be added at the end of an experiment to confirm presence of suspected peaks.

For water samples, concentration of target compounds is required, as the sensitivity of ^{31}P NMR is around 50 mg P/L (Reitzel, 2006) while natural surface waters are typically >>1 mg

P/L. Of the few studies that characterize dissolved and particulate phosphorus of natural waters, a common theme is the need for a unified method of concentration and extraction (e.g. Cade-Menun et al., 2006; Nanny & Minear, 1997; Reitzel et al., 2009). Concentration techniques such as tangential flow filtration and reverse osmosis (Nanny & Minear, 1997), concentration by precipitation with aluminum (Reitzel et al., 2009), rotary vacuum evaporation (Hupfer et al., 2004; Reitzel et al., 2009), and lyophilization of frozen samples (Cade-Menun et al., 2006) have been used. Freezing-lyophilization has benefits over tangential flow filtration and concentration by precipitation, in that samples are immediately frozen following initial filtration, and remain frozen until completely dry, limiting degradation at room temperature under tangential flow filtration, or chemical transformation during precipitation. Lyophilization requires only basic laboratory equipment, effectively concentrates surface water samples as small as 4 L, allows for routine collection, and has recently been shown to be suitable for recovery of P compounds from river water samples (Cade-Menun et al., 2006).

The use of solution ^{31}P NMR spectroscopy for dissolved constituents of lake water samples was first published in 1994 by Nanny and Minear, who worked to enhance methodological sensitivity with the use of Lanthanide shift reagents to reduce line broadening to resolve spectral shifts, increase sensitivity, and reduce T_1 relaxation time (Nanny & Minear, 1994). Nanny and Minear later found organic P concentration in lakes range from <5 μg/L in oligotrophic lakes to ~100 μg/L in a eutrophic lake (1997). Phosphate mono- and di-esters, pyrophosphates, and polyphosphates were found in eutrophic Crystal Lake, IL; the ratios of these compounds varied with season (Nanny & Minear, 1997).

In a methodological paper showing the efficacy of poly aluminum chloride as a concentration agent, Reitzel et al. performed ^{31}P NMR of dissolved P from the hypolimnetic

waters of five Danish lakes (Reitzel et al., 2006). The authors found orthophosphate, orthophosphate mono- and di-esters, and pyrophosphate, which appeared in different proportions across lakes. In a ^{31}P NMR study of river waters (Cade-Menun et al., 2006), the authors separated samples into the dissolved (0.45 μm filter) and particulate (matter collected on filter) P fractions from two river samples. In dissolved samples, the authors found primarily orthosphosphate, but also phosphonate, orthophosphate mono- and di-esters, and pyrophosphates. Pyrophosphate and orthophosphate monoesters were of higher concentration in the particulate samples than the dissolved samples (~ 12% and 25%, respectively).

Phytoplankton samples from healthy *C. vulgaris* and *O. rubescens* cultures, P-starved culture, P-recovered culture, and environmental samples collected from Lake Nantua, France, were analyzed by ^{31}P NMR by Feuillade and colleagues (1995). Healthy cultures had significant peaks of orthophosphate, sugar, pyro- and polyphosphate, and orthophosphate mono-and di-esters, while P starved and natural phytoplankton samples contained much less pyro- and polyphosphates (Feuillade et al., 1995). The authors concluded that it was possible for cyanobacteria to exist under low external P conditions without internal P stores. As much of the particulate P in lakes is of biogenic origin, and given the potential connection between phytoplankton internal stores and trophic status, other groups have explored the relationship between trophic status and particulate P forms, but found no relationship (Selig et al., 2006).

Cade-Menun and Paytan characterized several algal cultures under different conditions, high and low light, temperature, and phosphorus conditions. The authors found that low P and high P nutrition affected C:N and C:P ratios, but only high P altered P forms present intracellularly, by increasing pyrophosphate. Neither light, temperature, nor P stress induced changes in intracellular polyphosphate speciation (Cade-Menun & Paytan, 2010).

Other techniques, namely mass spectrometry, have been used to characterize specific compounds, but not to broadly classify organic P in natural environments (Cooper et al., 2005). But, given recent advances in the technology, techniques such as mass spectrometry may also contribute to our understanding of organic P in natural systems in the future.

6.2.4 Aims of this work

For Lake Mendota, Wisconsin, as a representative eutrophic temperate lake, we used ^{31}P NMR spectroscopy to determine (1) dynamics of P speciation during summer stratification to fall mixis in the epilimnion and hypolimnion of a eutrophic lake during the open water period, when epilimnetic DRP concentrations ranges from significant (0.05 mg/L) to below the limit of detection and (2) speciation of dissolved and particulate P composition of hydrologic inflows under base-flow and high-flow conditions.

We hypothesized that during periods of P-limitation (~ July-Sept), concentrations of labile dissolved and particulate organic P (pyrophosphate and phosphate esters) would be reduced and that some standing stock of recalcitrant organic P (phosphonate and polyphosphate) will be maintained through the open water season. Particulate P, due to physical and steric constraints, may be more recalcitrant than dissolved fractions. These measurements will be novel for Lake Mendota, and will be complemented by the routine water quality monitoring of 32 environmental variables by the North Temperate Lakes Long Term Ecological Research program (NTL LTER), which were monitored concurrently with the in-lake collection of phosphorus collected for this study.

6.3 Methods

6.3.1 Site description

Lake Mendota (lat 43.0984, long -89.402) is a temperate, dimictic, eutrophic lake located in the south central Wisconsin, in a watershed (686 km^2) dominated by dairy, cattle, and forage crop agriculture. The lake has surface area of 36 km^2 with maximum and mean depths of 25 and 12m, respectively. The mean hydrological residence time is ~ 4.5 years and the lake has three main hydrologic inflows and one outflow. Deforestation of the watershed for agriculture in the mid 1850's has been implicated as the cause of eutrophication, and the lake's eutrophic status has not changed significantly in the past century (Brock 1985). Like many eutrophic surface waters, Lake Mendota is dominated by *Cyanobacteria* biomass from mid-June through fall mixis, which typically occurs in October. *Microcystis* and *Aphanizomenon* species dominate epilimnetic *Cyanobacterial* biomass.

6.3.2 Sample collection and processing

We sampled on at approximately biweekly frequency from May through October 2011 at the location of maximum depth from Lake Mendota, and on three occasions (July and October 2011 and March 2012) from two major hydrologic inflows to the lake: Pheasant Branch (lat 43.107, long -89.483) and the Yahara River at 113 (lat 43.151, long -89.402). On Lake Mendota at the location of maximum depth, samples were drawn from 0.5 and 14m depths using a horizontal Van Dorn sample, and from 0.5m depth at the surface of two inflowing rivers using a grab sampler. Water was stored in acid washed bottles on ice until further processing. Approximately 8-10 l was collected from each site/depth (Table 6.1). Within one hour of sample collection, water was filtered through 0.45 μm nitrocellulose filters, pre-soaked in de-ionized water from between 1-3 hours prior to filtration. Filtrate was immediately frozen in acid washed

ice cube trays at -20C and filters were stored at -20C, both remaining frozen until further processing. Prior to extraction, filtrate was concentrated to dry solids by lyophilization. Sample starting volume of 8L typically resulted in ~ 2.5g solids.

Colorimetric determination was used to quantify dissolved reactive phosphorus (DRP, after 0.45 μm filtration), and total and total dissolved phosphorus (TP and TDP, after potassium persulfate acid digestion) using the ammonium molybdate method of Murphy and Riley (1962) with ascorbic acid reductant. All reported values reflect mean value of three replicates. NMR-ready sample solutions were sub sampled for analysis of manganese (Mn) and P using ICP OES performed by by the Wisconsin State Lab of Hygiene analytical laboratory. The ratio of P to Mn is shown in Table 1. Iron (Fe) was analyzed for a subset of samples (epilimnetic and hypolimnetic particulate sample prior to extraction and in concentrated NMR-ready solute) from day 123 (May 5 2011) through day 193 (July 12 2011). Fe concentration never exceeded the limit of detection for the SLOH ICP (0.1 mg Fe/L) in the pre-extracted samples, nor in the ~3000 fold concentrated samples (data not shown). For that reason, we considered only P/Mn ratios when considering the effect of paramagnetic ions on T_1 relaxation time (McDowell et al., 2006).

Alkaline phosphatase activity of whole water and 0.45 μm filtrate was measured fluorometrically using methylumbellieferone-phosphate (MUF-P) (Hoppe, 1983; Rengefors et al., 2003; Sinsabaugh et al., 1997). Alkaline phosphatase is an enzyme of the class hydrolase that cleaves orthophosphate monoesters to an alcohol and orthophosphate. Briefly, 0.4 mL of sample water was incubated at room temperature in the dark in triplicate for 4 hours with MUF-P; triplicate blanks (no MUF-P added) were treated identically and used to correct for native fluorescence. Fluorescence was measured for each sample every hour; the slope of the increase

in fluorescence was used as a proxy for alkaline phosphatase activity. Bulk activity rates (μmol MUF-P/L/hr) were used for comparison.

6.3.3 Extraction and preparation

Particulate phosphorus (PP) samples were extracted in 50mL acid-washed falcon tubes with 15mL each of 0.5M NaOH and 0.1M EDTA for 16 hours at room temperature on a shaking plate. Following shaking, tubes were centrifuged for 20 minutes at 2000 rpm; supernatant was decanted and filtered through pre-soaked 0.45 μm nitrocellulose filter (Millipore) and frozen at -80C. After freezing, samples were lyophilized, and solids were stored at -20C until final preparation for NMR experiment.

Following filtration through 0.45 μm pre-soaked nitrocellulose filters, dissolved phosphorus (DP) samples were frozen in acid-washed plastic ice-cube trays at -20C. Frozen sample was lyophilized in acid-washed freeze dry flasks; solids were collected after all water was removed, and were stored at -20C until extraction.

Lyophilized DP solids underwent one of two extraction methods: (1) solids were extracted as described above for PP samples, or (2) solids were pre-extracted: solids were dissolved in 15mL 0.1M EDTA and shaken for 15 minutes, then centrifuged at 2000 rpm for 10 minutes (Hupfer et al., 2004). Supernatant was decanted and discarded, and remaining solids were extracted in the same manner as the particulate fraction: samples were extracted with 15mL each of 0.1 M EDTA and 0.5M NaOH for 16 h, on a shaker plate. Samples were then centrifuged at 2000 rpm for 10 min and liquid was decanted and frozen. Following freezing, samples were lyophilized and stored at -20C until just prior to NMR experiment.

Lyophilized PP and DP samples were re-suspended in D_2O, 0.5 and 1M NaOH, 0.1M EDTA, and H_2O following methods of Cade-Menun et al. (2006) to a total volume of 1.4-2.4 mL or ~ 4mL, depending on the use of 5mm or 10mm probe. In some cases, extra D_2O was added to 5mm samples in order to decrease the viscosity to allow for adequate shimming. Samples underwent ^{31}P NMR experiment within 1 hour of preparation.

For most samples external standardization, H_3PO_4 was added after adequate signal from sample was achieved, at the end of the NMR experiment. Adenosine monophosphate (AMP) was also added to several samples to confirm peak assignment of this compound. Preliminary standardization for all samples was done using D_2O, which typically resulted in assignment of PO_4 peak within +/- 0.2 ppm from 6.0ppm.

6.3.4 ^{31}P NMR Experiments and data processing

Particulate phosphorus spectra were acquired on a 500 MHz Varian Unity spectrometer equipped with a 5mm broadband probe and dissolved phosphorus spectra on a 360 MHz Bruker Avance spectrometer equipped with a 10mm broadband probe. The data was acquired at 24°C, using a 90° pulse, a 0.70 sec acquisition time and a 4.5 sec relaxation delay, with 20Hz spinning (5mm probe) and 12 Hz spinning (10mm probe). The number of scans varied from 1200 (particulate P) to 11000 (dissolved P). Data was processed using the MestReNova NMR processing program, using a 7Hz exponential for full spectral integrations and a 2Hz exponential for integration of specific regions (7ppm to 2.5ppm and 2.5ppm to -4.5ppm).

Samples were spiked with a small amount of H_3PO_4, which peak was referenced to 6.0 ppm as an internal standard. Several samples were spiked with adenosine monophosphate, showing a ^{31}P chemical shift of 4.34ppm.

Peak assignments were made using ^{31}P NMR chemical shifts of orthophosphate (6 ppm, assigned by external H_3PO_4 standard), pyrophosphate (-4 ppm) and polyphosphate (-17 - -22 ppm), phosphonate (18-22 ppm), and orthophosphate monoesters (5.9-3.6 ppm) and diesters (2.5- -1 ppm), which are well established in the environmental chemistry literature from river, lake, and marine samples (e.g. Kolowith et al. 2001, Cade-Menum et al. 2006), addition to an assignment of adenosine monophosphate (4.34ppm) made based on external standards. Relative proportion of phosphorus species were estimated by the integration of ^{31}P NMR spectral peaks (Figure 6.1 ad 6.2). For relative proportions of polyphosphate and pyrophosphate, we combined peak height into one class (PolyP+PyroP), as polyphosphate end groups are detected as pyrophosphate, and polyphosphate can be hydrolyzed to pyrophosphate during alkaline extraction.

6.4 Results

6.4.1 Experimental parameters

Two experimental parameters were tested with the goal of enhancing signal-to-noise in for dissolved P samples: pre-extraction with EDTA, as described by (Hupfer et al., 2004); the use of larger probe. The use of larger (10mm) probe and an EDTA pre-extraction increased sensitivity (Figures 6.3 and 6.4) and were used for all DP samples with results shown.

6.4.2 Environmental Samples

Surface epilimnetic (0.5m) total and soluble reactive phosphorus concentrations decreased from May through September, with epilimnetic DRP falling below limits of detection from July 12 through September 21 (Figure 6.5). Epilimnetic TP and DRP both increased significantly by October 5, following cold weather and an extreme wind event, which resulted in thermal mixing of the lake. Hypolimnetic TP and DRP both increased from May through September 21, with DRP comprising the bulk of TP at 14m (Figure 6.5). Mean epilimnetic TDP increase from 0.015 mg/L on day 123 to 0.065 mg/L on day 153, after which it remained at or near the limit of detection from day 193-264. Epilimnetic TDP was 0.041 mg/L on day 278. Hypolimnetic TDP increased monotonically from day 123 through day 264, from 0.021 to 0.295 mg/L, and decreased again after thermal mixing to 0.115 mg/L on day 278. The difference between TDP and DRP, termed DNRP, was estimated for both epilimnetic and hypolimnetic samples. Epilimnetic DNRP was <0.010 mg/L for all observations, while hypolimnetic DNRP ranged from <0.010 to 0.033 mg/L.

Alkaline phosphatase activity (APA) for whole water samples always exceeded APA of filtrate. APA was highest for both fractions in the epilimnion around day 200, while hypolimnetic activity peaked around day 260 (Figure 6.5).

Samples from two main hydrologic inflows of Lake Mendota were collected under a range of flow conditions, from 72-110 cubic feet per second (cfs) for the Yahara River to 2-4 cfs for Pheasant Branch.

6.4.2.1 Lake particulate phosphorus

Twenty particulate phosphorus samples from discrete depths within the epilimnion (0.5m) and hypolimnion (14m) of Lake Mendota from May 3, 2011 (day 123) through October 5,

2011 (day 278) were analyzed by ^{31}P NMR spectroscopy (Table 1). Total particulate P from estimated after digestion of particulate P ranged from 0.010 to 0.035 mg P/L (*TPP*, Table 6.1). Total phosphorus following extraction and preparation (*NMR TP*) ranged from 0.001 to 0.027 mgP/L, with extraction efficiencies of 4-99%. Inorganic P, the sum of orthophosphate (Ortho), polyphosphate (PolyP) and pyrophosphate (PyroP) accounted for between 31-69% of P, while more organic P compounds accounted for the remainder. For both the epilimnetic and hypolimnetic samples, PolyP, PyroP and phosphonate (Phos) represented relatively greater proportion of P present during mid- summer through fall (after day 180), particularly for epilimnetic samples (Figure 6.5). The maximum fraction of PolyP observed in the epilimnion on day 248, while the maximum fraction observed in the hypolimnion occurred two weeks later on day 264). Epi- and hypolimnetic pyrophosphate (PyroP) was consistently present in low proportions, except for on days 179 and 206 when none was observed in the hypolimnion. Orthophosphate monoesters (MonoP) and diesters (DiP) represented significant fractions of PP for both epilimnetic and hypolimnetic samples (11-44% and 0-31%, respectively).

6.4.2.2 Lake dissolved phosphorus

Dissolved phosphorus, when detected, was more diverse in relative proportions of different P species than were particulate samples, and also was variable across depths (Table 1). Inorganic P accounted for all P detected in several samples (day 178 epilimnetic and hypolimnetic samples), while on day 278, only organic P (phosphonate) was observed in the hypolimnetic DP sample. Day 206 epiliminetic and day 278 hypolimnetic samples contained the greatest diversity of compounds. Day 278 hypolimnetic P more closely resembled lake and river

particulate samples, unlike day 206 epilimnetic signature, for which monoesters were conspicuously missing, while PO_4, DiP, and PyroP were present.

6.4.2.3 Phosphorus from hydrologic inflows

For the Yahara River and Pheasant Branch, DRP ranged from below limit of detection (<10 μg/L) to 0.041 μg/L and TP ranged from 0.035-0.276 μg/L (Table 2). Inorganic P comprised the largest fraction of detected PP in Pheasant Branch (60-82%), while inorganic P from the Yahara represented 35-47% of P detected. MonoP was the most dominant form of organic P of the Yahara samples (28-48% of total P), and represented 9-28% of TP from Pheasant Branch samples. Phosphonate was detected only once, on day 67 (of 2012) in the Yahara River.

Dissolved P from the Yahara on day 209 and 67 and from Pheasant Branch on day 67 were also analyzed. On day 209, DRP and TDP were near or below the limit of detection, and no DP was detected in in the NMR experiment. For day 67, 100% of P detected by NMR from the Yahara River was in the phosphonate region, while for Pheasant Branch, P was comprised of PO_4 (66%) and MonoP (34%). Day 67 at the Yahara river was the only day in which phosphonate was detected, and the compound was detected in both the PP and DP fractions.

6.5 Discussion

6.5.1 Experimental methods and detection of dissolved P

We tested the efficacy of an experimental parameter (probe width), an extra extraction step (EDTA pre-extraction), both with the goal of improving signal to noise ratio of dissolved P. Increasing probe width from 5 to 10mm had the expected result of increasing sensitivity (Figure

6.3). This step, together with a pre-extraction step, allowed detection of dissolved P forms, which was not possible without the use of these two steps (e.g. Figure 6.3, bottom panel). TDP and DRP were below our limit of detection in several cases, which corresponded to low/no detection of P in NMR experiment. For samples in which no DP was observed (day 206 and 234 epilimnetic and day 209 Yahara River samples), it is possible that we did not detect P that was indeed present, particularly when TDP and DRP were detected (e.g. day 209 Yahara River). However, in the cases of epilimnetic samples on day 206 and 234, TDP and DRP were both below our limit of detection, indicating that out limit of detection for colorimetry for filtered water samples was comparable to the limit of detection of NMR, following ~ 3000 fold concentration for NMR experimentation. For many of these samples, H_3PO_4 standard and AMP standards were added after the experiment was completed; in all cases, external standards were detected. Pre-extraction with EDTA likely complexed paramagnetic ions, which reduced line broadening and increased spectral resolution. That, together with increased probe size, allowed detection of lake and river dissolved P, after concentration of ~6-10L of surface water samples.

6.5.2 Seasonal trends in Lake Mendota particulate and dissolved P

Particulate P in the epilimnion was more consistent through time than in the hypolimnion (Figure 6.5), and was dominated by monoesters, PO_4 PO_4hosphate, and pyro-and polyphosphates. The relative contribution of Phos and PyroP+PolyP increased through time until day 264, after which MonoP dominated again. The mixing even occurring between day 264 and 278 typically results in increased epilimnetic DRP, reduced TP, and increased NO_3 and NO_2; this pulse of inorganic nutrients typically results in a phytoplankton bloom event that is often dominated by *Microcystis* (Brock, 1985). The shift in dominance of PolyP+PyroP to more prevalence of Phos

and MonoP may be due to shift in the speciation of phytoplankton biomass after the mixing event.

Hypolimnetic P observed was more variable in relative contribution of different species due to the variability of PolyP+PyroP observed. Ranging from 0-56% contribution, this variable component may have been due to sinking phytoplankton-derived detritus falling through the water column at inconsistent rates, perhaps due to entrainment or rapid deepening of the thermocline due to storm or wind events. Once in the hypolimnion, PolyP and PyroP would be rich substrates for energy and could be rapidly degraded by heterotrophic bacteria under hypolimnetic anaerobic conditions. This degradation of PyroP and PolyP could likely occur more rapidly than, e.g. phosphonate. Phosphonate observed from day 193-264 consistently represented between 17-27% of P observed. After the fall mixing event (between day 264-278), relative contribution of PolyP+PyroP and Phos decreased, while the relative contribution of PO_4 increased.

For particulate P samples are mainly comprised of planktonic biomass, namely phytoplankton. Typically from mid-June (~ day 165) through October (~day 273), Cyanobacterial cells dominate phytoplankton biomass, and the particulate phosphorus pool. In cells, phosphorus is present as nucleic acids (diesters), lipids (diesters), lipopolysaccharides (monoesters and diester degradation products), and intracellular solutes (orthophosphates, soluble polyphosphates, and others). Polyphosphate and pyrophosphate can also be accumulated by a numerous bacterial species (Brown & Kornberg, 2008), including several cyanobacterial types, and have been observed intracellularly in cultured phytoplankton and natural samples using ^{31}P NMR (Cade-Menun & Paytan, 2010; Feuillade et al., 1995). Phosphonates are also produced by cyanobacteria (Namikoshi & Rinehart, 1996), and although there is evidence for

greater recalcitrance of this compound of organic P in marine environments as compared to mono- and diesters (Clark et al., 1998), there are also many examples of phytoplankton utilization of phosphonates as P sources (Beversdorf et al., 2010; Lipok et al., 2007; Lipok et al., 2009). In Lake Mendota, more constant levels of phosphonate than poly- or pyrophosphate in both epilimentic and hypolimnetic (presumably dominated by particulates of epilimnetic origin) particulate P may be due to the recalcitrance of phosphonate as compared to polyphosphate.

The large contribution of polyphosphate and pyrophosphate to total particulate epilimnetic P from day 123 through day 248 is interesting in light of the dogma of Lake Mendota as a P-limited system during summertime stratification in the epilimnion (Brock, 1985). Evidence in the literature flr nutrient limitation as a cause of intracellular polyP accumulation is not in agreement (e.g. see (Cade-Menun & Paytan, 2010; Feuillade et al., 1995)) and additionally points to potential stresses beyond nutrient limitation (Kornberg et al., 1999).

6.5.3 The Yahara River and Pheasant Branch

Distinct differences in particulate P speciation between the hydrologic inflows were observed (Table 1). In particular, Pheasant Branch PP was dominated by orthophosphate, while monophosphates dominated the Yahara River PP. Yahara and Pheasant Branch river particulate and dissolved samples were similar in composition to those found in a previous study (Cade-Menun et al., 2006)

The hydrologic inflows sampled during this study were distinct in two important ways: 1) the Yahara River is a 4^{th} order stream while Pheasant Branch is 3^{rd} order, resulting in the Yahara delivering ~ 20-100 times greater mean discharge to Lake Mendota than Pheasant Branch; and 2) Pheasant Branch underwent fish habitat restoration construction at the sampling site prior and

during sampling events. The construction resulted in a shallower, wider, braided channel, to enhance aquatic macrophyte and fish spawning habitat. Although geo-membranes, plants, and hay berms were installed to prevent erosion, particulate P from Pheasant Branch was always darker in color than the Yahara particulate P, likely because of higher concentration of sediments suspended as a result of the restoration construction. Urban and agricultural construction runoff is regulated at the regional level to protect downstream water quality (Jones et al., 2010), and because our sampling occurred during construction, we have an interesting opportunity to see how construction particulate P looks. However, we do not yet have reference samples against which to compare.

6.6 Conclusions

Lake samples from late spring through early fall, including fall mixis, were characterized for particulate and dissolved phosphorus using ^{31}P NMR. We found particulate samples were dominated by orthophosphate monoesters, diesters, orthophosphate, polyphosphate and pyrophosphate. Epilimnetic samples were more consistent in the relative proportions of the compound classes than hypolimnetic samples, which could be due to epilimentic production of polyphosphate, pyrophosphate, and phosphonate and differential degradation of these materials as they sink through the water columns. Dissolved phosphorus contained all of the compound classes also found in particulate samples, but were typically dominated by orthophosphate, and in some cases contained no detectable phosphorus. Hydrologic inflows from 3rd and 4th order streams entering the lake were distinct from each other: one site was undergoing extensive habitat restoration construction during the sampling period, and typically contained significantly more orthophosphate as a relative proportion of total particulate phosphorus detected. River

dissolved phosphorus, like that of in-lake dissolved phosphorus, was generally much lower in concentration and dominated by orthophosphate. Phosphonate was detected in river samples only on one occasion (7 March 2012), and on that day, was found in both particulate and dissolved samples from the Yahara River.

Our results show that both dissolved and particulate organic and inorganic phosphorus speciation in a stratified eutrophic lake are dynamic in both time and space. Epilimnetic particulate phosphorus had the most consistent signature, while hypolimnetic particulate phosphorus, hypolimnetic dissolved phosphorus, and river dissolved and particulate P were much more dynamic in speciation. Our expectation that more labile dissolved and particulate P forms (orthophosphate esters and pyrophosphate) would be reduced and that polyphosphate and phosphonate would be maintained through the season was met. We did not find hypolimnetic particulate P to be mainained in composition through time, which may be due to differential uptake rates under hypolimnetic conditions.

6.7 Acknowledgements

Many thanks to Jay Hawley, Aaron Besaw, James Mutschler, Tingxi Zhang for laboratory assistance in APA fluorometry and sample preparation. NTL LTER, UW Chemistry Department NMR Facility.

6.8 References

Ahlgren, J., Tranvik, L., Gogoll, A., Waldeback, M., Markides, K., & Rydin, E. (2005). Sediment depth attenuation of biogenic phosphorus compounds measured by 31P NMR. *Environmental science & technology*, *39*(3), 867-72. Retrieved from http://www.ncbi.nlm.nih.gov/pubmed/15757351

Beversdorf, L. J., White, A. E., Björkman, K. M., Letelier, R. M., & Karl, D. M. (2010). Phosphonate metabolism by Trichodesmium IMS101 and the production of greenhouse gases. *Limnology and Oceanography*, *55*(4), 1768-1778. doi:10.4319/lo.2010.55.4.1768

Brock, T. D. (1985). *A Eutrophic Lake: Lake Mendota, Wisconsin* (p. 308). Springer Verlag.

Brown, M. R. W., & Kornberg, A. (2008). The long and short of it - polyphosphate, PPK and bacterial survival. *Trends in biochemical sciences*, *33*(6), 284-90. doi:10.1016/j.tibs.2008.04.005

Cade-Menun, B. J. (2005). Characterizing phosphorus in environmental and agricultural samples by 31P nuclear magnetic resonance spectroscopy. *Talanta*, *66*(2), 359-71. doi:10.1016/j.talanta.2004.12.024

Cade-Menun, B. J., Liu, C. W., Nunlist, R., & McColl, J. G. (2002). Soil and litter phosphorus-31 nuclear magnetic resonance spectroscopy: extractants, metals, and phosphorus relaxation times. *Journal of environmental quality*, *31*(2), 457-65. Retrieved from http://www.ncbi.nlm.nih.gov/pubmed/11931434

Cade-Menun, B. J., Navaratnam, J., & Walbridge, M. (2006). Characterizing dissolved and particulate phosphorus in water with 31P nuclear magnetic resonance spectroscopy. *Environmental science & technology*, *40*(24), 7874-80. Retrieved from http://www.ncbi.nlm.nih.gov/pubmed/17256541

Cade-Menun, B. J., & Paytan, A. (2010). Nutrient temperature and light stress alter phosphorus and carbon forms in culture-grown algae. *Marine Chemistry*, *121*(1-4), 27-36. Elsevier B.V. doi:10.1016/j.marchem.2010.03.002

Carpenter, S. R., Benson, B., Biggs, R., Chipman, J. W., Foley, J. A., Golding, S. A., Hammer, R. B., et al. (2007). Understanding Regional Change : A Comparison of Two Lake Districts. *BioScience*, *57*(4), 323-335.

Clark, L. L., Ingall, E. D., & Benner, R. (1998). Marine phosphorus is selectively remineralized. *Nature*, *393*(June), 1998.

Cooper, W., Llewelyn, J., Bennett, G., Stenson, A., & Salters, V. (2005). Organic Phosphorus Speciation in Natural Waters by Mass Spectrometry. In B. L. Turner, E. Frossard, & D. Baldwin (Eds.), *Organic Phosphorus in the Environment* (1st ed., pp. 45-74). Cambridge, MA: CABI Publishing.

Dillon, P., & Rigler, F. (1974). The phosphorus-chlorophyll relationship in lakes. *Limnology and Oceanography*, *19*(5), 767-773.

Ding, S., Xu, D., Li, B., Fan, C., & Zhang, C. (2010). Improvement of (31)P NMR spectral resolution by 8-hydroxyquinoline precipitation of paramagnetic Fe and Mn in

environmental samples. *Environmental science & technology*, *44*(7), 2555-61. doi:10.1021/es903558g

Eisenreich, S. J., & Armstrong, D. E. (1977). Chromatographic Investigation of Inositol Phosphate Esters in Lake Waters. *Environmental Science & Technology*, *11*(5), 497-501.

Falkowski, P., Scholes, R., Boyle, E., Canadell, J., Canfield, D., Elser, J., Gruber, N., et al. (2000). The Global Carbon Cycle: A Test of Our Knowledge of Earth as a System. *Science*, *290*(5490), 291-296. doi:10.1126/science.290.5490.291

Feuillade, J., Bielicki, G., & Renou, J. (1995). 31P NMR study of natural phytoplankton samples. *Hydrobiologia*, *300*.

Hoppe, H. (1983). Significance of exoenzymatic activities in the ecology of brackishwater: measurements by means of methylumbelliferyl-substrates. *Marine Ecology Progress Series*, *11*, 229-308.

Hupfer, M., Ru, B., Berlin, D.-, & Schmieder, P. (2004). Origin and diagenesis of polyphosphate in lake sediments : A 31 P-NMR study. *Limnology*, *49*(1), 1-10.

Jeppesen, E., Sondergaard, M., Jensen, J. P., Havens, K. E., Anneville, O., Carvalho, L., Coveney, M. F., et al. (2005). Lake responses to reduced nutrient loading - an analysis of contemporary long-term data from 35 case studies. *Freshwater Biology*, *50*(10), 1747-1771. doi:10.1111/j.1365-2427.2005.01415.x

Jones, S., Josheff, S., Presser, D., & Steinhorst, G. (2010). *The Yahara Capital Area Environmental Assessment and Needs 2010 Report* (p. 138). Madison, WI. Retrieved from www.yaharawatershed.org

Kornberg, A., Rao, N. N., & Ault-riché, D. (1999). Inorganic Polyphosphate: A molecule of many functions. *Annual Review of Biochemistry*, *68*, 89-125.

Kuenzler, E. (1970). Dissolved organic phosphorus excretion by marine phytoplankton. *Journal of Phycology*, *6*, 7-13.

Lathrop, R., Carpenter, S. R., Stow, C., Soranno, P., & Panuska, J. (1998). Phosphorus loading reductions needed to control blue-green algal blooms in Lake Mendota. *Spring*.

Lean, D. (1973). Phosphorus dynamics in lake water. *Science*, *179*(4074), 678-680. doi:10.1126/science.187.4175.454

Lipok, J., Owsiak, T., Młynarz, P., Forlani, G., & Kafarski, P. (2007). Phosphorus NMR as a tool to study mineralization of organophosphonates—The ability of Spirulina spp. to degrade glyphosate. *Enzyme and Microbial Technology*, *41*(3), 286-291. doi:10.1016/j.enzmictec.2007.02.004

Lipok, J., Wieczorek, D., Jewgiński, M., & Kafarski, P. (2009). Prospects of in vivo 31P NMR method in glyphosate degradation studies in whole cell system. *Enzyme and Microbial Technology*, *44*(1), 11-16. doi:10.1016/j.enzmictec.2008.09.011

McDowell, R. W., Stewart, I., & Cade-Menun, B. J. (2006). An examination of spin-lattice relaxation times for analysis of soil and manure extracts by liquid state phosphorus-31 nuclear magnetic resonance spectroscopy. *Journal of environmental quality*, *35*(1), 293-302. doi:10.2134/jeq2005.0285

Minear, R. (1972). Characterization of Naturally Occuring Dissolved Organophosphorus Compounds. *Environmental science & technology*, *6*(5), 431-437.

Murphy, J., & Riley, J. (1962). A modified single solution method for the determination of phosphate in natural waters. *Analytica chimica acta*, *27*, 31-36.

Namikoshi, M., & Rinehart, K. (1996). Bioactive compounds produced by cyanobacteria. *Journal of Industrial Microbiology and Biotechnology*, *17*(5-6), 373-384.

Nanny, M., & Minear, R. (1994). Use of Lanthanide Shift Reagents with 31P FT-NMR Spectroscopy To Analyze Concentrated Lake-Water Samples. *Environmental science & technology*, *28*(8), 1521-7. doi:10.1021/es00057a022

Nanny, M., & Minear, R. (1997). Characterization of soluble unreactive phosphorus using 31P nuclear magnetic resonance spectroscopy. *Marine Geology*, *139*(1-4), 77-94. doi:10.1016/S0025-3227(96)00098-9

Paerl, H. W., & Downes, M. T. (1978). Biological Availability of Low Versus High Molecular Weight Reactive Phosphorus. *Journal of Fisheries Research Board of Canada*, *35*(1978), 1639-1643.

Peters, J., & Lean, D. (1973). The Characterization of Soluble Phosphorus Released by Limnetic Zooplankton. *Limnology and Oceanography*, *18*(2), 270-279.

Reitzel, K., Ahlgren, J., Debrabandere, Æ. H., Adolf, Æ., & Lars, G. Æ. (2007). Degradation rates of organic phosphorus in lake sediment. *Biogeochemistry*, 15-28. doi:10.1007/s10533-006-9049-z

Reitzel, K., Ahlgren, J., Gogoll, A., & Rydin, E. (2006). Effects of aluminum treatment on phosphorus, carbon, and nitrogen distribution in lake sediment: a 31P NMR study. *Water research*, *40*(4), 647-54. doi:10.1016/j.watres.2005.12.014

Reitzel, K., Jensen, H. S., Flindt, M., & Andersen, F. Ø. (2009). Identification of dissolved nonreactive phosphorus in freshwater by precipitation with aluminum and subsequent 31P NMR analysis. *Environmental science & technology*, *43*(14), 5391-7. Retrieved from http://www.ncbi.nlm.nih.gov/pubmed/19708371

Rengefors, K., Ruttenberg, K. C., Haupert, C. L., Taylor, C., Howes, B. L., & Anderson, D. M. (2003). Experimental investigation of taxon-specific response of alkaline phosphatase activity in natural freshwater phytoplankton. *Limnology and Oceanography*, *48*(3), 1167-1175. doi:10.4319/lo.2003.48.3.1167

Rigler, F. (1956). A tracer study of the phosphorus cycle in lakewater. *Ecology*, *37*, 550-562.

Schaus, M. H., Vanni, M. J., Wissing, T. E., Bremigan, M. T., & Garvey, J. E. (1997). Nitrogen and Phosphorus Excretion by Detritivorous Gizzard Shad in a Reservoir Ecosystem. *Limnology and Oceanography*, *42*(6), 1386-1397.

Selig, U., Michalik, M., & Hübener, T. (2006). Assessing P status and trophic level of two lakes by speciation of particulate phosphorus forms, *65*(1), 17-26.

Sinsabaugh, R. L., Findlay, S., Franchini, P., Fischer, D., & Sinsabaugh, L. (1997). Enzymatic analysis of riverine bacterioplankton production. *Limnology and Oceanography*, *42*(1), 29-38.

Soranno, P., Carpenter, S. R., & Lathrop, R. (1997). Internal phosphorus loading in Lake Mendota : response to external loads and weather. *Methods*, *1893*, 1883-1893.

Turner, B. L., Newman, S., & Reddy, K. R. (2006). Overestimation of organic phosphorus in wetland soils by alkaline extraction and molybdate colorimetry. *Environmental science & technology*, *40*(10), 3349-54. Retrieved from http://www.ncbi.nlm.nih.gov/pubmed/16749704

Wetzel, R. G. (2001). *Limnology: Lake and River Ecosystems* (3rd ed.). San Diego, CA: Academic Press.

White, E., & Payne, G. (1980). Distribution and Biological Availability of Reactive High Molecular Weight Phosphorus in Natural Waters in New Zealand. *Journal of Fisheries and Aquatic Science*, *34*, 664-669.

Worsfold, P. J., Gimbert, L. J., Mankasingh, U., Omaka, O. N., Hanrahan, G., Gardolinski, P. C. F. C., Haygarth, P. M., et al. (2005). Sampling, sample treatment and quality assurance issues for the determination of phosphorus species in natural waters and soils. *Talanta*, *66*(2), 273-93. doi:10.1016/j.talanta.2004.09.006

6.9 Tables

Table 6.1. ^{31}P NMR P speciation and extraction efficiency of water samples collected in-lake and from hydrologic inflows to Lake Mendota, WI. Phosphonate (Phos), orthophosphate (PO_4), orthophosphate monoesters (MonoP), orthophosphate diesters (DiP), pyrophosphate plus polyphosphate (PyroP + PolyP) were discriminated and quantified using ^{31}P NMR. Total phosphorus (TP), total particulate phosphorus (TPP), total dissolved phosphorus (TDP) and dissolved reactive phosphorus (DRP) were measured colorimetrically after acid digestion (for TP, TDP, and TPP). NMR extract was subsampled prior to experiment for TP analysis by ICP OES (NMR TP). Extraction efficiency (%) was calculated as [NMR TP/TPP or TDP]. Inorganic phosphorus (P_i) and organic phosphorus (P_o) are shown as a percent of total P observed in NMR analysis. The ratio of phosphorus to manganese (P/Mn) of the NMR-ready extract is shown for lake particulate samples.

Lake Particulate Phosphorus

Sample ID	Depth (m)	Date	Day of Year	Phos	PO_4	Mon oP	DiP	PyroP + PolyP	TPP (mg/L)	DRP (mg/L)	NMR TP (mg/L)	Extraction Efficiency (%)	Pi (%)	Po (%)	P/ Mn
20	0.5	05/03/11	123	0	27	41	16	15	0.031	0.018	n/d	n/d	42	58	n/d
26	0.5	05/18/11	138	0	24	35	23	17	0.035	0.035	0.020	55	41	59	2.9
24	0.5	06/01/11	152	0	17	23	31	30	0.018	0.056	0.005	27	46	54	3.5
35	0.5	06/28/11	179	0	30	35	9	25	0.023	< 0.01	0.021	91	56	44	48.9
38	0.5	07/12/11	193	5	27	21	14	33	0.030	< 0.01	0.027	89	60	40	26.8
41	0.5	07/25/11	206	16	11	24	22	27	0.020	< 0.01	0.009	45	38	62	13.0
47	0.5	08/09/11	221	3	9	31	21	36	0.013	<0.01	0.01	77	45	55	3.4
53	0.5	09/05/11	248	15	9	19	16	42	0.017	< 0.01	0.009	53	51	49	2.6
51	0.5	09/21/11	264	0	15	38	10	37	0.024	< 0.01	0.007	29	51	49	1.6
60	0.5	10/05/11	278	17	11	36	8	27	0.033	0.041	0.018	55	38	62	3.3
22	14	05/03/11	123	0	24	43	12	21	0.031	0.013	0.011	35	46	54	1.2
27	14	05/18/11	138	0	25	39	18	17	0.034	0.038	0.001	4	42	58	1.7
30	14	06/01/11	152	0	31	44	15	10	0.027	0.060	0.015	54	41	59	5.2
32	14	06/12/11	165	14	14	17	0	55	0.014	0.107	0.014	98	69	31	2.1
36	14	06/28/11	179	0	37	33	30	0	0.019	0.131	0.014	75	37	63	1.7
40	14	07/12/11	193	18	19	17	14	32	0.018	0.171	0.018	99	51	49	16.7
42	14	07/25/11	206	22	25	20	27	7	0.014	0.224	0.010	71	31	69	0.9
54	14	09/05/11	248	17	11	18	28	26	0.014	0.248	0.011	79	37	63	39.8
52	14	09/21/11	264	18	3	11	11	56	0.006	0.292	0.006	100	59	41	28.9
61	14	10/05/11	278	0	35	27	17	21	0.033	0.102	0.019	58	56	44	1.0

River Particulate Phosphorus

Sample ID	Location	Date	Day of Year	Phos	PO_4	Mon oP	DiP	PyroP + PolyP	TPP (mg/L)	DRP (mg/L)	NMR TP (mg/L)	Extraction Efficiency (%)	Pi (%)	Po (%)
49	Yahara	07/28/11	209	0	28	41	15	17	0.276	< 0.01	n/d	n/d	45	55

43	Yahara	09/21/11	264	0	23	48	18	12	0.112	< 0.01	n/d	n/d	35	65
44	Ph. Branch	09/21/11	264	0	49	28	12	12	0.048	0.017	n/d	n/d	60	40
62	Ph. Branch	03/07/12	67	0	64	9	9	18	0.273	0.041	n/d	n/d	82	18
63	Yahara	03/07/12	67	16	15	28	10	32	0.035	0.003	n/d	n/d	47	53

Lake Dissolved Phosphorus

Sample ID	Depth (m)	Date	Day of Year	Phos	PO_4	MonoP	DiP	PyroP + PolyP	TDP (mg/L)	DRP (mg/L)	NMR TP (mg/L)	Extraction Efficiency (%)	Pi (%)	Po (%)
69	0.5	06/28/11	179	0	100	0	0	0	0.051	0.02	n/d	n/d	100	0
55	0.5	07/24/11	206	0	0	0	0	0	< 0.01	< 0.01	n/d	n/d	0	0
65	0.5	08/22/11	234	0	0	0	0	0	<0.01	<0.01	n/d	n/d	0	0
58	0.5	10/05/11	278	20	29	24	12	6	0.048	0.041	n/d	n/d	43	57
64	14	06/28/11	179	0	100	0	0	0	0.141	0.131	n/d	n/d	100	0
56	14	07/24/11	206	0	87	0	7	7	0.229	0.224	n/d	n/d	94	6
66	14	08/22/11	234	0	100	0	0	0	0.225	0.192	n/d	n/d	100	0
59	14	10/05/11	278	100	0	0	0	0	0.115	0.102	n/d	n/d	0	100

River Dissolved Phosphorus

Sample ID	Location	Date	Day of Year	Phos	PO_4	MonoP	DiP	PyroP + PolyP	TDP (mg/L)	DRP (mg/L)	NMR TP (mg/L)	Extraction Efficiency (%)	Pi (%)	Po (%)
57	Yahara	07/28/11	209	0	0	0	0	0	0.012	< 0.01	n/d	n/d	0	0
	Yahara	09/21/11	264						0.037	<0.01	n/d	n/d		
	Ph. Branch	09/21/11	264						0.024	0.017	n/d	n/d		
68	Yahara	03/07/12	67	100	0	0	0	0	<0.01	<0.01	n/d	n/d	0	100
67	Ph. Branch	03/07/12	67	0	66	34	0	0	0.053	0.042	n/d	n/d	66	34

6.10 Figures

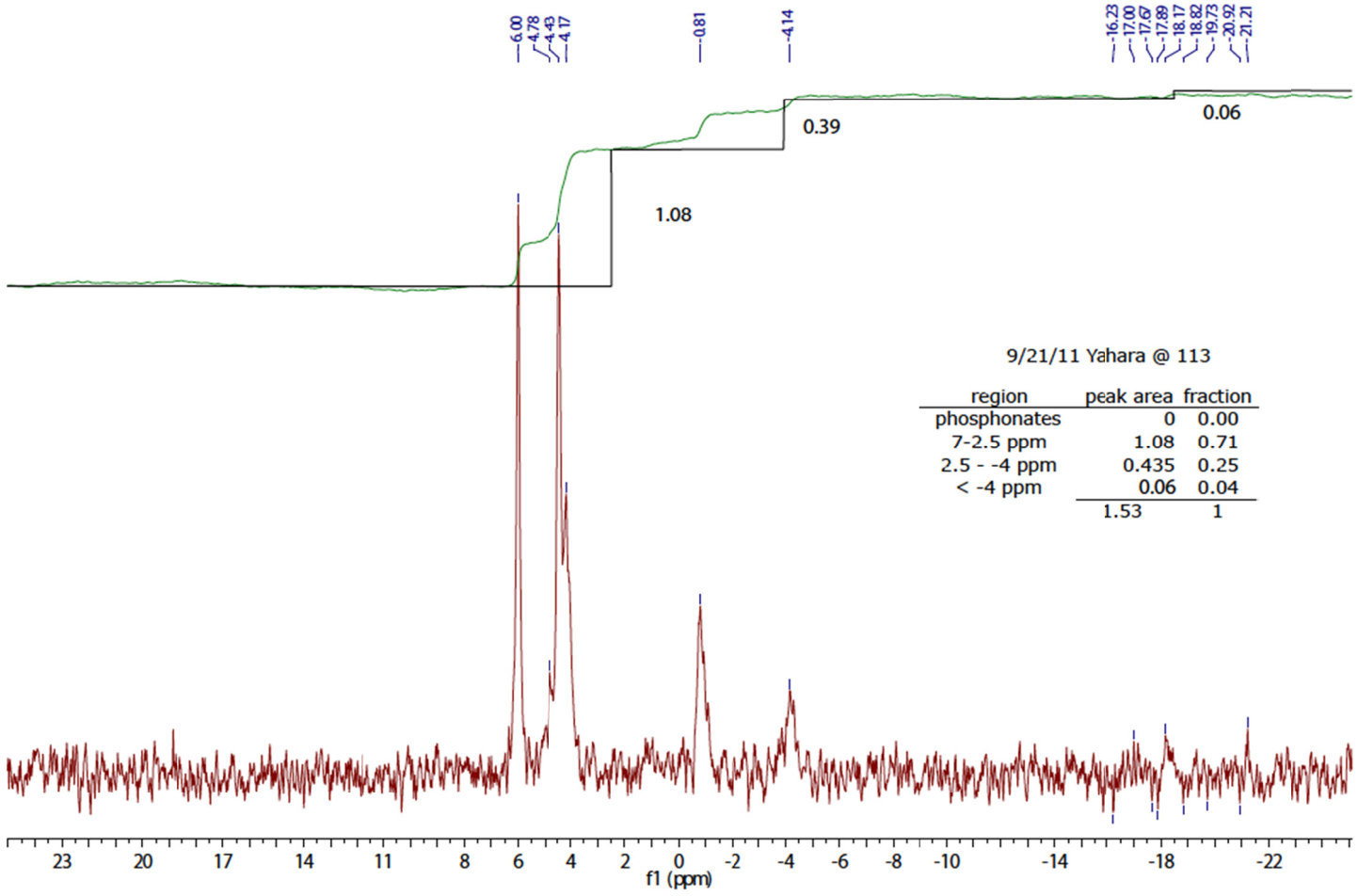

Figure 6.1 Example of full integrated particulate P NMR spectrum, collected from the Yahara River on September 13, 2011. Peak assignments and integration (green line) made using NUTS software. Peaks within regions defined above are further discriminated and quantified using the same integration technique to give P fractions shown in Table 6.1

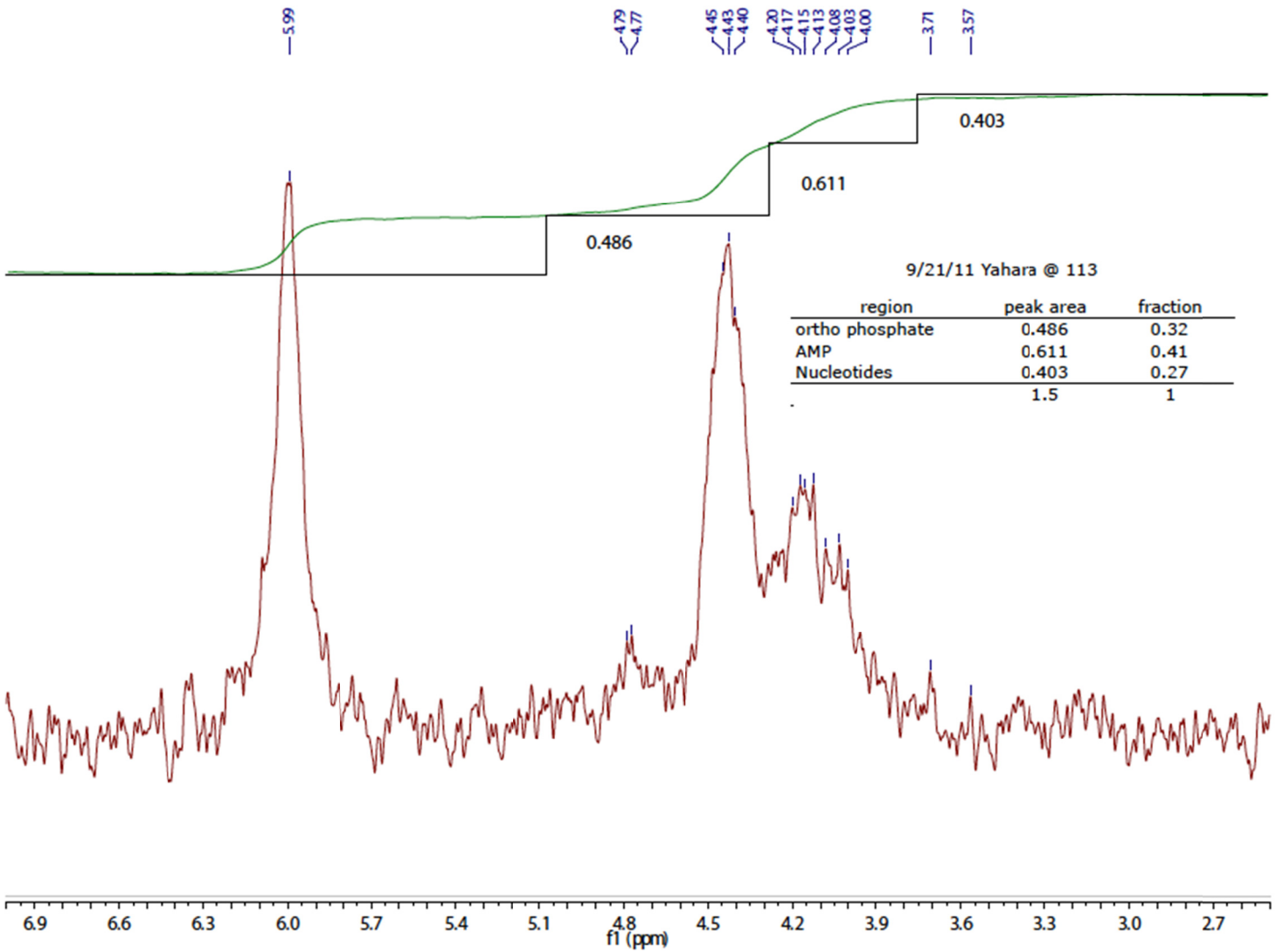

Figure 6.2 Example of integrated particulate P NMR spectrum zoomed into 7-2.5 ppm range for discrimination of orthophosphate (6ppm), APM (4.3ppm) and nucleotides (~4.1ppm).

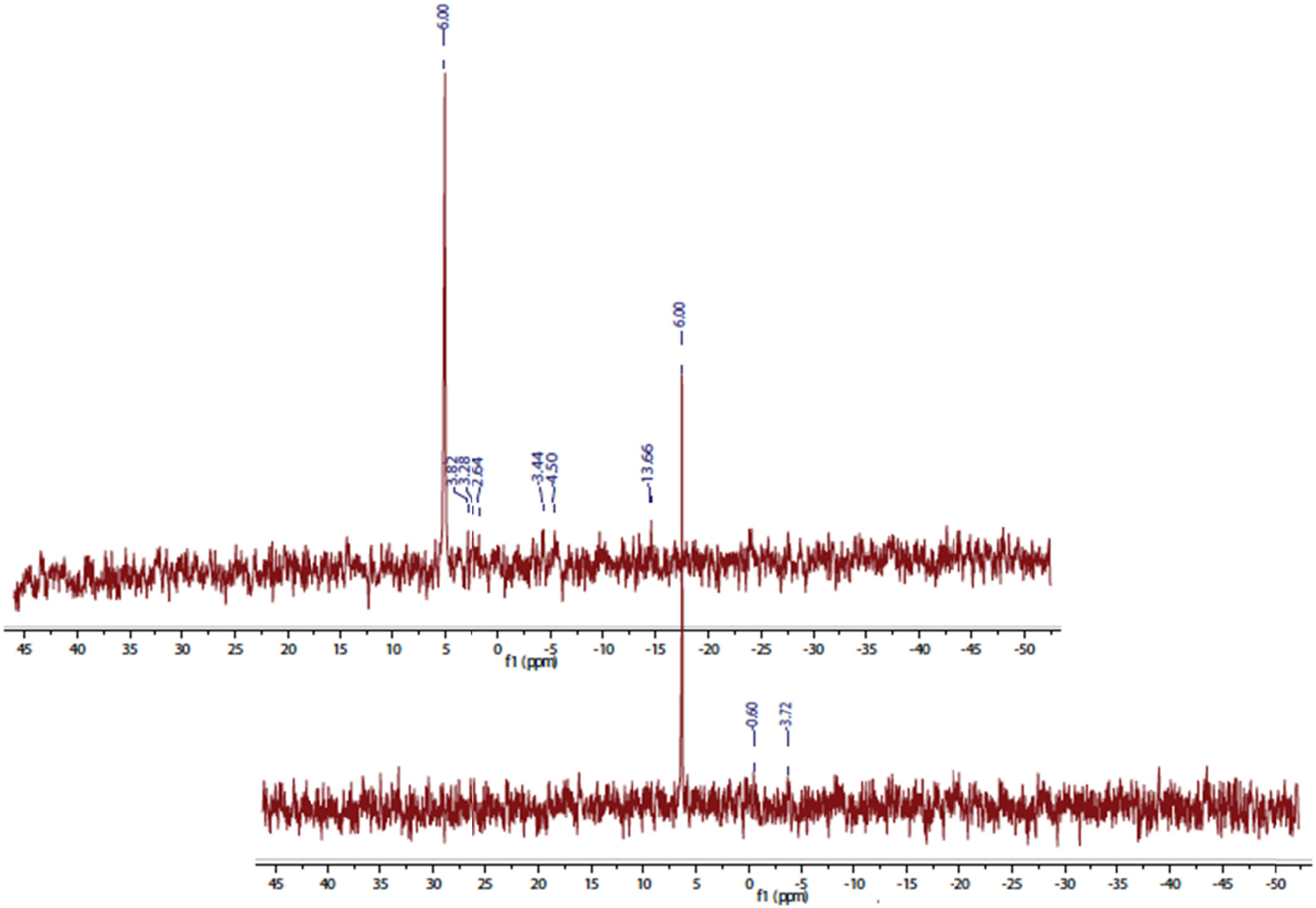

Figure 6.3 Epilimnetic dissolved P sample run using a 10mm probe on 360MHz Bruker instrument (top) versus using a 5mm probe on a 500MHz instrument (bottom).

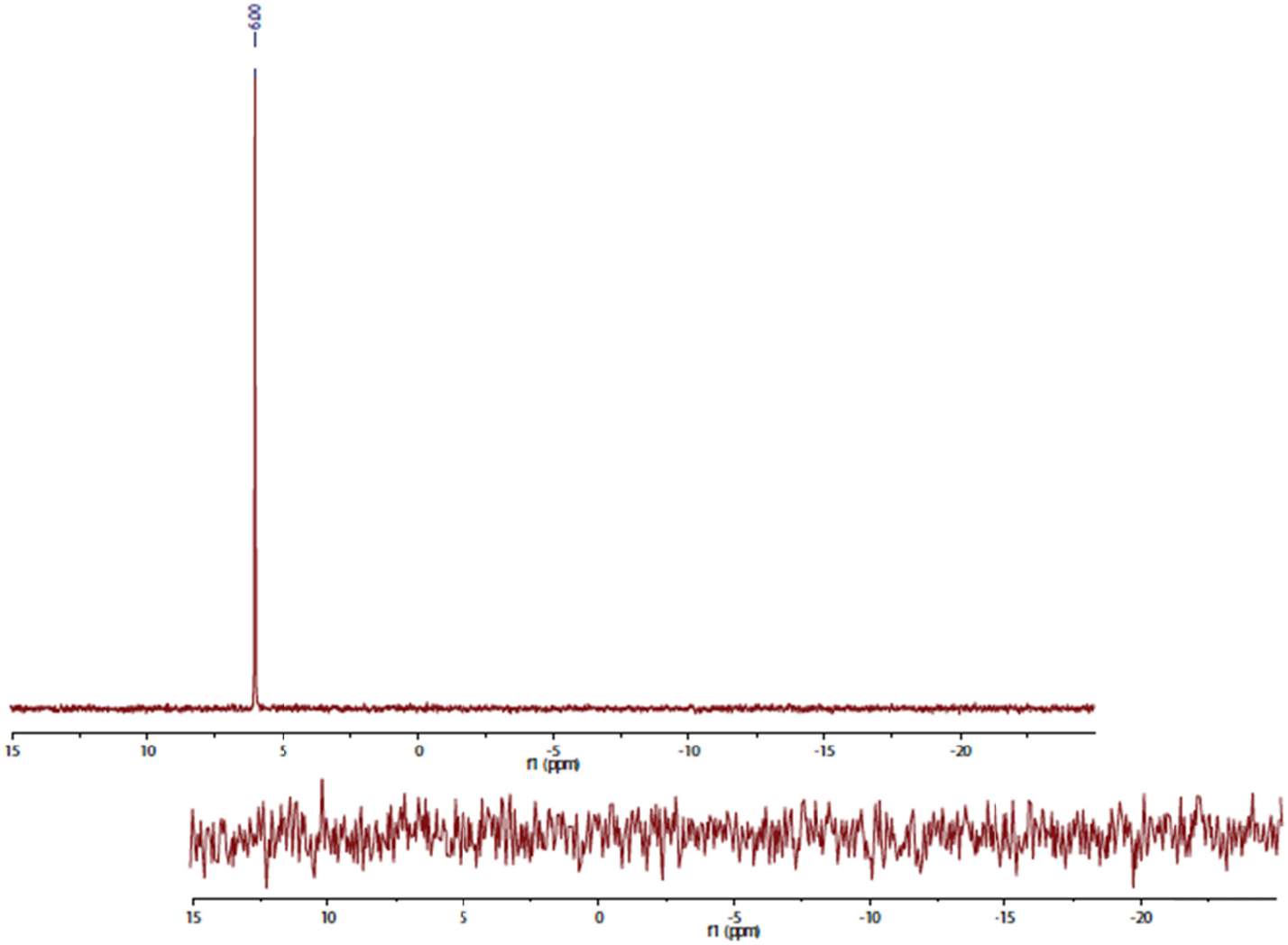

Figure 6.4 Epilimnetic dissolved phosphorus sample from June 1, 2011 analyzed after standard NaOH-EDTA extraction (bottom spectrum) and after pre-extraction with EDTA, followed by standard NaOH-EDTA extraction (top spectrum).

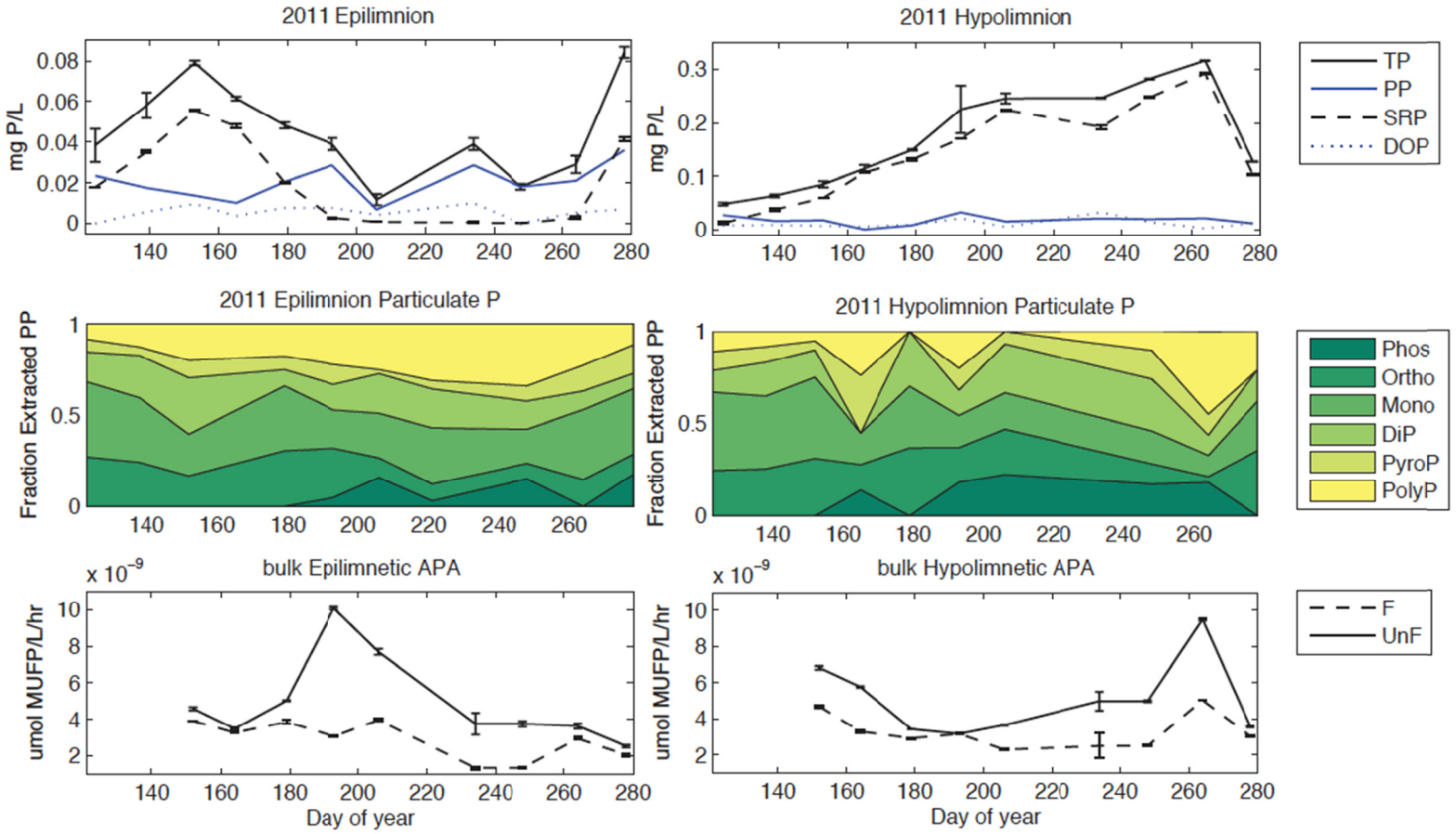

Figure 6.5 Temporal dynamics of phosphorus and alkaline phosphatase activity from epilimnion (0.5m) and hypolimnion (14m) depths in Lake Mendota, WI. **Top panel:** Temporal dynamics of total phosphorus (TP) and soluble reactive phosphorus (SRP) and, by subtraction, particulate (PP: TP-total dissolved P) and organic P (OP: total dissolved P-SRP) shown for epilimnetic (left) and hypolimnetic samples (right). **Center panel:** Fraction of extracted particulate P (PP) from epilimnion and hypolimnion shown in center panels: phosphonate (Phos), orthophosphate (PO_4), orthophosphate monoesters (MonoP), orthophosphate diesters (DiP), pyrophosphate (PyroP) and polyphosphate (PolyP) were discriminated and quantified using ^{31}P NMR. **Bottom panel:** alkaline phosphatase activity of filtered (F) and unfiltered (UF) bulk water sample

Chapter 7 – Conclusions and future work

Emily L. Kara

The goals of this dissertation were to address questions related to phosphorus management, speciation, and cycling; to determine the predictive ability of a water quality model for harmful cyanobacterial blooms and to assess the simulated effects of nutrient loading on water quality; and finally to understand drivers and characteristics of lake bacterial communities over a decade of observations. The research focuses on eutrophic Lake Mendota, Wisconsin, but the findings can be extended to other systems, and in some cases, are indicative of the potential and limitations of particular tools, i.e. numerical water quality simulation. Below, the major findings and recommend future research directions are briefly described.

7.1 The effects of phosphorus management on a watershed phosphorus budget

Efforts to reduce phosphorus loading in the Lake Mendota, Wisconsin watershed, including implementation of best management practices among farmers for nutrient and manure management, reduced use of chemical P feed supplements by dairy farmers, and an urban P fertilizer ban, reduced accumulation of P in watershed soils by ~ 50% from 1995 to 2007. However, we estimated accumulation of P in soils continues at a rate of 279,000 kg P/year. Our results indicate that watershed soils may be saturated in P, thus limiting the ability of watershed managers to accurately quantify and track further P inputs: under P-saturated conditions, excess P is not retained by soil. We found that crop chemical fertilizers continue to be the largest source of P inputs to the watershed (and thus modification of this source has the greatest potential for

reducing watershed P accumulation), while installation of riparian buffers represents an effective strategy for preventing P export from the watershed soils to the Yahara chain of lakes.

The efficacy of nutrient management to improve water quality is well established (Jeppesen et al., 2005). For the Lake Mendota watershed, there seems to be a disparity between the goals of stakeholders (Jones et al., 2010) and the desired outcomes (Kara et al., 2012). I believe that the sociological and political aspects (i.e. 'human' problems) are the barrier to improvement in water quality, as opposed to our ability to implement or assesses the management effects. For the goal of improving the water quality of the Yahara chain of lakes, stakeholders should look to examples of effective nutrient management, particularly, perhaps, for surface waters surrounded by agriculturally-dominated land and economies. Recently, the Wisconsin Department of Natural Resources (DNR) worked with the US Environmental Protection Agency (EPA) to revise the total maximum daily load (TMDL) standards for point sources in the Rock River Basin of Wisconsin. The new rules were written to allow point sources to either meet new, more stringent water quality requirements, or to implement nutrient management commensurate with the more stringent standards elsewhere in the basin, e.g. by working with farmers to mitigate non-point sources elsewhere in the watershed. One requirement for the alternative mitigation is that water quality improvements must be documented, as opposed to simply reducing nutrient criteria elsewhere in the watershed. This system, known as adaptive management, is unique in Wisconsin for surface water quality TMDL rules, and perhaps in the US. Madison Metropolitan Sewerage District (MMSD) has been leading the effort as a point source that is seeking to improve water quality elsewhere in the watershed as opposed to attempting to reduce nutrients in wastewater effluent, based on a cost comparison of additional removal of phosphorus versus migration of nutrient watershed elsewhere in the Lake Mendota

watershed. The outcome of this management 'experiment' is unknown as of yet, but it may represent potential success where other programs have fallen short.

7.2 Prediction of algal blooms and the effect of external drivers

We determined that a one-dimensional hydrodynamic biogeochemical numerical model had good predictive ability for temperature and water chemistry over 90 days over the open water period of 2008, but only moderate ability for cyanobacterial biomass concentrations (Kara et al., 2012). We used both high frequency water quality observations and manual observations to assess predictive ability, and novel application of wavelet analysis to determine assessment of the magnitude of variability predicted versus observed. We determined that pattern in short term (daily to hourly) scales were not reproduced by the model as expected, which led to closer consideration of model configuration and assumptions.

We found that cyanobacterial biomass responded more significantly to phosphorus loading than to external nitrogen loading or initial temperature conditions. Phytoplankton biomass was also insensitive to the type of nutrients loaded to the system (e.g. particulate versus dissolved, labile versus recalcitrant, or organic versus inorganic.

For a lake as large as Mendota, a three dimensional (3D) hydrodynamic model coupled to a biogeochemical model is likely require to reproduce biological patterns at short time scales, which may be driven by spatial heterogeneity not accounted for in a one dimensional model. Although the expertise of several research groups might be required to rigorously setup and run a 3D hydrodynamic biogeochemical model, without such an effort we will never know the extent to which bloom forecasting is possible. Additionally, from a management perspective, the effect of nutrient loading on this one lake is interesting, but if we could test the effect on multiples

lakes across gradients of size, mixing regime, and trophic status, we might be able to identify particular sensitivity classes of lakes that would respond to a greater extent than others.

7.3 Long-term bacterioplankton community dynamics

For time series of unprecedented length, we analyzed the bacterioplankton communities from a decade of observations from Lake Mendota, Wisconsin. We used local similarity analysis and network analysis to investigate differences in community patterns across seasons. We found that seasons controlled diversity, richness, and interaction network complexity, such that spring was least diverse but most complex and connected, while fall was most diverse but least connected. Cumulative time since ice-off or cumulative primary productivity may drive patterns in diversity. Implications of network structure on community function, resilience, and resistance are unknown, but findings from macro-ecological food webs indicate that greater complexity is typically associated with greater stability.

Network analysis gives information about communities across temporal or spatial gradients. The technique goes beyond the traditional toolbox of multivariate statistics that are typically used to distinguish differences between complex communities, to allow characterization of differences, as opposed to just identification of differences. It also allows for detailed taxon-level analysis of intra-taxon and taxon-environment interactions. Network analysis could be used to give insights into existing datasets of observations in the natural environment and in engineered systems. There are large opportunities for testing the following hypotheses either using existing datasets or new, experimentally derived ones: 1) interaction network complexity is a proxy for stability, as has been found for many other types of networks

and 2) network stability and diversity are positively related. Network analysis can give us greater insights into the functional capacity of complex communities.

There is also a unique opportunity for comparison of the molecular fingerprinting technique used for this study (automated ribosomal intergenic spacer analysis, ARISA) against the results of next generation sequencing results (i.e. Illumina 16S rRNA tag sequencing). This large dataset with robust patterns from ARISA data would useful for comparison to new techniques, in part because much of our knowledge of microbial ecology rests on more traditional molecular tools. The rise of the 'omics' age (genomics, metagenomics, proteomics, transcriptomics) is a new frontier for microbial ecologists with both great opportunities for discovery and great challenges for managing vast quantities of data.

7.4 Phosphorus speciation in a eutrophic lake and its hydrologic inflows

Using ^{31}P NMR to characterize the structure of phosphorus compounds in Lake Mendota and its inflows from May through October 2011, we made several surprising findings: 1) Epilimnetic particulate P is more constant in composition (relative proportion of orthophosphate, orthophosphate esters, polyphosphate and pyrophosphates) than hypolimnetic particulate P, river particulate P, and all dissolved P; 2) Epilimnetic particulate P comprised of phosphonates and polyphosphates increased as thermal stratification persisted through the open water season, and as dissolved reactive phosphorus remained undetectable; and 3) Pheasant Branch, a hydrologic inflow undergoing significant restoration, was a source of relatively more inorganic P than an un-disturbed, larger order stream (Yahara River).

Only three samples from the hydrologic inflows were made. By additional sampling from these inflows over longer and more even sampling period, a clearer picture of the influence of P

compounds on water quality, particularly at different times of the year and under different flow regimes, could be completed to identify the relative lability of P compounds present in runoff events, and perhaps related to the onset of cyanobacterial dominance. The role of polyphosphate and phosphonate in particulate P cells was also very compelling. There is evidence for diel patterns polyphosphate and phosphonate in cyanobacteria in the P-limited Yellowstone hot springs, where polyphosphate dominates during the day and phosphonate at night. This kind of metabolism, if present in Lake Mendota cyanobacteria, may give additional insight into the success of cyanobacteria in competition for resources over other algal species.

7.5 References

Jeppesen, E., Sondergaard, M., Jensen, J. P., Havens, K. E., Anneville, O., Carvalho, L., Coveney, M. F., et al. (2005). Lake responses to reduced nutrient loading - an analysis of contemporary long-term data from 35 case studies. *Freshwater Biology*, *50*(10), 1747-1771. doi:10.1111/j.1365-2427.2005.01415.x

Jones, S., Josheff, S., Presser, D., & Steinhorst, G. (2010). *The Yahara Capital Area Environmental Assessment and Needs 2010 Report* (p. 138). Madison, WI. Retrieved from www.yaharawatershed.org

Kara, E. L., Hanson, P. C., Hamilton, D. P., Hipsey, M. R., Mcmahon, K. D., Read, J. S., Winslow, L., et al. (2012). Time-scale dependence in numerical simulations : Assessment of physical , chemical , and biological predictions in a stratified lake at temporal scales of hours to months. *Environmental Modelling and Software*, *35*, 104-121. Elsevier Ltd. doi:10.1016/j.envsoft.2012.02.014

Kara, E. L., Heimerl, C., Killpack, T., Bogert, M. C., Yoshida, H., & Carpenter, S. R. (2012). Assessing a decade of phosphorus management in the Lake Mendota, Wisconsin watershed and scenarios for enhanced phosphorus management. *Aquatic Sciences*, *74*(2), 241-253. doi:10.1007/s00027-011-0215-6